Atomic and Molecular Data Needs for Plasma Applications Workshop
In the aether somewhere, April 2021

Low energy plasma interactions at atmospheric pressure with:
high concentration H_2O vapour,
water dissociation products &
water clusters

Paul Maguire
Ulster University

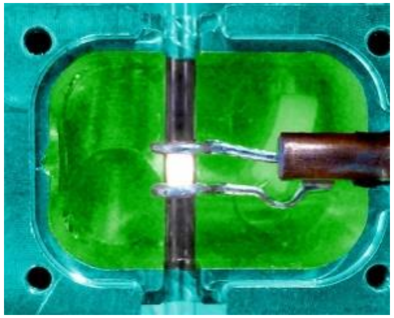

University of Ulster
Davide Mariotti
Sadegh Askari
Atta Haq
David Rutherford
Charles Mahony
Colin Kelsey
Nourhan Hendawy
Mark Tweedie
Manuel Macias-Montero
Harold McQuaid
Fatima Perez-Martin

University of Glasgow
Declan Diver

Outline

pd.maguire@ulster.ac.uk

- Introduction
  - Basics of the multiphase plasma systems and environments
  - A quick journey through some relevant applications
- Liquid droplet in plasma
  - Droplet statistics and flow
  - Temperature
  - Evaporation
  - Plasma structure and chemistry
  - Plasma charging of droplet
  - Plasma induced chemistry
- Electron flux to particle
  - Probe models
  - Solvation layer
- Ion, metastable flux
  - Recombination, energy transfer
  - Secondary electron emission
- New diagnostics
  - XPS/UPS/REELS/ISS of plasma treated liquid (then frozen)
  - Tunable midIR absorption

pd.maguire@ulster.ac.uk

Multiple phase system

- The beginning
  - ➲They say its "a very good place to start…"
- The ELEMENTS of the ancients
  - ➲*In no particular order*
  - ➲Earth:
  - ➲Wind:
  - ➲Fire:
  - ➲Water:
- Paper Scissors Rock
  - ➲***or***
  - ➲Liquid Wets Gas,
  - ➲Gas Dilutes Plasma,
  - ➲Plasma Surrounds Liquid…
  - ➲ and we make Nanorocks
- Multiphase systems
  - ➲Combining
  - ➲Multiphase flow
  - ➲Non-equilibrium Plasmas

Solid Gas Plasma Liquid

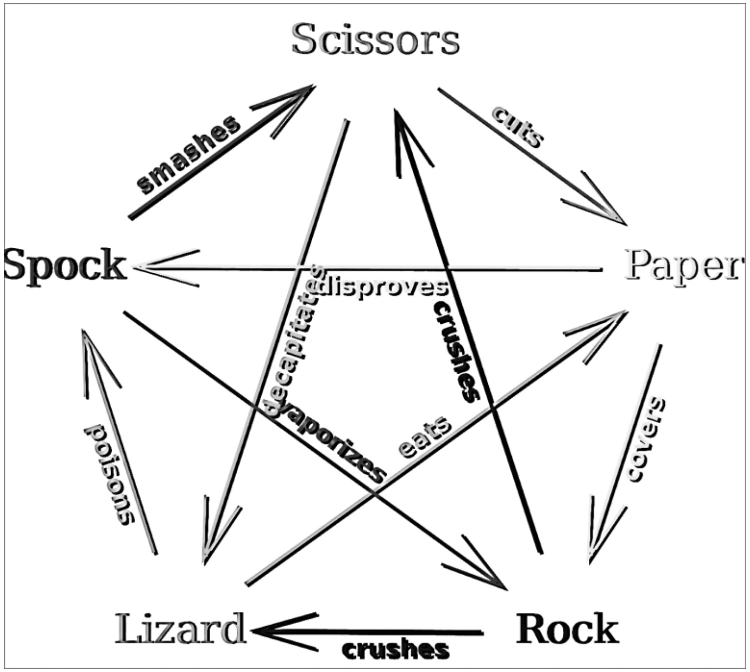

pd.maguire@ulster.ac.uk

Nanorocks

Solids from gas/plasma, with maybe a little liquid

Nanorocks (silicon)

pd.maguire@ulster.ac.uk

- Plasma interactions
  - ➲SiH_4 monomer dissociation
  - ➲Cluster formation
  - ➲Solid surface irradiation by charge & radicals
  - ➲Surface temperature elevation and melting
  - ➲Rapid local annealing and quenching

- Hot nanoparticles – Cold gas
  - ➲Tailored semiconductor properties
  - ➲Liquid phase present?
  - ➲Facilitates mass transfer gas → solid ?
- Charge collisional model

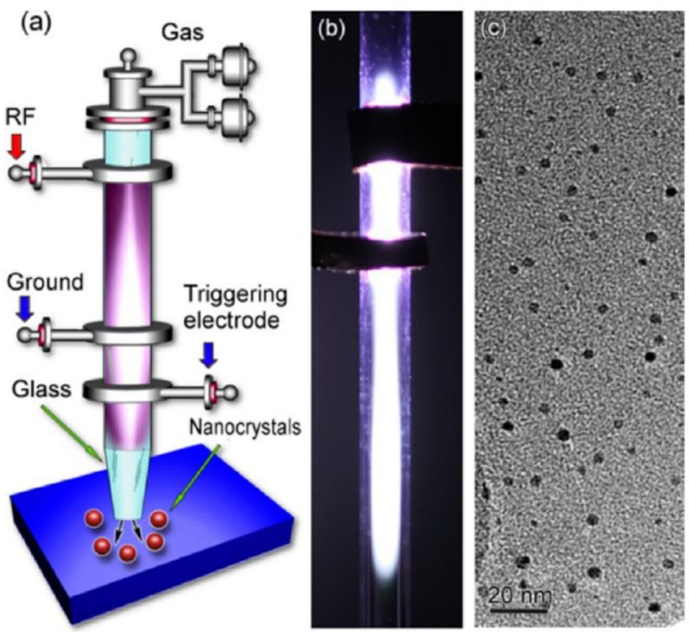

ADVANCED MATERIALS

The Interplay of Quantum Confinement and Hydrogenation in **Amorphous Silicon** Quantum Dots, Askari et al., 2015
10.1002/adma.201503013

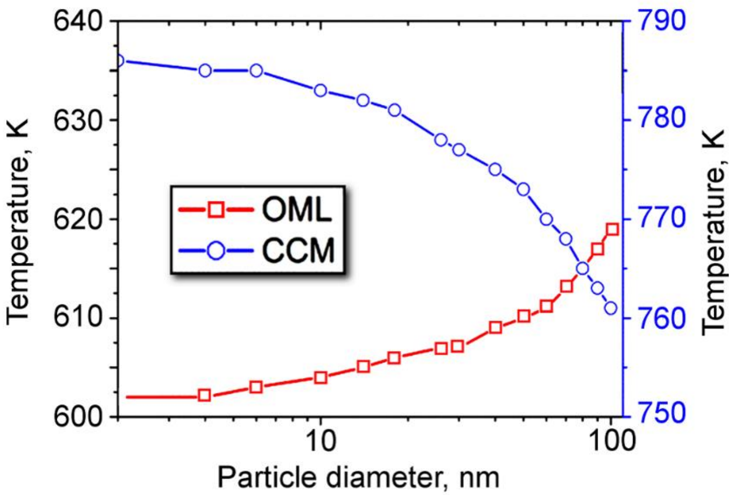

FIG. 4. Particle temperature for a range of nanoparticle diameter according to the two theoretical frameworks, OML, and CCM.

Crystalline Si nanoparticles below crystallization threshold: Effects of collisional heating in non-thermal atmospheric-pressure microplasmas
S. Askari, I. Levchenko, K. Ostrikov, P. Maguire, and D. Mariotti

Citation: Applied Physics Letters **104**, 163103 (2014); doi: 10.1063/1.4872254
View online: http://dx.doi.org/10.1063/1.4872254

- Plasma interactions
  - ➲SiH_4 monomer dissociation
  - ➲Cluster formation
  - ➲Solid surface irradiation by charge & radicals
  - ➲Surface temperature elevation and melting
  - ➲Rapid local annealing and quenching

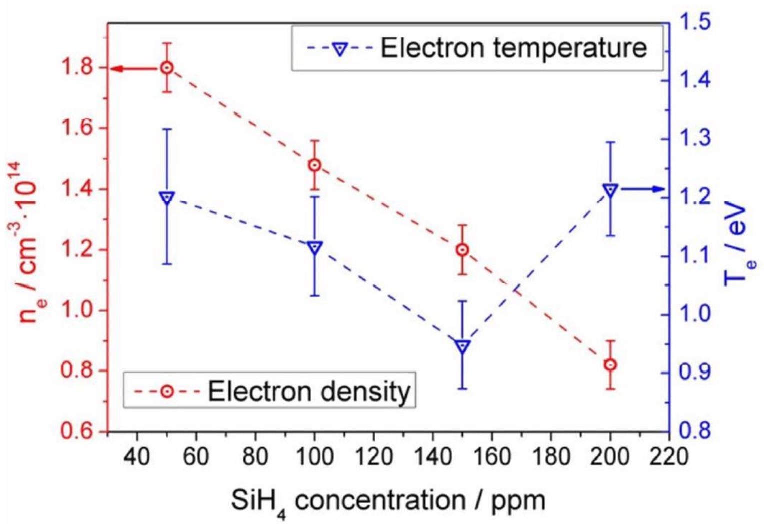

Electron density (left axis) and electron temperature (right axis) calculated

ADVANCED MATERIALS

The Interplay of Quantum Confinement and Hydrogenation in **Amorphous Silicon** Quantum Dots, Askari et al., 2015 10.1002/adma.201503013

- Hot nanoparticles – Cold gas
  - ➲Tailored semiconductor properties
  - ➲Liquid phase present?
  - ➲Facilitates mass transfer gas → solid ?
- Charge collisional model

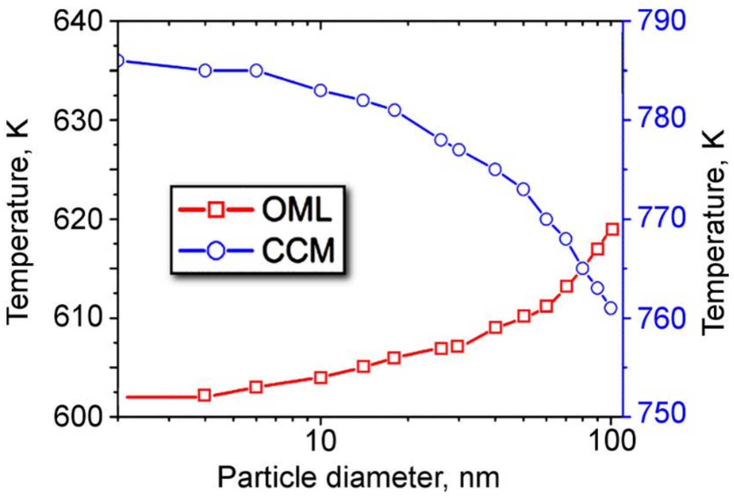

FIG. 4. Particle temperature for a range of nanoparticle diameter according to the two theoretical frameworks, OML, and CCM.

Crystalline Si nanoparticles below crystallization threshold: Effects of collisional heating in non-thermal atmospheric-pressure microplasmas

S. Askari, I. Levchenko, K. Ostrikov, P. Maguire, and D. Mariotti

Citation: Applied Physics Letters **104**, 163103 (2014); doi: 10.1063/1.4872254
View online: http://dx.doi.org/10.1063/1.4872254

- Crystallisation
  - ➲Amorphous – crystalline temperature contour
  - ➲Charge flux – size dependent
  - ➲Local surface heating – local melting?
  - ➲Facilitates mass transfer from gas/plasma to solid state

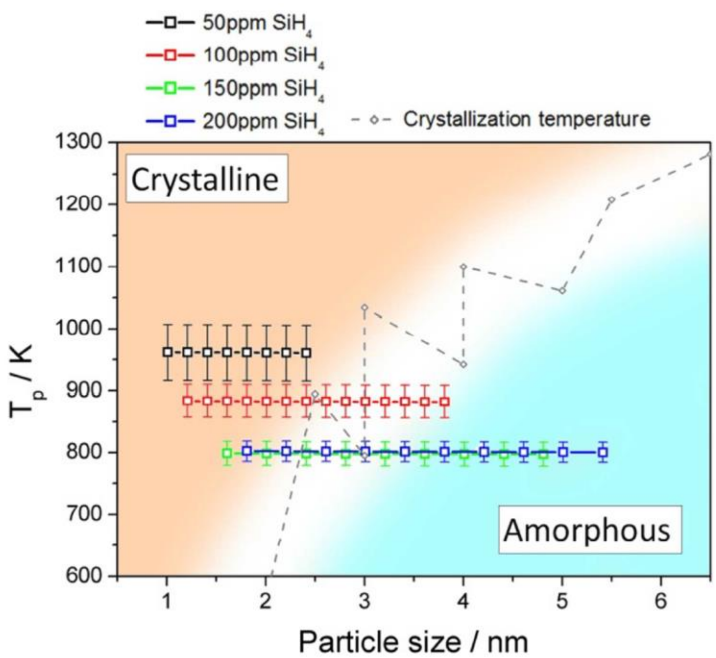

Figure 4. Particle temperature calculated using the collision-corrected model (CCM)

ADVANCED MATERIALS

The Interplay of Quantum Confinement and Hydrogenation in **Amorphous Silicon** Quantum Dots, Askari et al., 2015 10.1002/adma.201503013

- Hot nanoparticles – Cold gas
  - ➲Tailored semiconductor properties
  - ➲Liquid phase present?
  - ➲Facilitates mass transfer gas → solid ?
- Charge collisional model

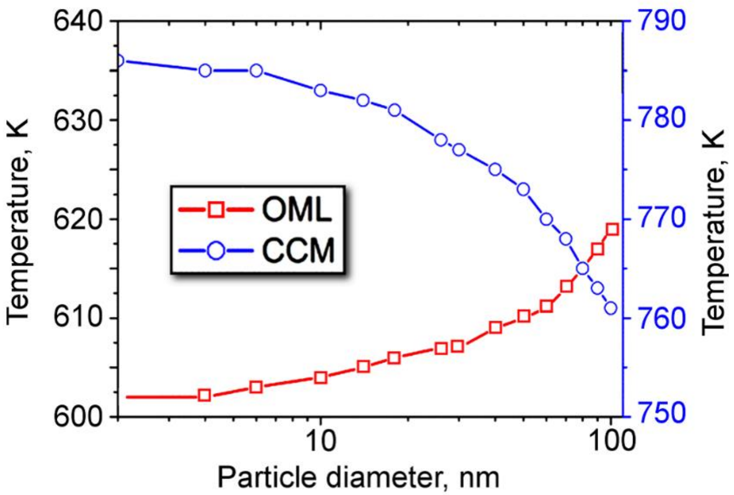

FIG. 4. Particle temperature for a range of nanoparticle diameter according to the two theoretical frameworks, OML, and CCM.

Crystalline Si nanoparticles below crystallization threshold: Effects of collisional heating in non-thermal atmospheric-pressure microplasmas
S. Askari, I. Levchenko, K. Ostrikov, P. Maguire, and D. Mariotti

Citation: Applied Physics Letters **104**, 163103 (2014); doi: 10.1063/1.4872254
View online: http://dx.doi.org/10.1063/1.4872254

pd.maguire@ulster.ac.uk

- Crystallisation
  - ➲Amorphous – crystalline temperature contour
  - ➲Charge flux – size dependent
  - ➲Local surface heating – local melting?
  - ➲Facilitates mass transfer from gas/plasma to solid state

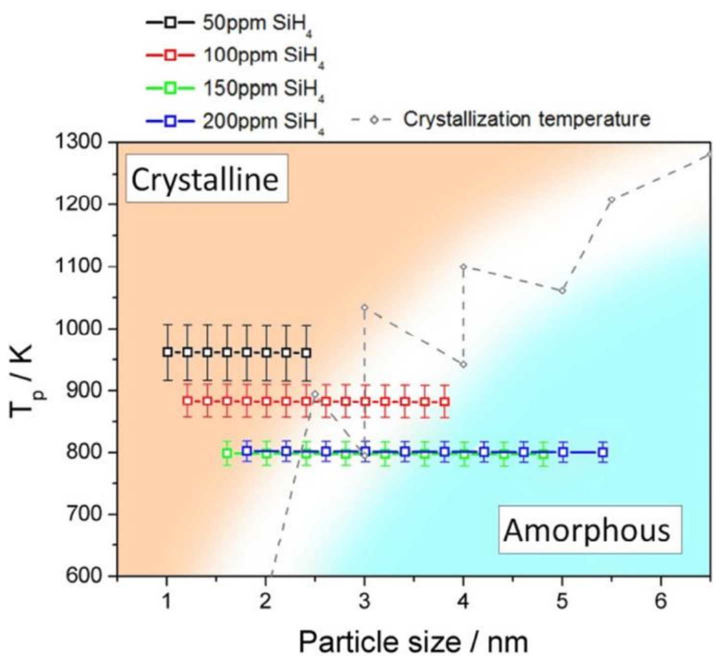

Figure 4. Particle temperature calculated using the collision-corrected model (CCM)

ADVANCED MATERIALS

The Interplay of Quantum Confinement and Hydrogenation in **Amorphous Silicon** Quantum Dots, Askari et al., 2015 10.1002/adma.201503013

- Hot nanoparticles – Cold gas
  - ➲Tailored semiconductor properties
  - ➲Energy bandgap
  - ➲ conduction & Valence band edges

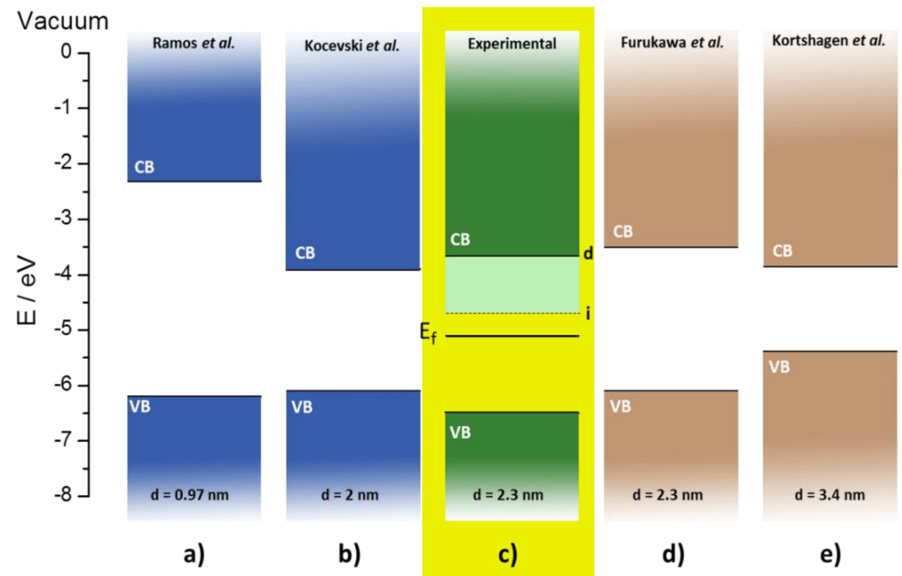

First experimental measurements of conduction band, valence band and fermi-level alignments. Comparison with theoretical predictions

Energy bands diagrams of: a) Ramos *et al.* theoretical calculations of Si quantum dots (QDs) with 85 atoms [26], b) Kocevsky *et al.* theoretical calculations of 2 nm Si QDs [31], c) present experimental measurements of 2.3 nm Si QDs, d) and e) Furukawa *et al.* and Kortshagen *et al.* experimental bandgap with theoretical assignment of bands positions of Si QDs [14,32].

Understanding the depletion of electrons in dusty plasmas at atmospheric pressure
Nabiel H Abuyazid *et al* 2020 *Plasma Sources Sci. Technol.* **29** 075011
Sankaran group

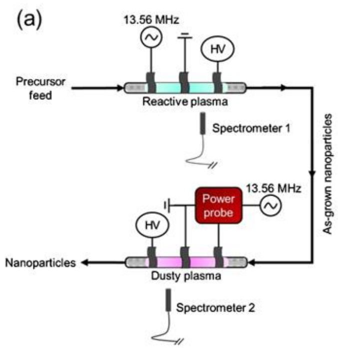

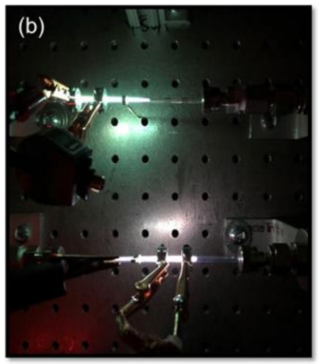

(a) tandem atmospheric-pressure plasma system, and
(b) corresponding image of 'reactive' (top) and 'dusty' (bottom) atmospheric-pressure plasmas during standard particle-containing operation.
(c) Hexane vapour (80ppm) in Ar: C_x NPs (~50nm)

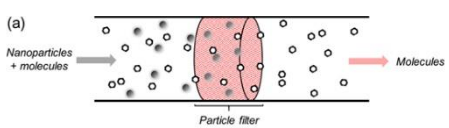

Electron densities measured by power probe for various conditions in the dusty plasma reactor: particle-free (Ar only), nanoparticles (NPs) produced in the reactive plasma, particle-free with inline filter (Ar only), and NPs produced in the reactive plasma with inline filter.

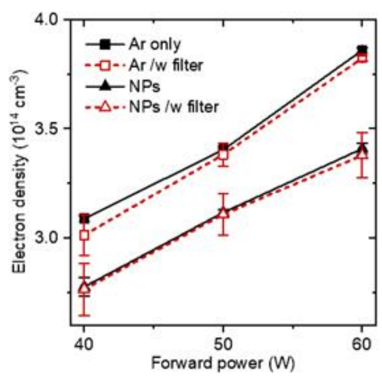

Electron density decrease not due to NPs but to reactions with vapour phase precursor molecules

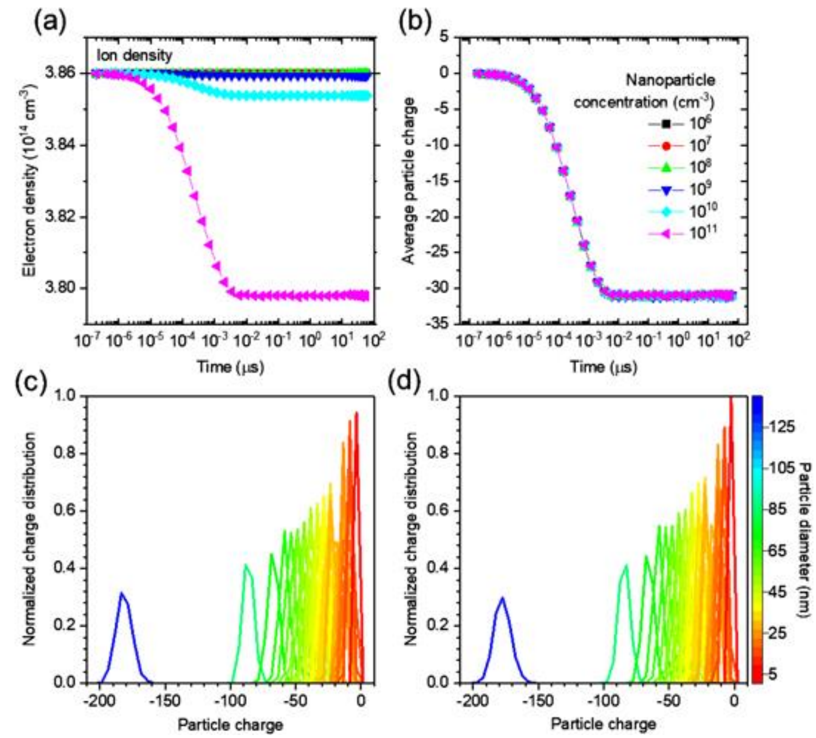

Simulation:
Constant number Monte Carlo
(a) electron density
(b) average NP charge vs residence time for different particle concentrations (measured: 10^6 cm^{-3})
(c) Time-averaged particle charge distribution using measured n_e for particle-free plasma and
(d) using measured n_e for particle-containing plasma.
For measured range of NP diameters

Droplet In Plasma (DiP)

pd.maguire@ulster.ac.uk

- Microscale droplets
  - ➲A stream of microdroplets transported through a low temperature RF plasma.
  - ➲Low gas temperature, “large” size of droplet and short residence means evaporation is incomplete
- Non-thermal equilibrium plasma
  - ➲Gas, ion temperature << electron temperature
  - ➲$T_{gas} \sim T_{ion} << T_e$.
- Plasma - Microdroplets
  - ➲Stream of microdroplets flows through plasma
  - ➲50,000 droplets / sec
  - ➲Exposed to plasma for **~120 μs**
  - ➲Droplet mean velocity **~10 ms^{-1}**

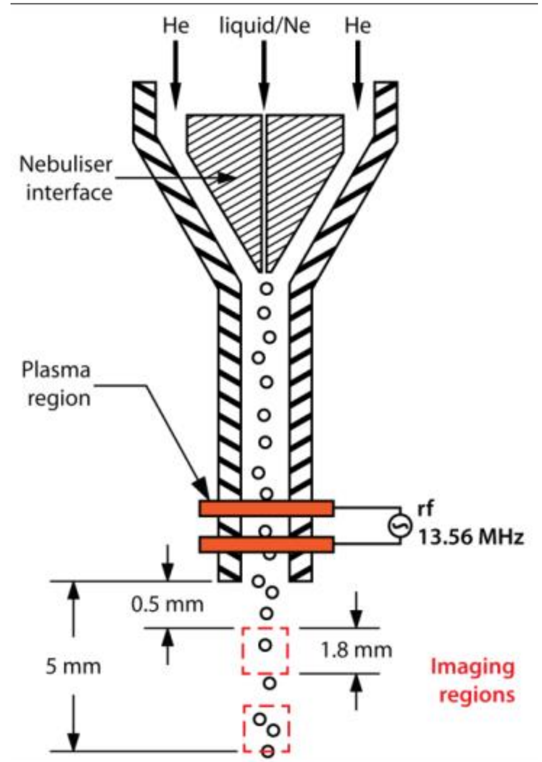

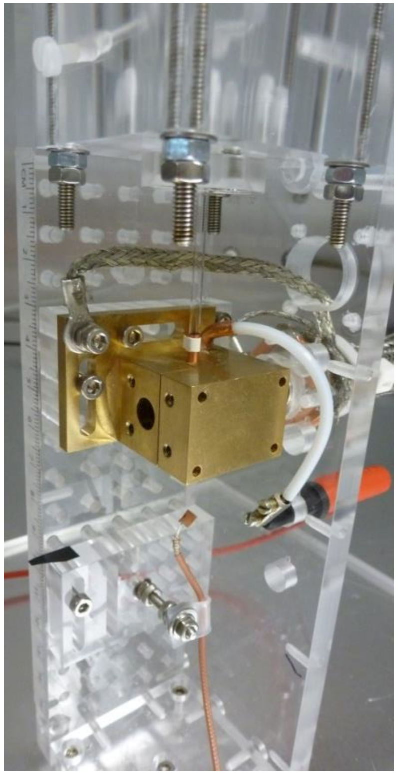

RF 13.56 MHz,
He: 3.5 slm,
Ne (aerosol): 1 slm
or Ar (aerosol): 1 slm

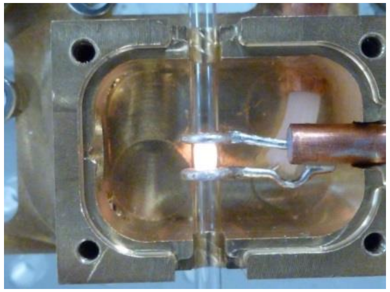

Maguire et al., Appl. Phys. Lett. 106, 224101 (2015);

Liquid metal, metal clusters

pd.maguire@ulster.ac.uk

- Sn nanocrystals:
  - ➲new stable crystal phase
- Plasma interactions
  - ➲Solid Sn metal precursor
  - ➲Atomic “sputtering” or molten droplet (?)
  - ➲High density microplasma ~10^{20} m^{-3}.
  - ➲Cluster formation or liquid metal droplet
  - ➲Solid surface irradiation by charge & radicals
  - ➲Surface temperature elevation
  - ➲Rapid local annealing and quenching

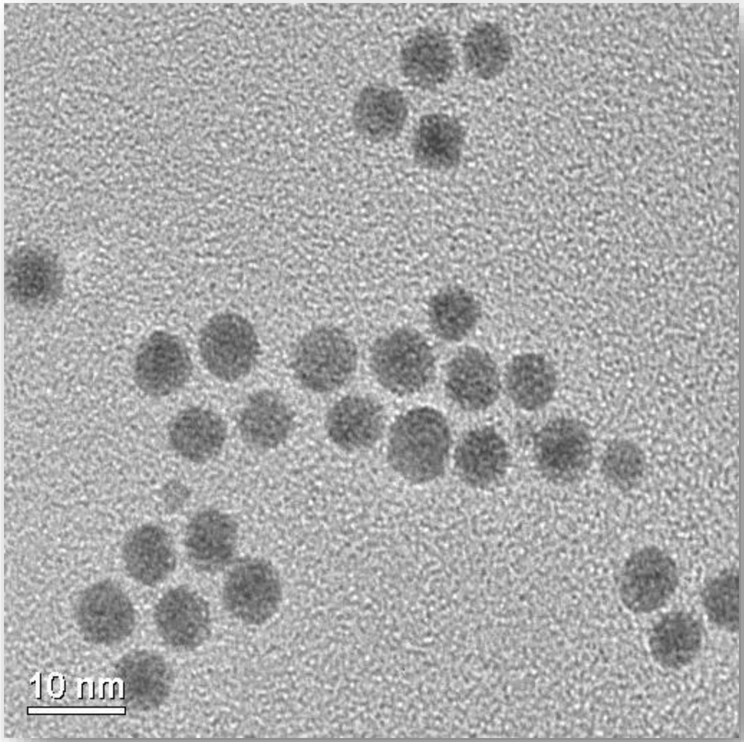

nature COMMUNICATIONS

Haq, A. U. et al Size-dependent stability of ultra-small a-/ß-phase tin nanocrystals synthesized by microplasma. *Nat. Commun.* **2019**, *10* **DOI**:10.1038/s41467-019-08661-9

Applications

Plasma synthesis of nanomaterials

pd.maguire@ulster.ac.uk

- Unique High Value Materials
  - ➲Atmospheric Pressure Plasma Sources
  - ➲Collisional
  - ➲Non-thermal equilibrium
- Multiple Phases
  - ➲Gas-phase synthesis
  - ➲Plasma – cluster
  - ➲Plasma – molten solid - solid
  - ➲Plasma-bulk liquid
  - ➲Plasma-droplet (low evaporation)
  - ➲H2O, ethanol, hydrocarbons, monomers

ACS APPLIED MATERIALS & INTERFACES

Microplasma Processed Ultrathin Boron Nitride Nanosheets for Polymer Nanocomposites with Enhanced Thermal Transport Performance

Ri-Chao Zhang†‡§, Dan Sun‡, Ai Lu‡, Sadegh Askari§, Manuel Macias-Montero§, Paul Joseph#, Dorian Dixon§, Kostya Ostrikov¶⊥, Paul Maguire§, and Davide Mariotti§
† Department of Chemical and Biological Engineering, Zhejiang University, Hangzhou, 310002, PR China
‡ School of Mechanical and Aerospace Engineering, Queen's University Belfast, BT9 5AH, U.K.
§ Nanotechnology and Integrated Bioengineering Centre (NIBEC), University of Ulster, Newtownabbey, BT37 0QB, Northern Ireland, U.K.
∥ Institute of Chemical Materials, China Academy of Engineering Physics, Mianyang 621900, Sichuan People's Republic of China
⊥ Department of Physics, Chemistry and Biology (IFM)/Plasma and Coatings Physics (PLASM), Linköping University, 581 83 Linköping, Sweden
Centre for Environmental Safety and Risk Engineering (CESARE), College of Engineering and Science, Victoria University, Room 4206, Level 2, Building 4 Hoppers Lane, Werribee Campus Victoria 3030, Melbourne, Australia
¶ School of Chemistry, Physics, and Mechanical Engineering, Queensland University of Technology, Brisbane, Queensland 4000, Australia
▲ Joint CSIRO-QUT Sustainable Materials and Devices Laboratory, CSIRO, P.O. Box 218, Lindfield, New South Wales 2070, Australia

ACS Appl. Mater. Interfaces, 2016, 8 (21), pp 13567–13572
DOI: 10.1021/acsami.6b01531
Cite this: ACS Appl. Mater. Interfaces 8, 21, 13567-13572

PLASMA PROCESSES AND POLYMERS

Feature Article

Plasma–Liquid Interactions at Atmospheric Pressure for Nanomaterials Synthesis and Surface Engineering

Davide Mariotti, Jenish Patel, Vladimír Švrček, Paul Maguire

First published: 06 August 2012 | https://doi.org/10.1002/ppap.201200007 | Cited by: 81

Nano Energy

Volume 50, August 2018, Pages 245-255
https://doi.org/10.1016/j.nanoen.2018.05.036

Full paper

Type-I alignment in $MAPbI_3$ based solar devices with doped-silicon nanocrystals

Conor Rocks[a], Vladimir Svrcek[b], Tamilselvan Velusamy[a], Manuel Macias-Montero[a], Paul Maguire[a], Davide Mariotti[a]

SCIENTIFIC REPORTS

Article | OPEN | Published: 26 October 2015

Enhanced Dispersion of TiO_2 Nanoparticles in a TiO_2/PEDOT:PSS Hybrid Nanocomposite via Plasma-Liquid Interactions

Yazi Liu, Dan Sun, Sadegh Askari, Jenish Patel, Manuel Macias-Montero, Somak Mitra, Richao Zhang, Wen-Feng Lin, Davide Mariotti & Paul Maguire

Scientific Reports 5, Article number: 15765 (2015) | Download Citation

Microplasma-assisted electrochemical synthesis of Co_3O_4 nanoparticles in absolute ethanol for energy applications

Chengsheng Ni,*abc Darragh Carolan,a Conor Rocks,a Jianing Hui,b Zeguo Fang,b Dilli Babu Padmanaban,a Jiupai Ni,c Deti Xie,c Paul Maguire,a John T. S. Irvineb and Davide Mariottia

NANO LETTERS

Continuous In-Flight Synthesis for On-Demand Delivery of Ligand-Free Colloidal Gold Nanoparticles

Paul Maguire†, David Rutherford†, Manuel Macias-Montero†, Charles Mahony†, Colin Kelsey†, Mark Tweedie†, Fátima Pérez-Martin†, Harold McQuaid†, Declan Diver‡, and Davide Mariotti†
† NIBEC, University of Ulster, Belfast, BT37 0QB, Northern Ireland
‡ SUPA, School of Physics and Astronomy, University of Glasgow, Glasgow G12 8QQ, United Kingdom

Nano Lett., 2017, 17 (3), pp 1336–1343
DOI: 10.1021/acs.nanolett.6b03440
Cite this: Nano Lett. 17, 3, 1336-1343

ADVANCED MATERIALS

Communication | Open Access

The Interplay of Quantum Confinement and Hydrogenation in Amorphous Silicon Quantum Dots

Sadegh Askari, Vladimir Svrcek, Paul Maguire, Davide Mariotti

First published: 02 November 2015 | https://doi.org/10.1002/adma.201503013 | Cited by: 12

nature COMMUNICATIONS

Article | OPEN | Published: 01 August 2017

Charge carrier localised in zero-dimensional $(CH_3NH_3)_3Bi_2I_9$ clusters

Chengsheng Ni, Gordon Hedley, Julia Payne, Vladimir Svrcek, Calum McDonald, Lethy Krishnan Jagadamma, Paul Edwards, Robert Martin, Gunisha Jain, Darragh Carolan, Davide Mariotti, Paul Maguire, Ifor Samuel & John Irvine

ROYAL SOCIETY OF CHEMISTRY

DOI: 10.1039/C7SE00158D (Paper) Sustainable Energy Fuels, 2017, 1, 1611-1619

Environmentally friendly nitrogen-doped carbon quantum dots for next generation solar cells†

Darragh Carolan*a, Conor Rocks a, Dilli Babu Padmanaban a, Paul Maguire a, Vladimir Svrcek b and Davide Mariotti a
a Nanotechnology & Integrated Bio-Engineering Centre (NIBEC), Ulster University, Jordanstown, Newtownabbey, Co. Antrim BT37 0QB, UK. E-mail: d.carolan@ulster.ac.uk
b Research Centre of Photovoltaics, National Institute of Advanced Industrial Science and Technology-AIST, Central 2, Tsukuba, Japan

Applications of nanomaterials

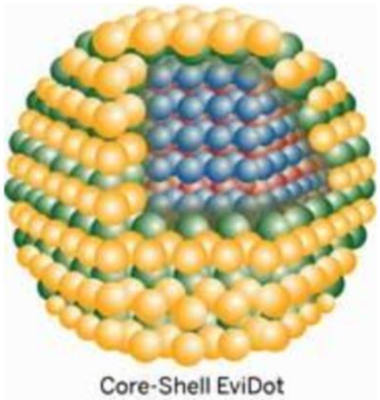

- Nanocrystals
- 2-10 nm diameter
- semiconductors

Melting point

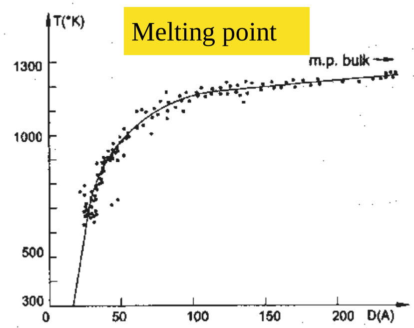

Strength of nanophase copper as a function of grain size

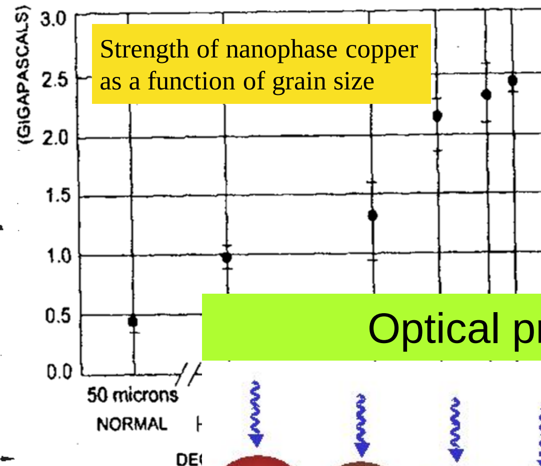

Optical properties v size

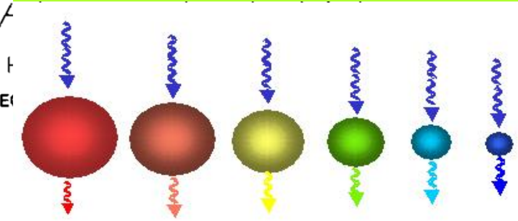

Nanocrystals absorb light then re-emit the light in a different color – the size of the nanocrystal (at the Angstrom scale) determines the color

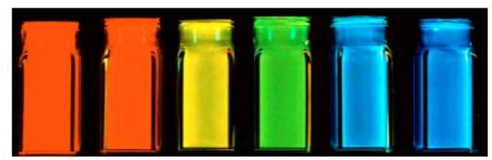

Six different quantum dot solutions are shown excited with a long wave UV lamp

Optical, electrical and chemical for biomedical

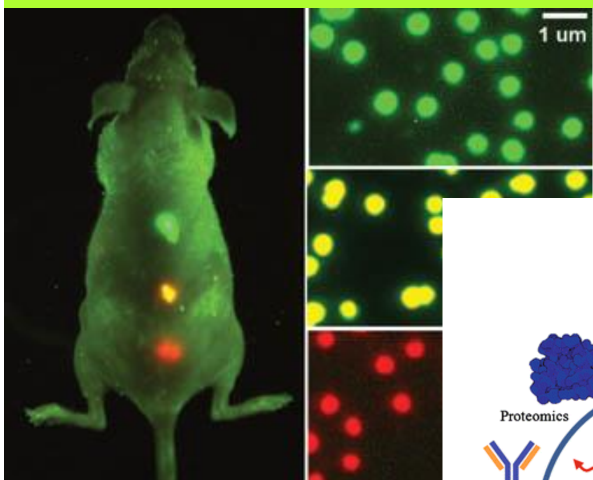

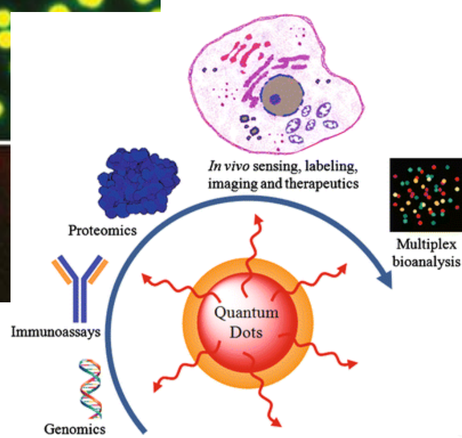

Optical and electrical for solar cells

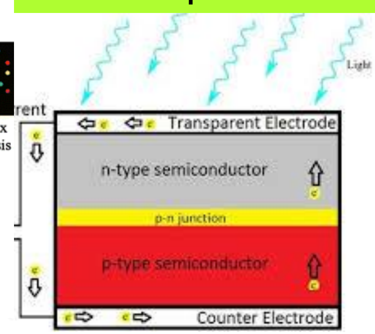

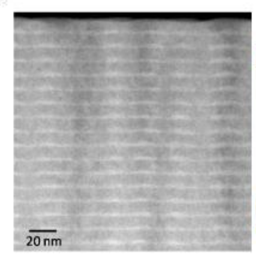

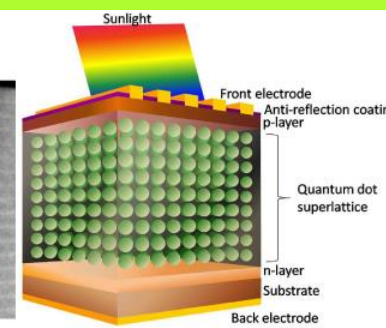

- Gold nanoparticles
  - ➲First discovered by Faraday
  - ➲Still being researched

ACS Publications
Most Trusted. Most Cited. Most Read.

Search Results

Search

gold nanoparticles

Results: 1 – 20 of 6990 Filter(s) Applied:

2014 - 2016 ×

SECTION	
Biochemical Methods	1004
Pharmaceuticals	881
Surface Chemistry And Colloids	814
Optical, Electron, And Mass Spectroscopy And Other Related Properties	760
Electrochemical, Radiational, And Thermal Energy Technology	437
Electric Phenomena	247
Radiation Chemistry, Photochemistry, And Photographic And Other Reprographic Processes	210
Electrochemistry	196
Catalysis, Reaction Kinetics, And Inorganic Reaction Mechanisms	152
Plastics Manufacture And Processing	111

PUBLICATION	
ACS Applied Materials & Interfaces	1125
The Journal Of Physical Chemistry C	1018
ACS Nano	705
Analytical Chemistry	592
Langmuir	562
Nano Letters	431
Journal Of The American Chemical Society	351
Chemical Reviews	214
Chemistry Of Materials	191
ACS Catalysis	176

Water microdroplet containing metal salt

pd.maguire@ulster.ac.uk

- Solids formed in liquids in gas/plasma

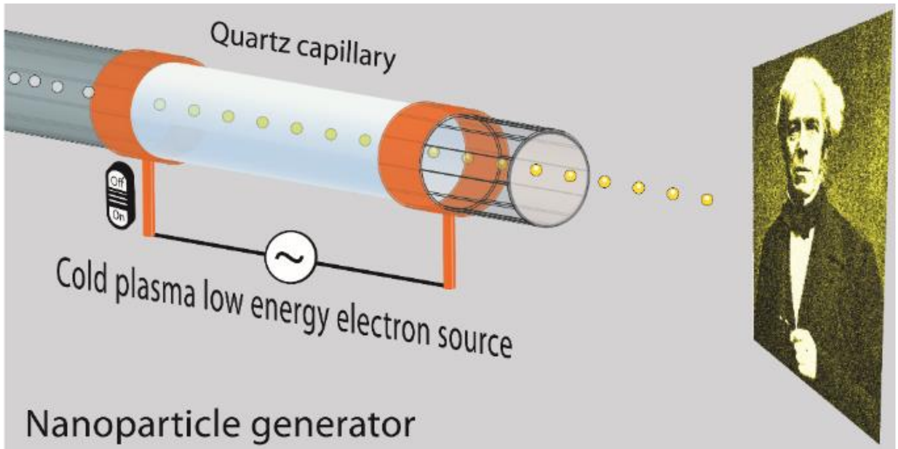

- Nanoparticles: on demand delivery
  - ➲$HAuCl_4$ in H_2O microdroplet
  - ➲Passed through plasma
  - ➲120 us time of flight
- Electron flux
  - ➲Direct reduction of Au^{3+} ions in liquid by solvated electrons from plasma

NANO LETTERS

Continuous In-Flight Synthesis for On-Demand Delivery of Ligand-Free Colloidal Gold Nanoparticles, Maguire et al., 2017, 10.1021/acs.nanolett.6b03440

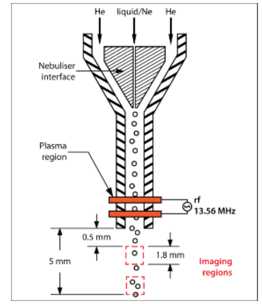

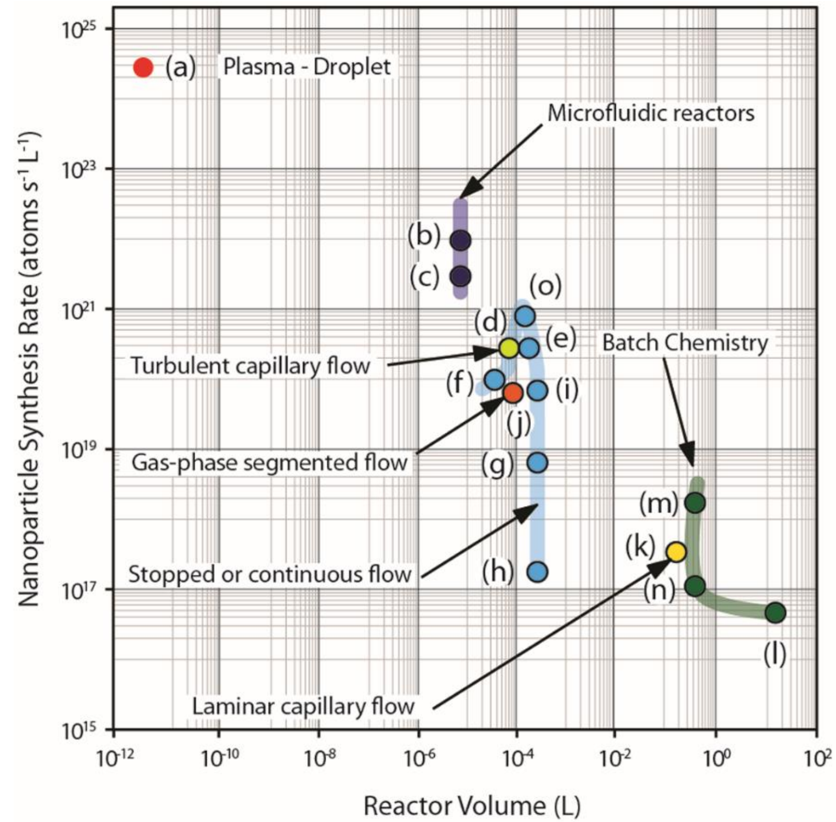

Comparison of plasma – droplet synthesis rate with batch and microreaction chemistry

- X $10^3 - 10^7$ faster
  - ➲**Similar dose rate as gamma radiation**
- Plasma-droplet
  - ➲Dose rate assuming **x%** plasma energy delivered to drop
  - ➲5×10^{-2} kGy s^{-1}.

$HAuCl_4$. The reduction of **Au^{III}** proceeds via reactions as:

II	$Au^{III}Cl_4^- + e_{aq}^- \rightarrow Au^{II}Cl_4^{2-}$	(R1)
III / I	$2\ Au^{II}Cl_4^{2-} \rightarrow Au^{III}Cl_4^- + Au^{I}Cl_2^- + 2Cl^-$	(R2a)
0	$\mathbf{Au^{I}Cl_2^- + e_{aq}^- \rightarrow Au^{0}Cl_2^{2-}}$	**(R3)**
I / II	$Au^{III} + Au^{0} \rightarrow Au^{I}$ and Au^{II}	(R4)

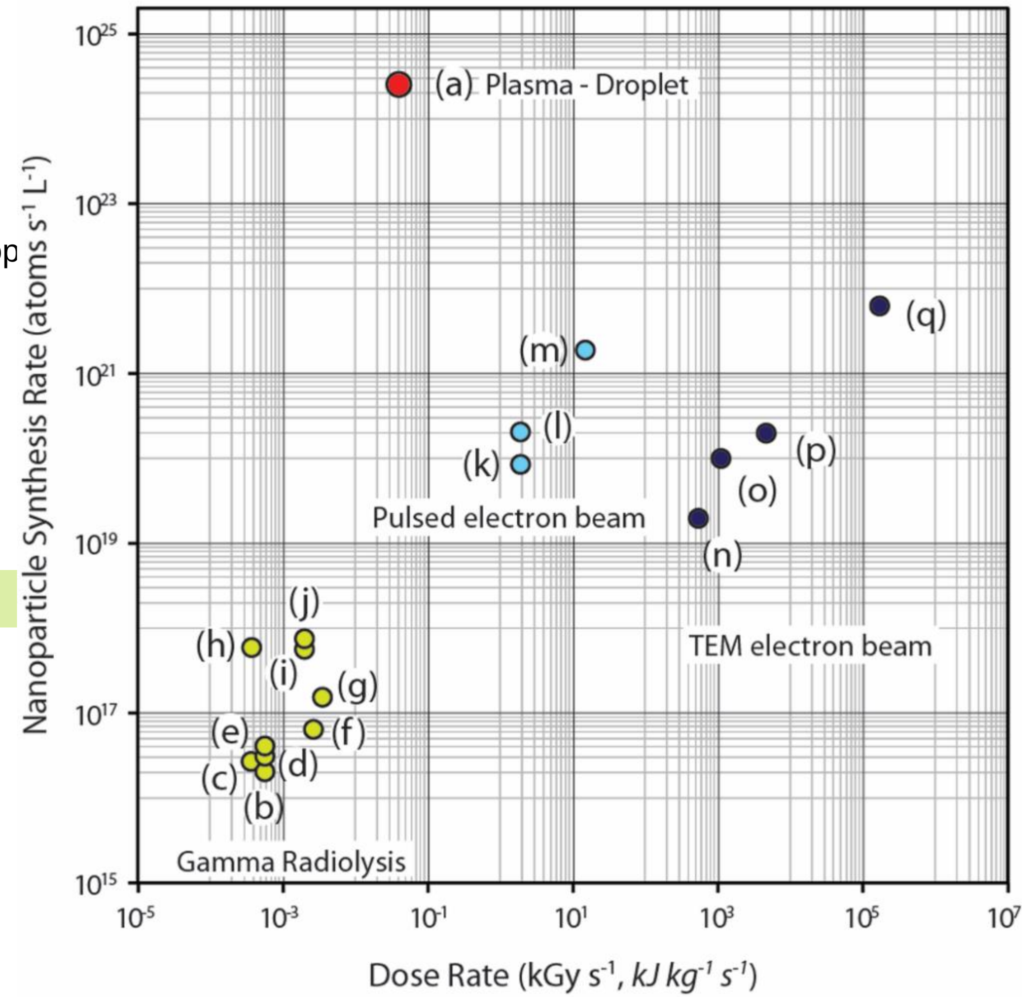

Comparison of plasma – droplet synthesis rate with high energy radiolysis or electron beam methods

Maguire et al., 2017, 10.1021/acs.nanolett.6b03440

Wound healing

Cancer treatment

Plasma Medicine

Plasma Medicine

Commercial medical plasma systems

pd.maguire@ulster.ac.uk

- kINPen MED

- SteriPlas

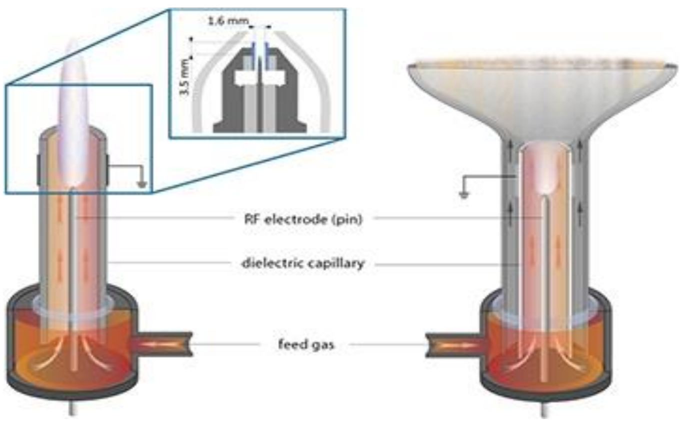

Left: pen, **right**: large-area treatment principle.
Inset: the kINPen head with gas curtain device

The kINPen—a review on physics and chemistry of the atmospheric pressure plasma jet and its applications
Stephan Reuter *et al* 2018 *J. Phys. D: Appl. Phys.* **51** 233001

Direct-contact plasmas

pd.maguire@ulster.ac.uk

- Direct-contact
  - ➲The plasma is in contact with tissue that is “far away” from the power source.
  - ➲Plasma species include radicals, UV, charge, ions
  - ➲Plasma species are continuously generated along the path.
- Maintains high concentration of active species “far away” at tissue.
- Issues
  - ➲Plasma still needs to be quite close
  - ➲Plasma very sensitive to local environment
  - ➲**Medical approval**: Gas temperature, UV exposure, ozone, current, electric fields – need to be continuously measured and certifiably controlled. **Difficult**.
  - ➲Less accessible treatment sites - problematic

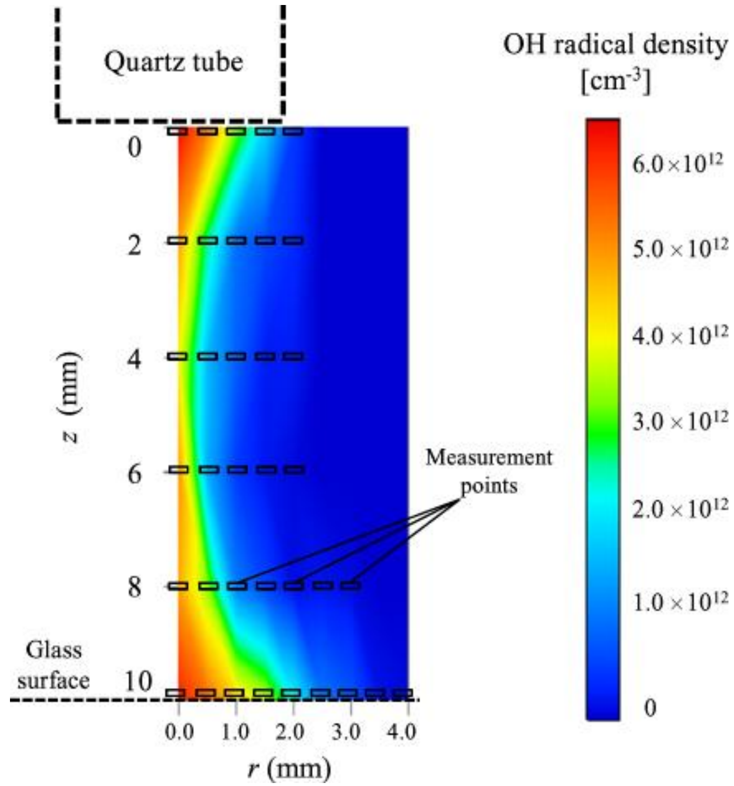

Yonemori, S. et al., *J. Phys. D* **2014**, *47*, 125401.

Plasma Activated Liquids (PAL)

pd.maguire@ulster.ac.uk

- PAL
  - ➲Also known as PAM
  - ➲Plasma treats liquid
  - ➲Liquid stored for use as chemotherapy agent
  - ➲Cocktail of short-, medium-, long-lived ROS, RNS radicals
- Effectiveness unclear
- Very sensitive to shelf-life
  - ➲(< seconds?)
- Droplet in Plasma system
  - ➲Delivers PAL in droplet stream
  - ➲Delivery time < milliseconds
  - ➲Distance > 200 mm

Options?

During open surgery

Minimally invasive techniques

Endoscopy: flexible tubing

Long metal needle

Injection – Plasma Activated Liquids

Plasma Treatment Inside the Body?

pd.maguire@ulster.ac.uk

- Prostate Biopsy
  - ➲Can we integrate with plasma device?

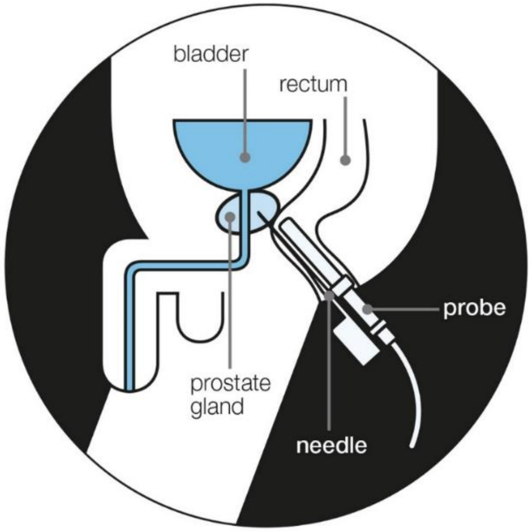

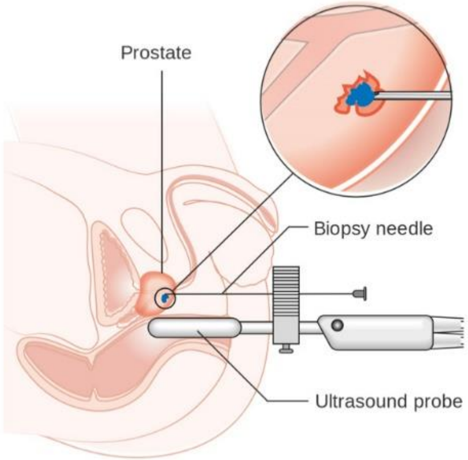

- Endoscope
  - ➲Can we integrate with plasma device?

Plasma Endoscopy

pd.maguire@ulster.ac.uk

- Plasma Endoscope

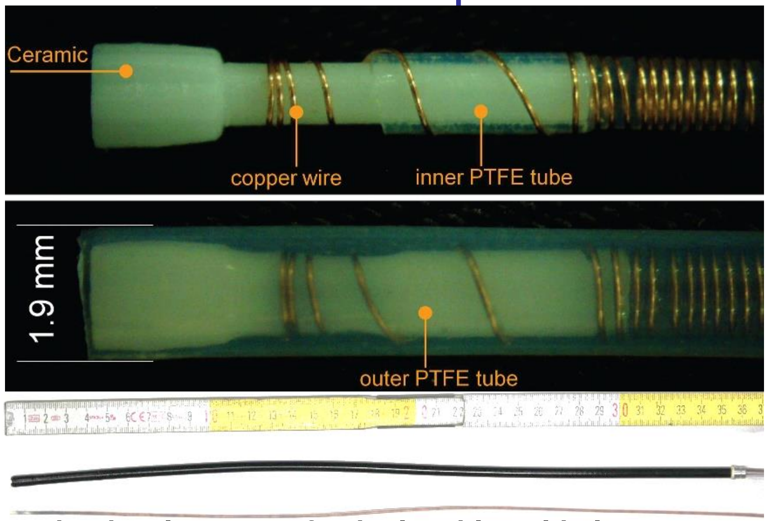

On the development of a deployable cold plasma endoscope, Jörn Winter et al., Contrib. Plasma Phys. (2018) https://doi.org/10.1002/ctpp.201700127

- Remote plasma
  - ➲Plasma generated at end of long tube
- Challenges
  - ➲High voltages inside the body – can they be isolated?
  - ➲Possible high temperature arcs
  - ➲Jet operation in cavities
  - ➲Unwanted tube & parasitic discharges
  - ➲Tube erosion

- Plasma Gun

Perspectives of endoscopic plasma applications, E. Robert, et.al, Clinical Plasma Medicine,**1** (2013) 8 -16

A flexible cold microplasma jet using biocompatible dielectric tubes for cancer therapy, Kim ey al**,** Appl. Phys. Lett. **96**, 203701 (2010); https://doi.org/10.1063/1.3431392

Long, biocompatible and highly flexible cold atmospheric microplasma jet device for precise endoscopic therapies, Tao Wang et al., 2018 IEEE Micro Electro Mechanical Systems (MEMS)

Flexible cold plasma jet with controllable length and temperature for hydrophilic modification, Geng et al, Physics of Plasmas **25**, 083508 (2018); https://doi.org/10.1063/1.5040331

Microdroplet OH

pd.maguire@ulster.ac.uk

- Significant increase in OH delivered using microdroplets

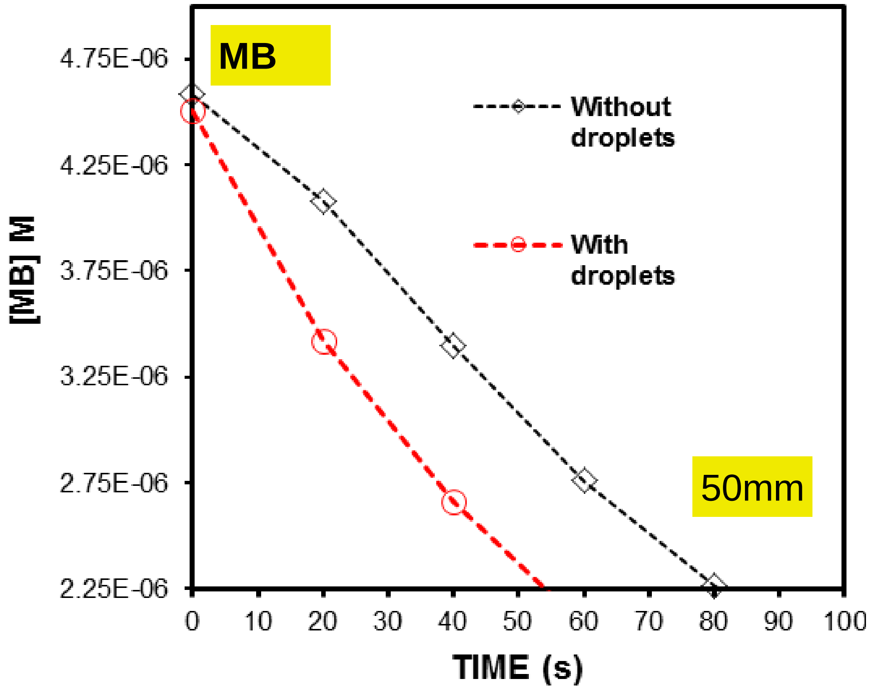

E coli interaction

pd.maguire@ulster.ac.uk

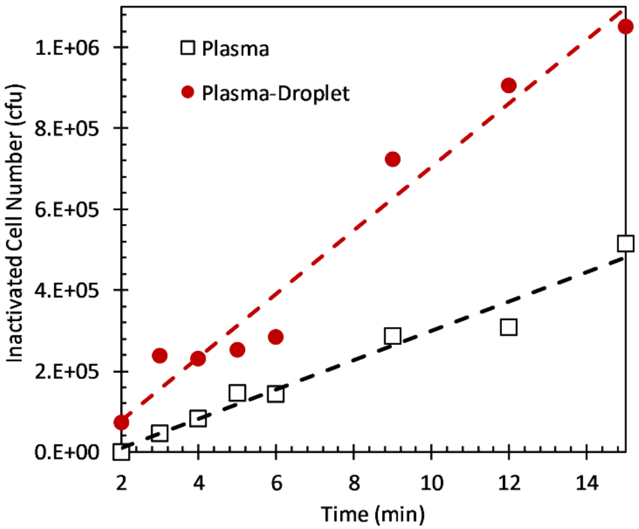

No of cells inactivated versus PE and PED exposure time at a fixed distance of 4.3 cm, calculated from ZoI diameter assuming ~4000 cfu mm^{-2}.

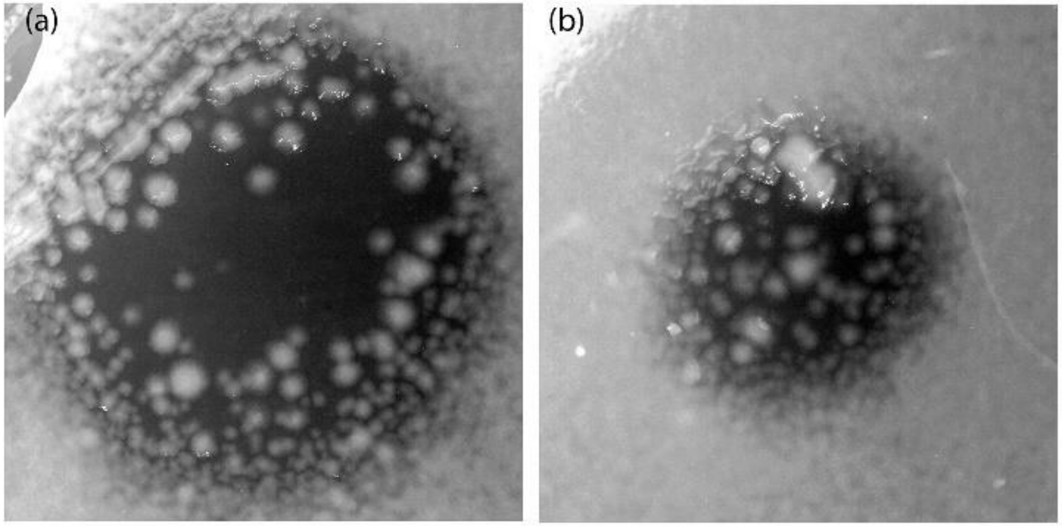

E coli growth inhibition zone (ZoI) at a distance of 40 mm from plasma, after 3 min exposure to
(a) plasma effluent with **droplets** and
(b) plasma effluent

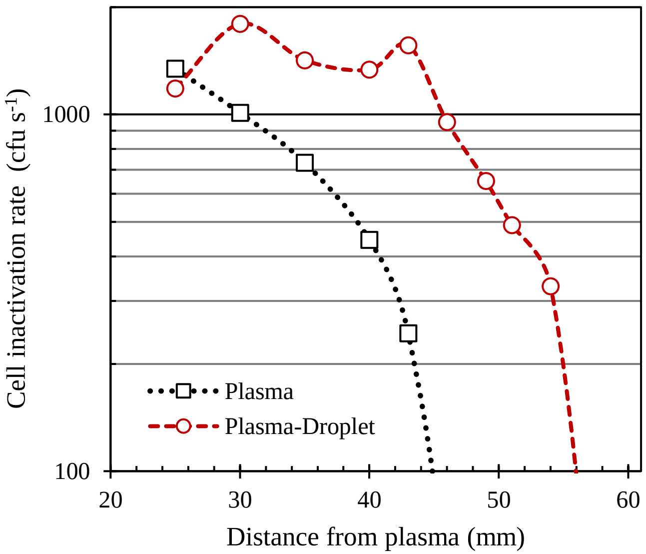

Increased efficacy in killing E coli with distance using droplets

Droplet in Plasma (DiP)

pd.maguire@ulster.ac.uk

Droplet In Plasma (DiP)

- Microscale droplets
  - ➲A stream of microdroplets transported through a low temperature RF plasma.
  - ➲Low gas temperature, “large” size of droplet and short residence means evaporation is incomplete
- Non-thermal equilibrium plasma
  - ➲Gas, ion temperature << electron temperature
  - ➲$T_{gas} \sim T_{ion} << T_e$.
- Plasma - Microdroplets
  - ➲Stream of microdroplets flows through plasma
  - ➲50,000 droplets / sec
  - ➲Exposed to plasma for **~120 μs**
  - ➲Droplet mean velocity **~10 ms^{-1}**

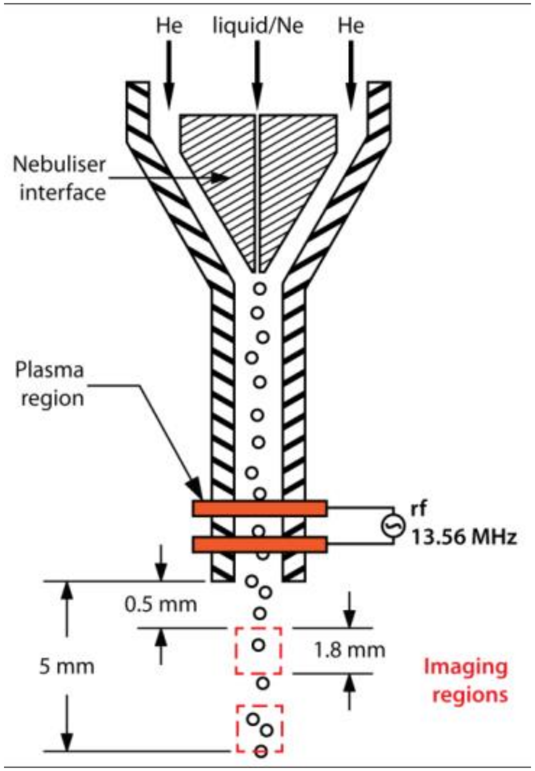

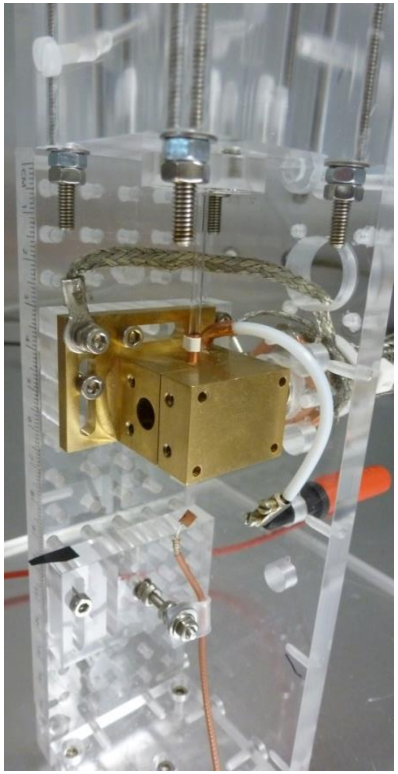

RF 13.56 MHz,
He: 3.5 slm,
Ne (aerosol): 1 slm
or Ar (aerosol): 1 slm

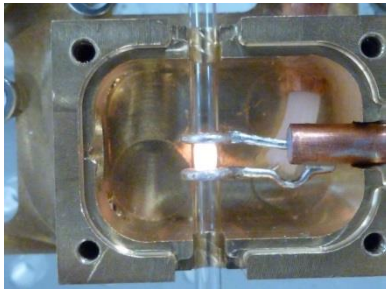

Maguire et al., Appl. Phys. Lett. 106, 224101 (2015);

- OH maximum
  - ➲Net input power decreases > 500ppm, as plasma becomes electronegative
  - ➲Power density (emission brightness) decreases at slower rate

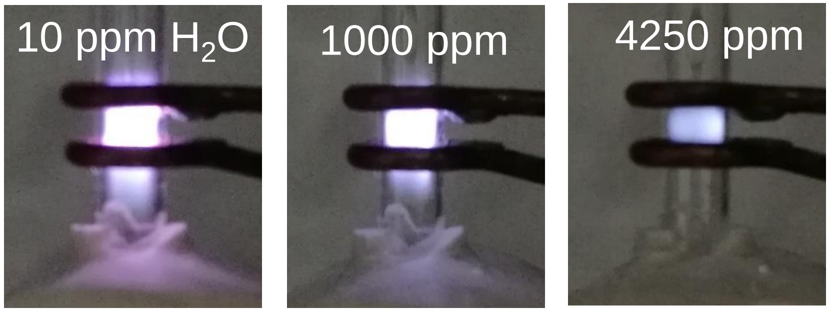

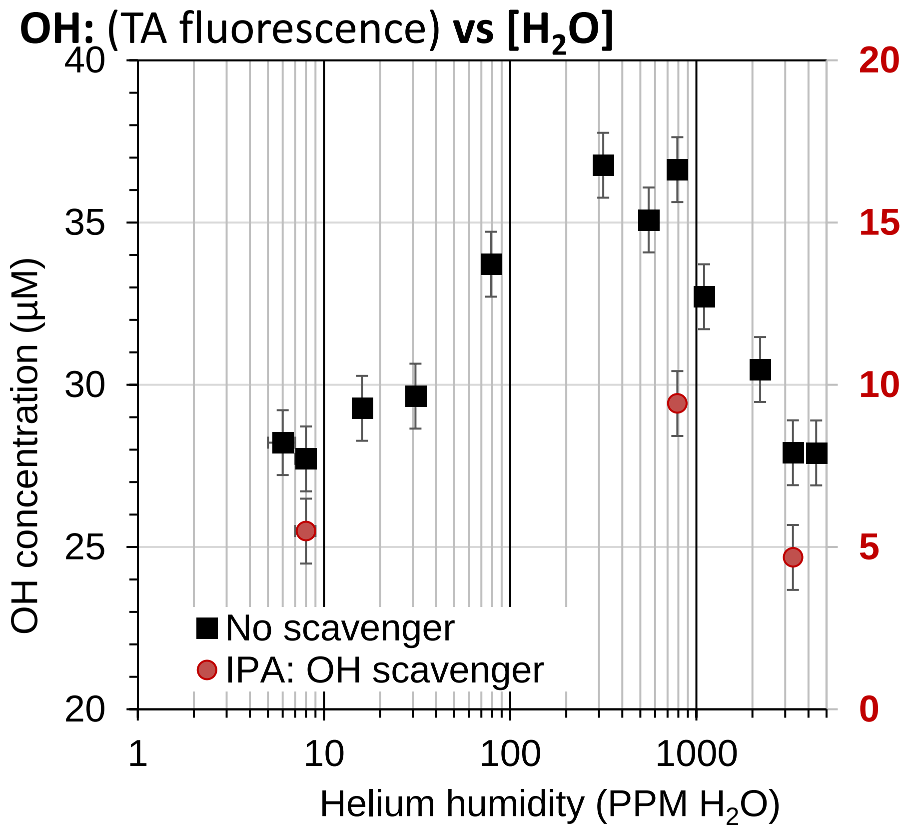

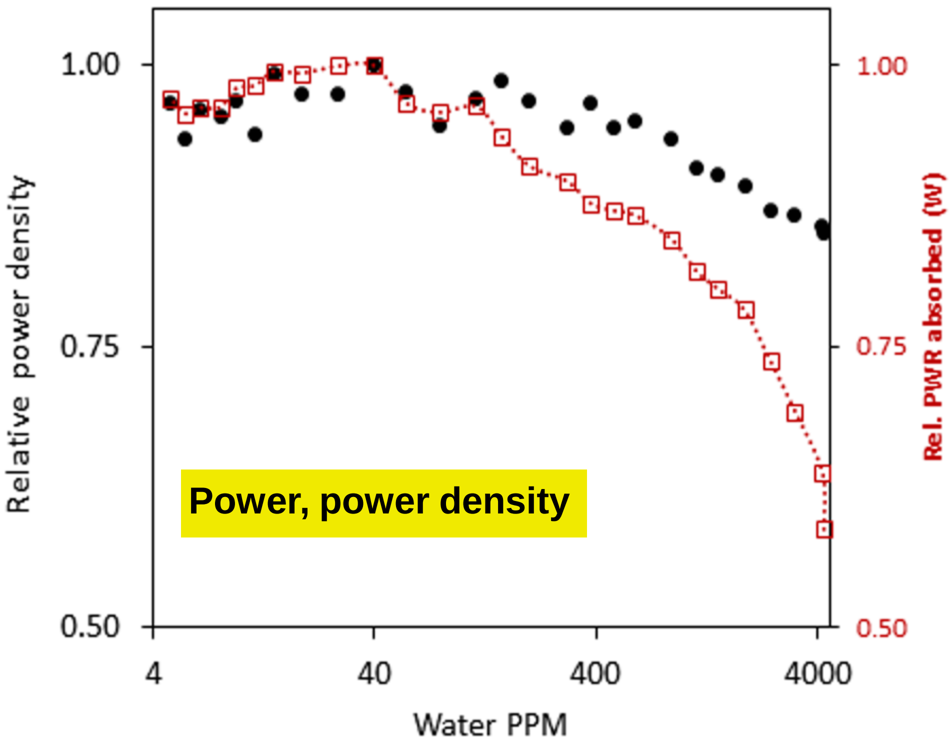

Basic conditions

pd.maguire@ulster.ac.uk

RF 13.56MHz
n_e: 10^{12} – 10^{14} cm^{-3}.
Reactor diameter: 2mm

HeNe plasma (5:1)
Laminar axial flow
~10^4 droplets per second
Residence time in plasma: ~100μs
Droplet diameter average: 15 μm

High speed imaging

~ 5 droplets in plasma region at any instant

He^0
He*
Ne^0
neutrals

He^+
Ne^+
ions

e^- e^- e^- e^- e^- e^- e^-

Droplet

Gas velocity ~10 ms^{-1}.

Water dissociation
$H_xO_y^+$
$O_xH_y^-$

Plasma region

Droplet Size and Velocity Distributions

pd.maguire@ulster.ac.uk

- Evaporation
  - ➲H2O production rate, delivered into plasma
- Droplet Size Distribution
  - ➲Obtained from imaging in flight
  - ➲15um (CMD), no plasma

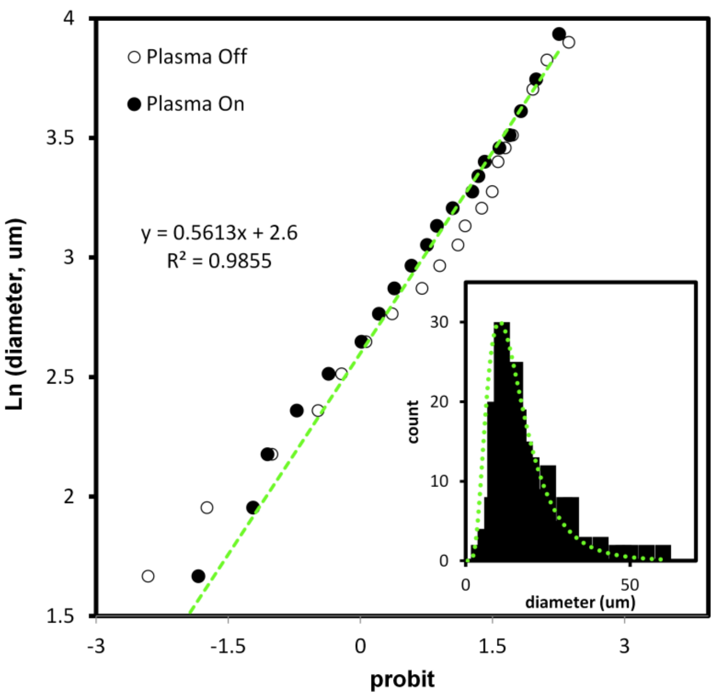

- Velocity Distribution
  - ➲V(r) measured by imaging (but outside tube)
  - ➲Drop travelling at 75% velocity of gas
  - ➲Is this true inside tube?
- Stokes Flow regime
  - ➲Determines whether convection or diffusion carries H2O away from droplet into plasma

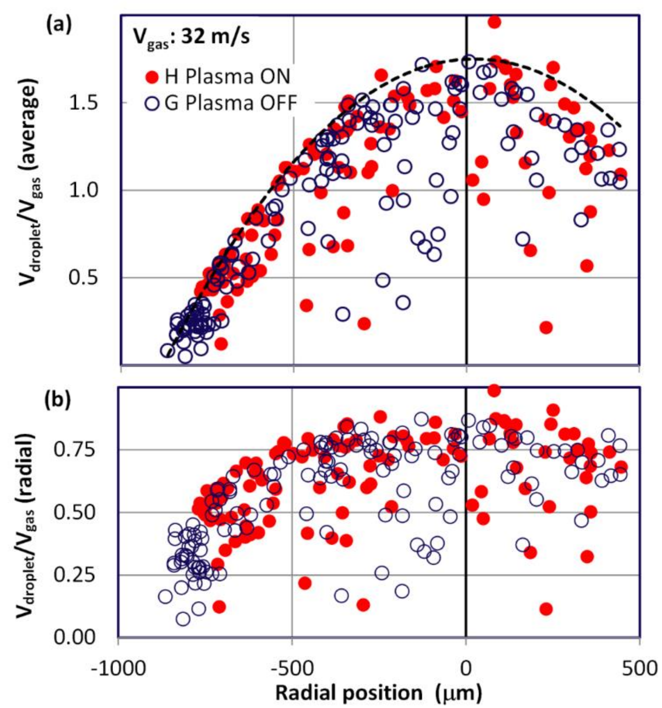

Evaporation

pd.maguire@ulster.ac.uk

RF 13.56MHz
n_e: $10^{12} – 10^{14}$ cm^{-3}.

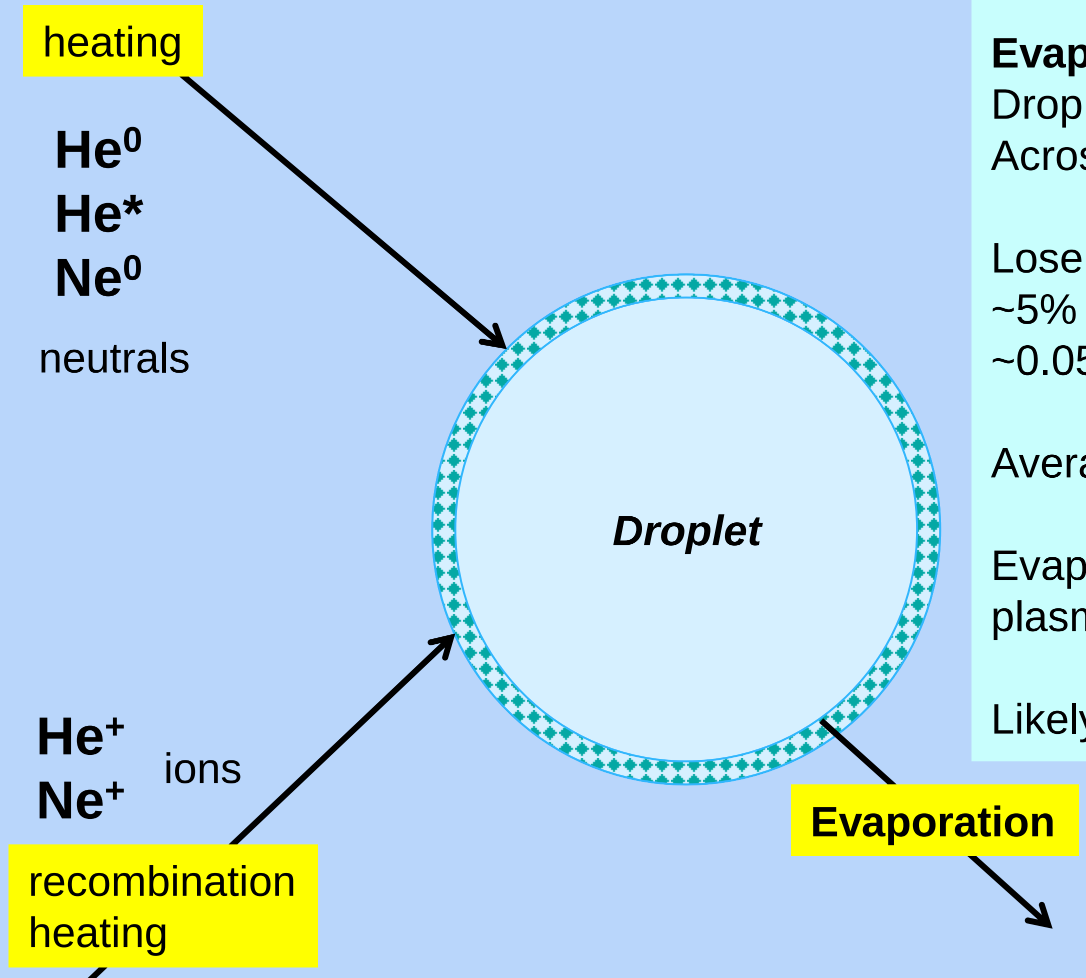

Evaporation
Droplet 15μm (CMD) → 13μm (CMD)

Evaporation ~ D^2
Droplet loss by evaporation
Across lognormal distribution

Lose smaller droplets <4um
~5% of the total droplet number and
~0.05% of the total liquid flow

Average Evaporation rate: 5×10^{-8} m^2 s^{-1}.

Evaporated vapour per drop: → **<100ppm** in plasma vol. $10^{-8} m^3$.

Likely vapour density is higher close to droplet

pd.maguire@ulster.ac.uk

RF 13.56MHz
n_e: 10^{12} – 10^{14} cm^{-3}.

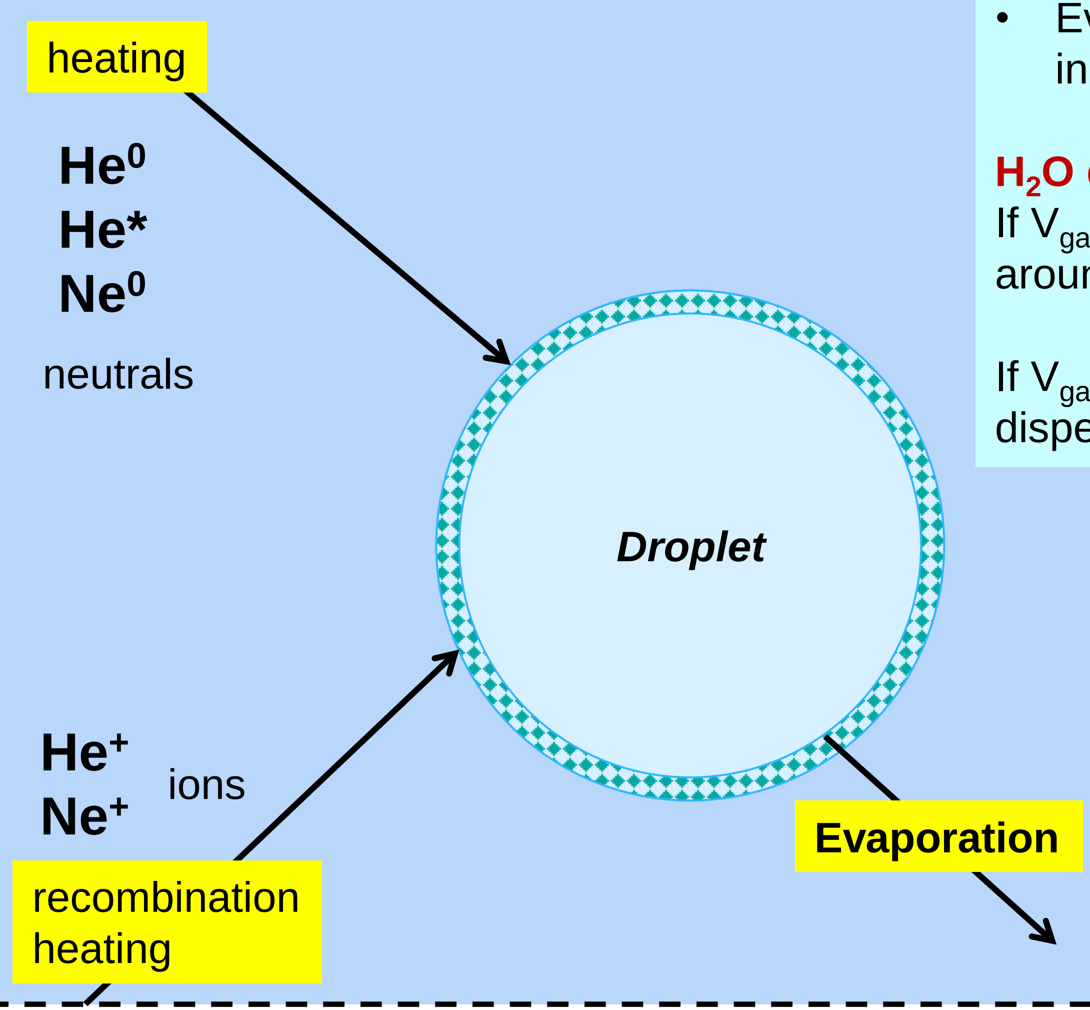

Evaporation

- Average Evaporation rate: 5 x 10^{-8} m^2 s^{-1}.
- Evaporated vapour per drop: → **<100ppm** in plasma vol. $10^{-8}m^3$.

H_2O distribution:

If V_{gas} ~ $V_{droplet}$: high density vapour halo around droplet. ~40,000 ppm H_2O.

If V_{gas} >> $V_{droplet}$: evaporated vapour will disperse → uniform humidity

Plasma region

Droplet/gas velocity ratio **inside** the plasma

pd.maguire@ulster.ac.uk

- Peak **gas** velocity at plasma entrance is 34 m s^{-1}
- Stoke's flow condition ($v_{drop}/v_g(r) > 0.95$)
- Droplet acceleration from nebuliser to plasma
- From literature: Nebuliser output velocity
  - $\mathbf{v_{gas}}$ >1000 m s^{-1}.
  - $\mathbf{v_{droplet}}$ > 25 m s^{-1} within a few millimetres
- The acceleration of a falling droplet, with local gas speed $v_g(r)$ is given by

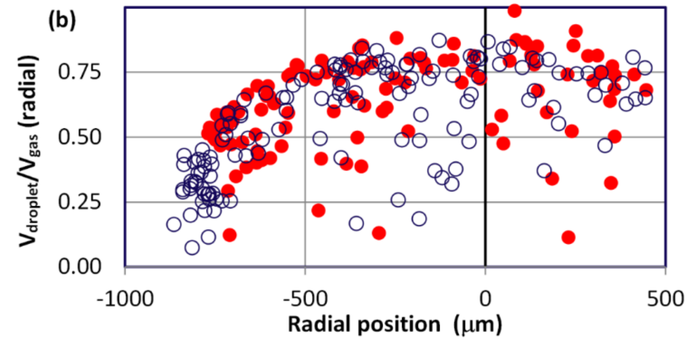

$$\frac{dv_d}{dt} = g + \frac{3\rho_g C_{Dr.}}{4\rho_d D} v_g^2(r)\left(1 - \frac{v_d}{v_g(r)}\right)$$

g is acceleration due to gravity, r is the radial distance, ρ_g and ρ_d are gas and droplet density respectively and C_{Dr} is the drag coefficient of a sphere.

Fraction nebuliser – plasma distance required to reach the Stoke's flow condition

- Depends on initial velocity (v_o) at nebuliser.
  - Diameter 20 μm: $v_o/v_g > 0.1$,
  - 20 μm < D < 30 μm: $v_o/v_g > 0.8$
- Across the velocity range, this accounts for ~75% of evaporated vapour

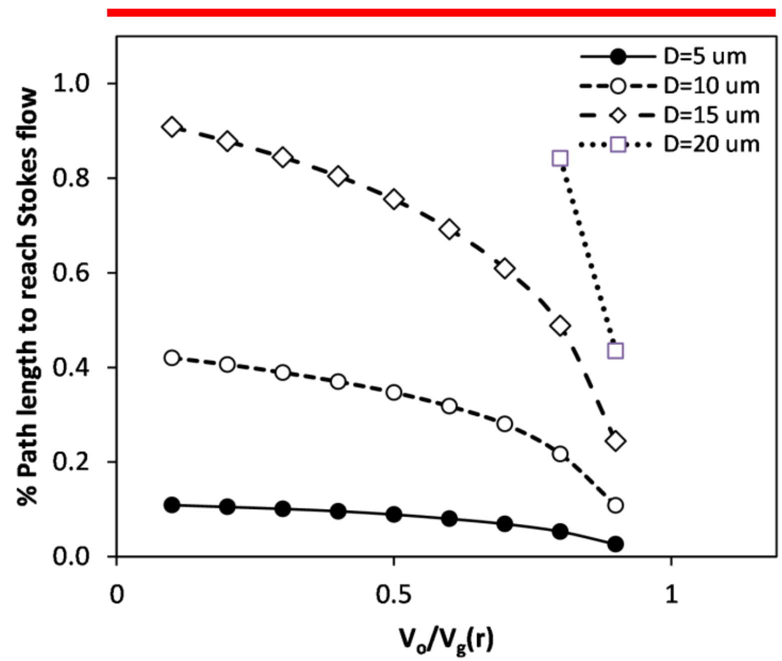

Figure 6. Fraction of path length between nebuliser and plasma (50 mm) required for droplet to reach Stokes flow condition, for various initial velocities, v_o, and diameters.

Evaporation and humidity

pd.maguire@ulster.ac.uk

- Humidity effect on plasma
  - ➲With added H_2O,
  - ➲electropositive → electronegative plasma
  - ➲Plasma impedance increases, NI mobility
  - ➲Power density reduced
- Droplet effect
  - ➲Addition of droplets
  - ➲No increase in impedance (slight reduction)
  - ➲No decrease in power absorbed
  - ➲Consistent with vapour halo formation
- Gas Temperature
  - ➲Temperature generally increases with humidity
  - ➲ However with droplets T_{gas} is lower
  - ➲ ~35 ^oC.
  - ➲Consistent with vapour halo formation
- Simulation
  - ➲Evaporation, Stokes flow
  - ➲Global
  - ➲Characteristic numbers

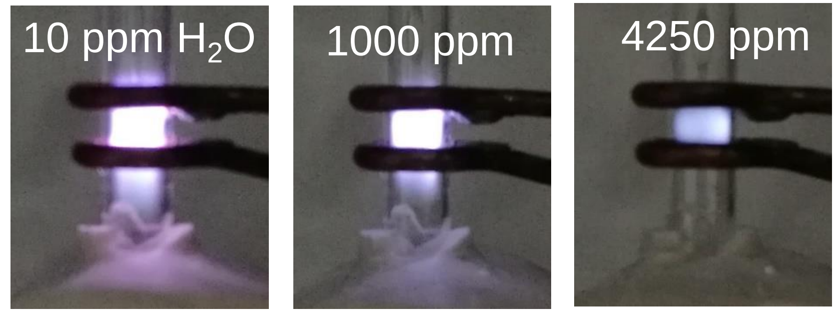

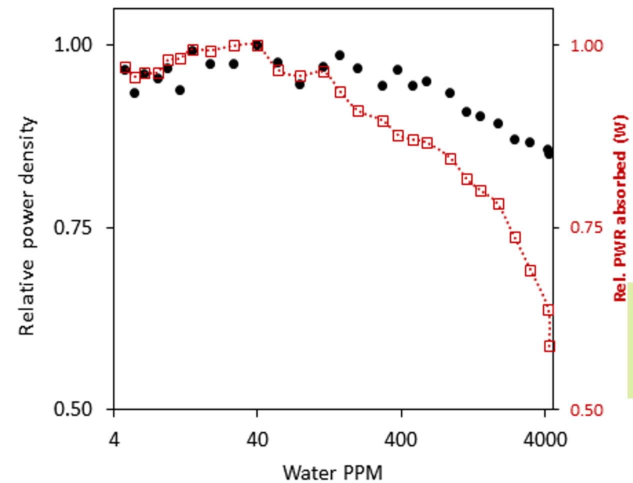

Power, power density

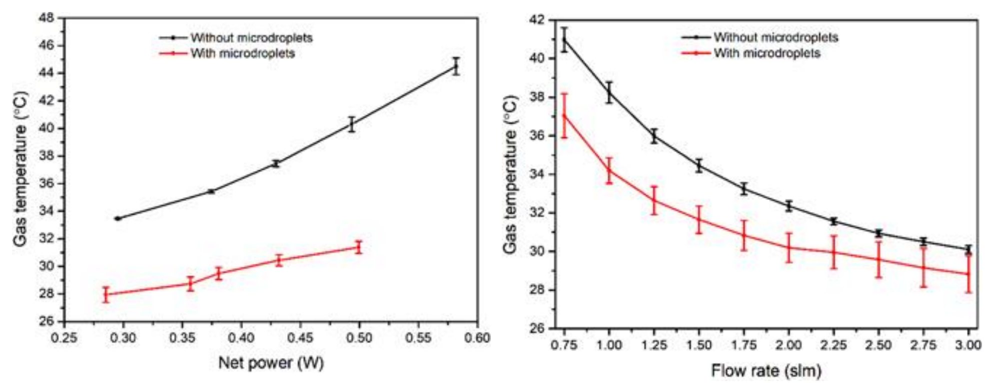

N Hendawy *et al* 2020 *Plasma Sources Sci. Technol.* **29** 085010

Plasma – droplet induced effects

pd.maguire@ulster.ac.uk

RF 13.56MHz
n_e: $10^{12} – 10^{14}$ cm^{-3}.

heating

He⁰
He*
Ne⁰

neutrals

Water dissociation
$H_xO_y^+$
$O_xH_y^-$

He^+
Ne^+ ions

recombination heating

e^- plasma chemistry

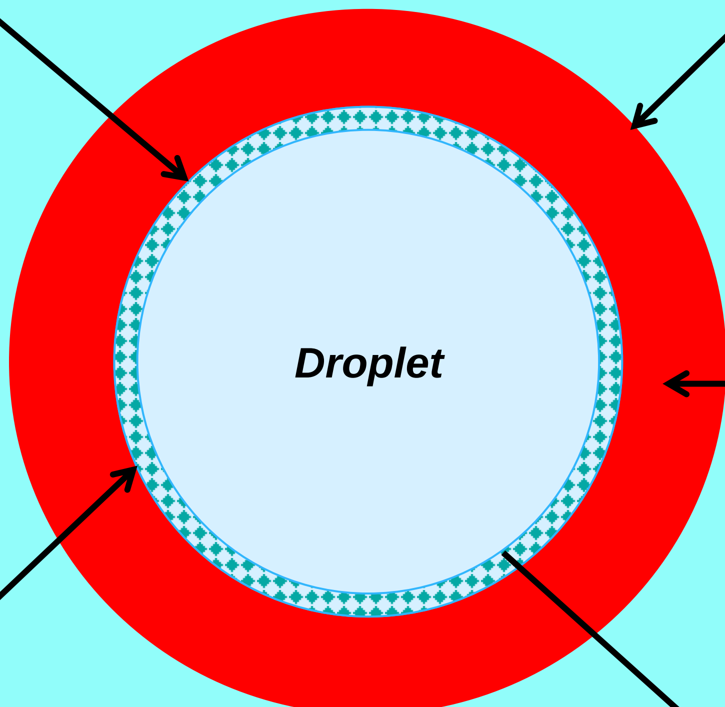

Saturated vapour layer

Evaporation

Plasma is set back from air impurity contamination

Low ppm H_2O without droplet. **Measured at <500ppm**

O_2, N_2: ~0

Plasma region

Droplet Halo Characteristics

pd.maguire@ulster.ac.uk

Evaporated H_2O density in halo around droplet against flight time in plasma

$$D^2 = D_0^2 - c_{av}t$$

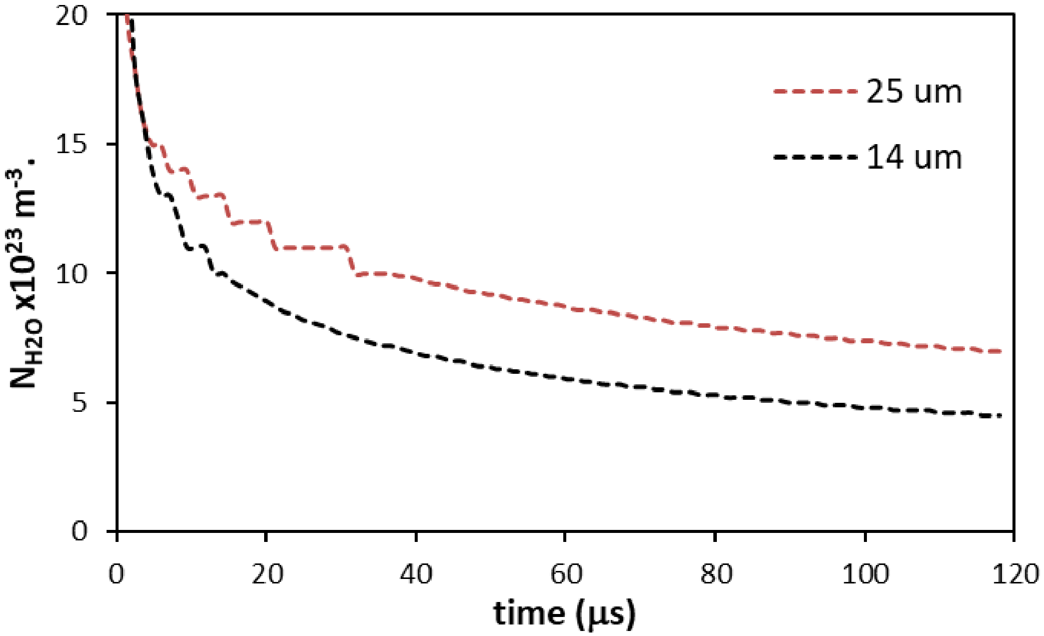

D_0: 14 µm and 25 µm,
Diffusion length of $\sqrt{(D_{H2O}.t)}$,
Gas temperature:350 K
Saturated vapour pressure, 350K: $\mathbf{P_{v.sat}}$ = 41.6 kPa
Evaporation constant: $\mathbf{c_{av}}$ = 5.5 x 10^{-8} m^2s^{-1}.
Halo width @ 120µs = ~100µm

- Droplet Halo Chemistry
  - Noble gas
  - Electrons
  - Water Dissociation

Chemical Flux to droplet
- e^-
- He^+, Ne^+.
- OH, H, H_2O_2.
- H^+, OH^+, Om^+, $H_3O^+(H2O)_n$ clusters
- OH^-, H^-, Om^-, $OH^-(H2O)_n$ clusters

Plasma – droplet induced effects

pd.maguire@ulster.ac.uk

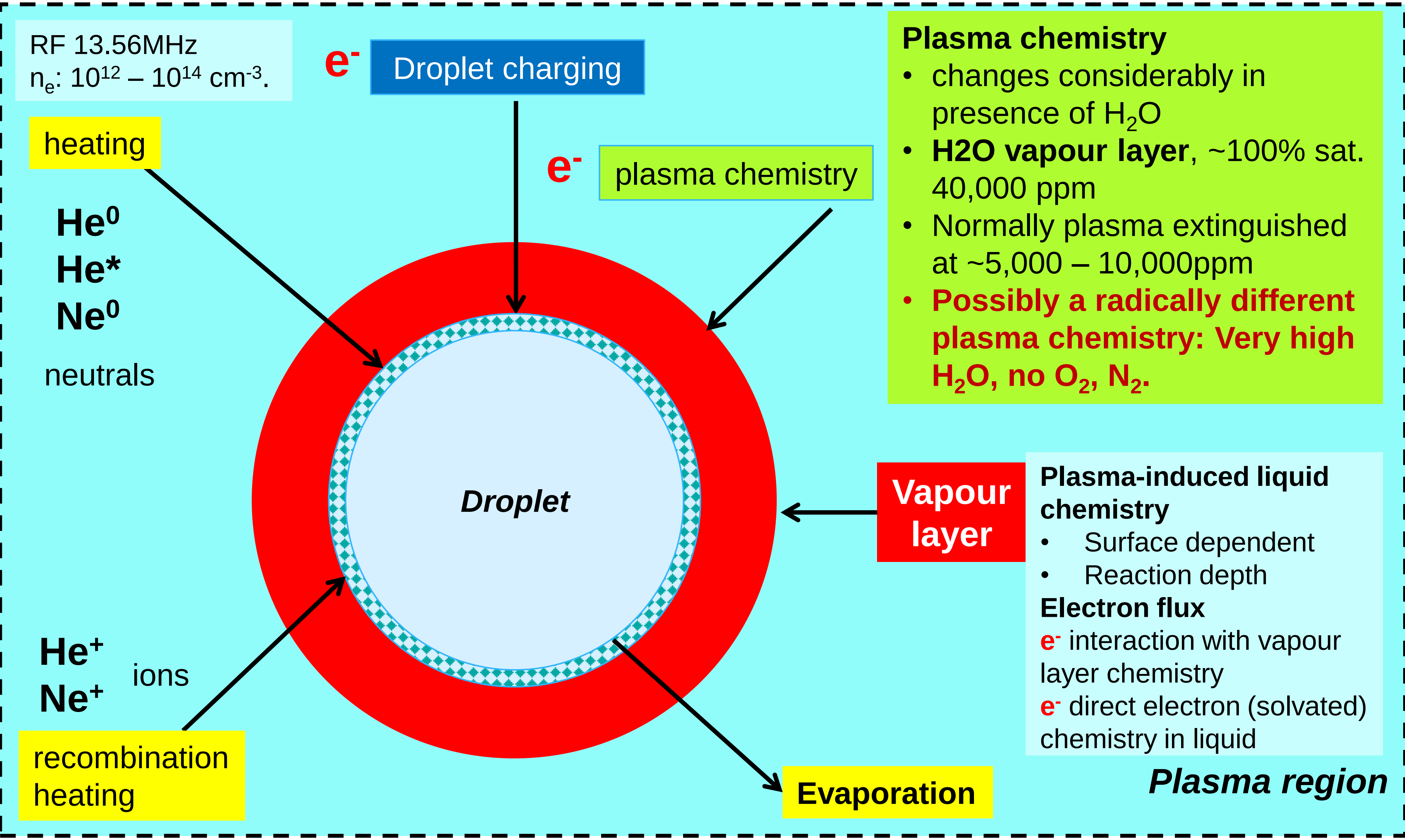

pd.maguire@ulster.ac.uk

Plasma – droplet induced effects

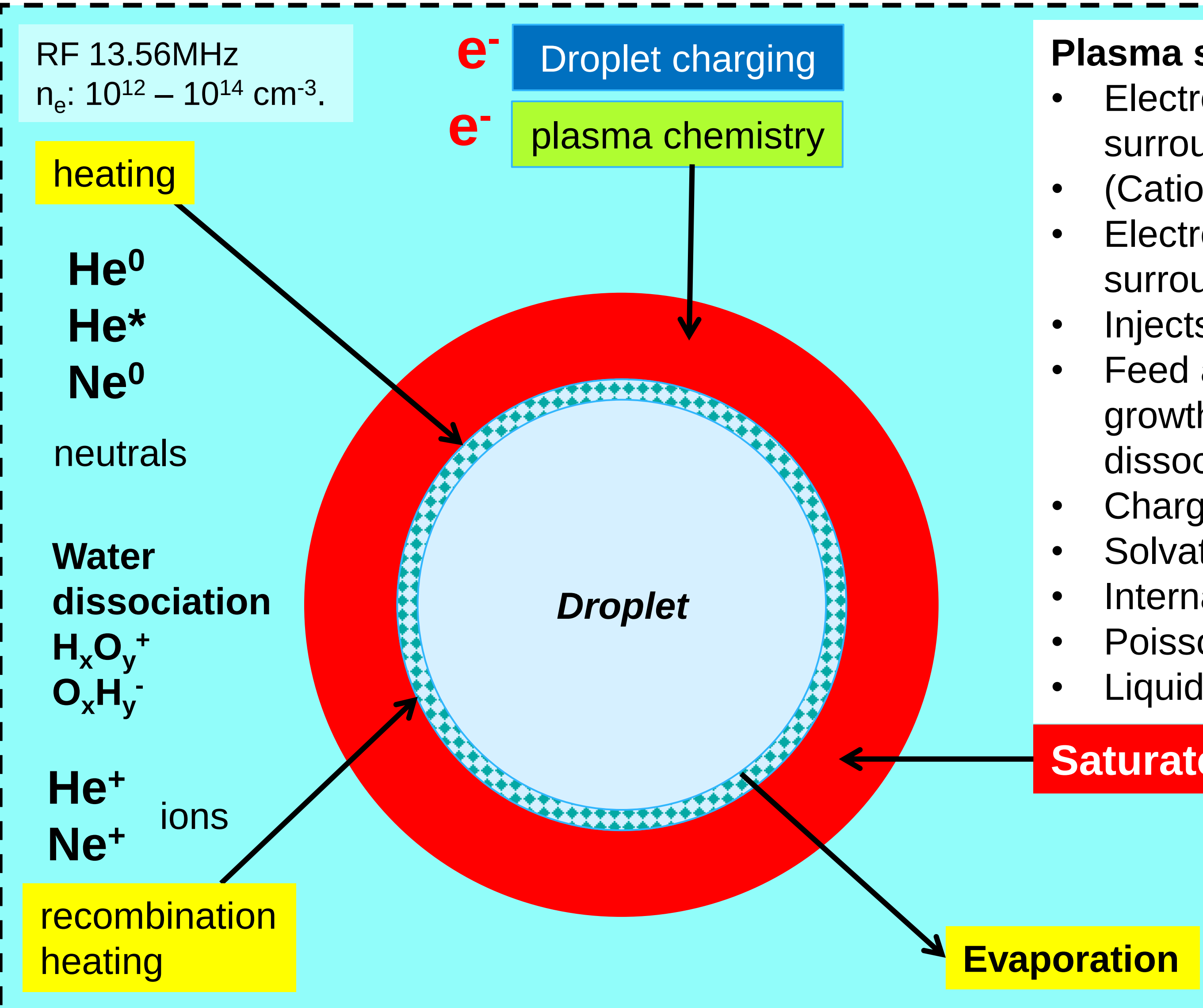

Plasma structure?

- Electronegative plasma surrounds droplet
- (Cation – Anion plasma?)
- Electropositive plasma surrounds halo
- Injects electrons
- Feed anion, cation H_2O cluster growth – depends on N_{H2O} and dissociation species
- Charges droplet
- Solvated electron chemistry
- Internal electric field
- Poisson-Boltzmann
- Liquid species redistribution

Saturated vapour layer

Plasma region

Plasma – droplet induced effects

pd.maguire@ulster.ac.uk

RF 13.56MHz
n_e: $10^{12} – 10^{14}\ cm^{-3}$.

e^- Droplet charging

e^- plasma chemistry

heating

He^0
He^*
Ne^0

neutrals

Water dissociation
$H_xO_y^+$
$O_xH_y^-$

He^+
Ne^+ ions

recombination heating

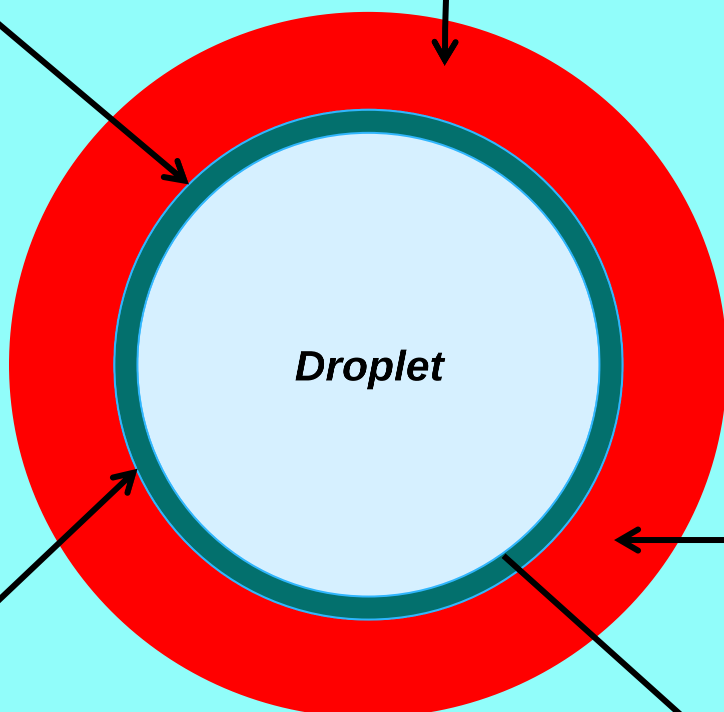

Plasma structure?

- Electronegative plasma surrounds droplet
- (Cation – Anion plasma?)
- Electropositive plasma surrounds halo
- Injects electrons
- Feed anion, cation H_2O cluster growth – depends on N_{H2O} and dissociation species
- Charges droplet
- Solvated electron chemistry
- Internal electric field
- Poisson-Boltzmann
- Liquid species redistribution

Saturated vapour layer

Droplet sheath

Plasma region

Plasma – droplet induced effects

pd.maguire@ulster.ac.uk

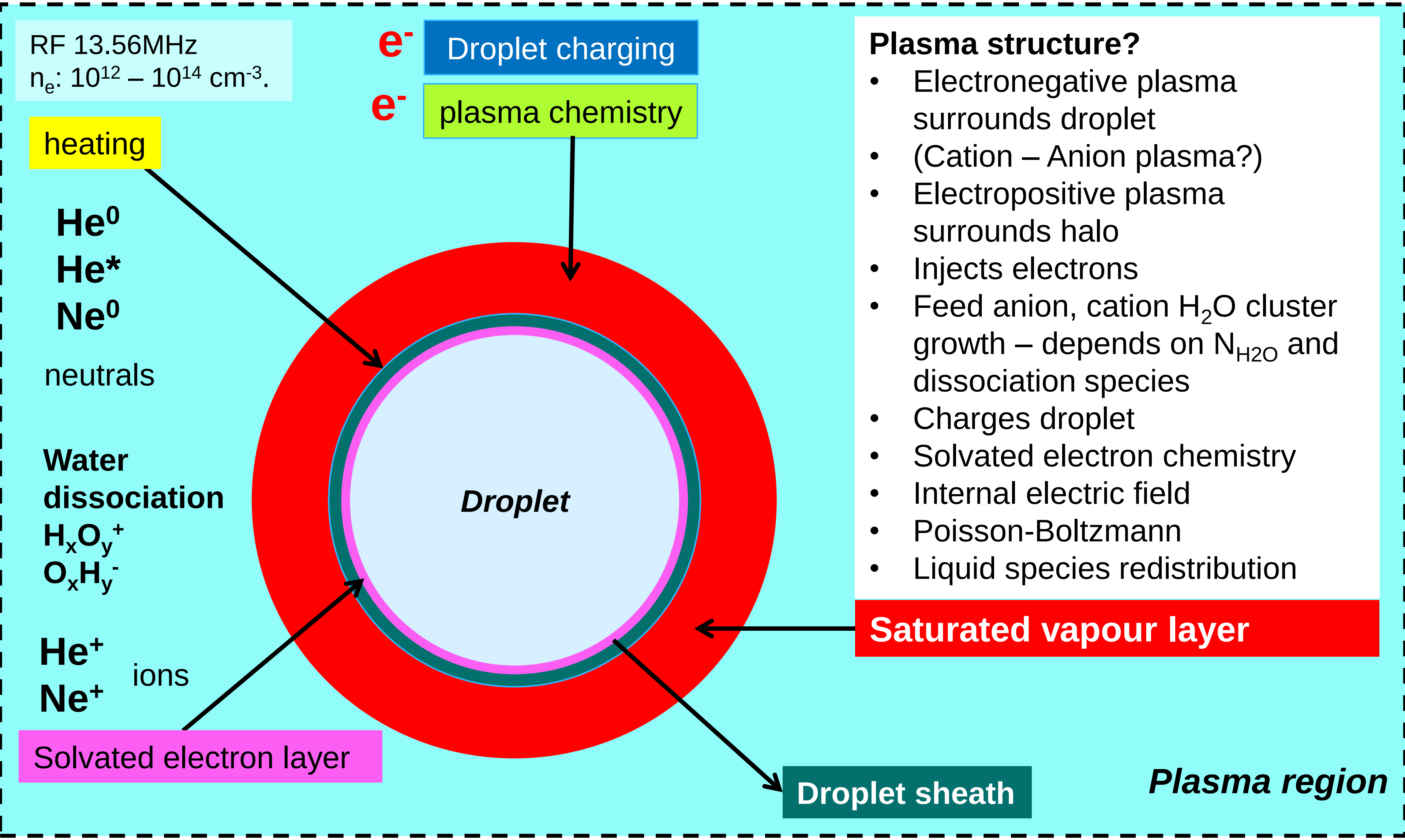

Plasma structure?

- Electronegative plasma surrounds droplet
- (Cation – Anion plasma?)
- Electropositive plasma surrounds halo
- Injects electrons
- Feed anion, cation H_2O cluster growth – depends on N_{H2O} and dissociation species
- Charges droplet
- Solvated electron chemistry
- Internal electric field
- Poisson-Boltzmann
- Liquid species redistribution

Plasma – droplet induced effects

pd.maguire@ulster.ac.uk

RF 13.56MHz
n_e: 10^{12} – 10^{14} cm^{-3}.

He^0
He* neutrals
Ne^0

e^- Droplet charging

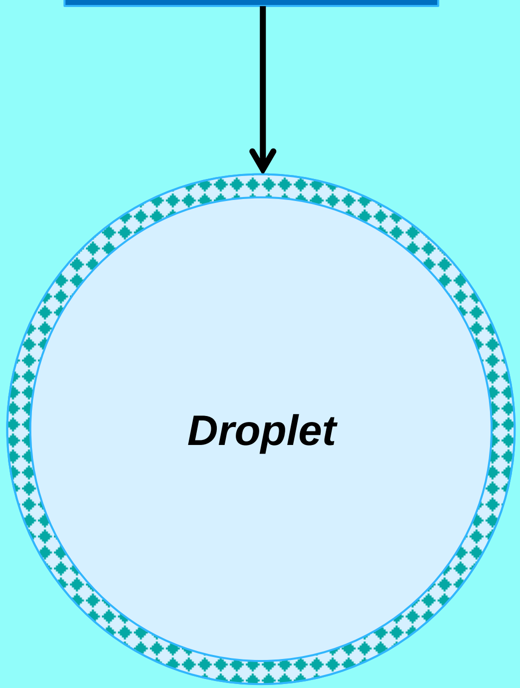

He^+
Ne^+ ions

Water dissociation
$H_xO_y^+$
$O_xH_y^-$

Net electron flux initially
Droplet charges rapidly until it reaches
Negative floating potential
Then electron flux = ion flux
Timescale ns, (ω_i)

Plasma region

Plasma – droplet induced effects

pd.maguire@ulster.ac.uk

RF 13.56MHz
n_e: 10^{12} – 10^{14} cm^{-3}.

He^0
He^* neutrals
Ne^0

e^- Droplet charging

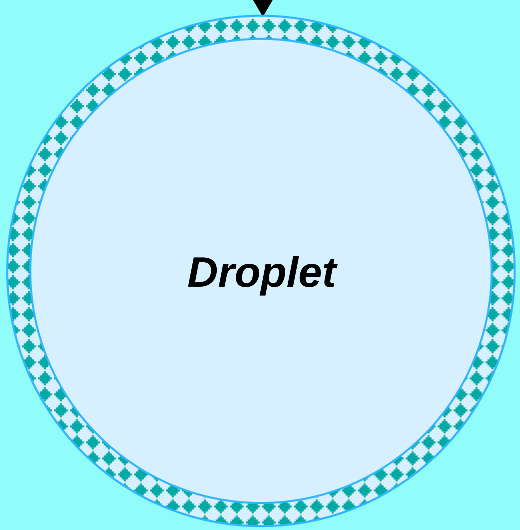

He^+
Ne^+ ions

Net electron flux initially
Droplet charges rapidly until it reaches
Negative floating potential
Then electron flux = ion flux
Timescale ns, (ω_i)

Plasma volume ~10^{-8} m^3.
Total no. electrons: > 10^{10}.
Max. electrons lost to droplet 0.1%

Plasma region

Droplet Halo Characteristics

pd.maguire@ulster.ac.uk

Evaporated H_2O density in halo around droplet against flight time in plasma

$$D^2 = D_0^2 - c_{av}t$$

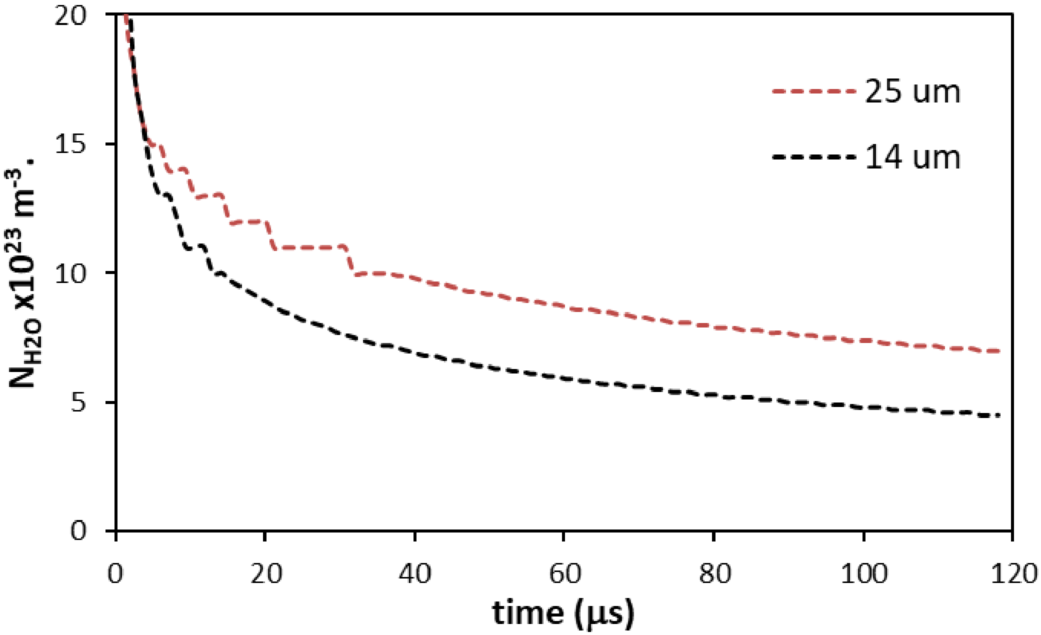

D_0: 14 µm and 25 µm,
Diffusion length of $\sqrt{(D_{H2O}.t)}$,
Gas temperature:350 K
Saturated vapour pressure, 350K: $\mathbf{P_{v.sat}}$ = 41.6 kPa
Evaporation constant: $\mathbf{c_{av}}$ = 5.5 x 10^{-8} m^2s^{-1}.
Halo width @ 120µs = ~100µm

- Droplet Halo Chemistry
  - Noble gas
  - Electrons
  - Water Dissociation
- Species flux to droplet
  - e^-
  - He^+, Ne^+.
  - OH, H, O_m, H_2O_2.
  - H^+, OH^+, O_m^+, $H_3O^+(H2O)_n$ clusters
  - OH-, H-, O_m-, OH-$(H2O)_n$ clusters
- With droplet at floating potential
  - e^-
  - He^+, Ne^+.
  - OH, H, ~~O_m~~, H_2O_2.
  - H^+, OH^+, ~~O_m^+~~, $H_3O^+(H2O)_n$ clusters
  - ~~OH-, H-, O_m-, OH-$(H2O)_n$ clusters~~

Simulation

pd.maguire@ulster.ac.uk

- Electron Flux to droplet
  - ➲Dusty plasma (?)
  - ➲But collisional
  - ➲But D >> λ_i, λ_{De}.
- Ion Flux to droplet
  - ➲Collisional
  - ➲Very low energy
  - ➲Water product ions ~ neutrals
  - ➲Noble gas ions?
- Flux induced droplet chemistry
  - ➲Charge and chemical species flux to droplet
- Model
  - ➲Plasma induced chemistry
  - ➲In liquid
  - ➲1D radial
  - ➲15 species, including solvated electrons
  - ➲100 reactions
- Charge flux (variable n_e)
- Neutral chemical flux
  - ➲OH, H, H2O2, H2, O2.
- $H_2O \rightarrow H_2O_2$ conversion efficiency
  - ➲Literature, up to 6000ppm
  - ➲Across plasma types and conditions
  - ➲Y_{H2O2} ~10^{-3}, from gas phase measurements
  - ➲Y_{H2O2} ~10^{-4}, from liquid measurements
- $H_2O \rightarrow$ OH, H conversion efficiency
  - ➲OH + OH $\rightarrow H_2O_2$. (but some show N_{OH} ~ N_{H2O2})

Plasma – droplet induced effects

pd.maguire@ulster.ac.uk

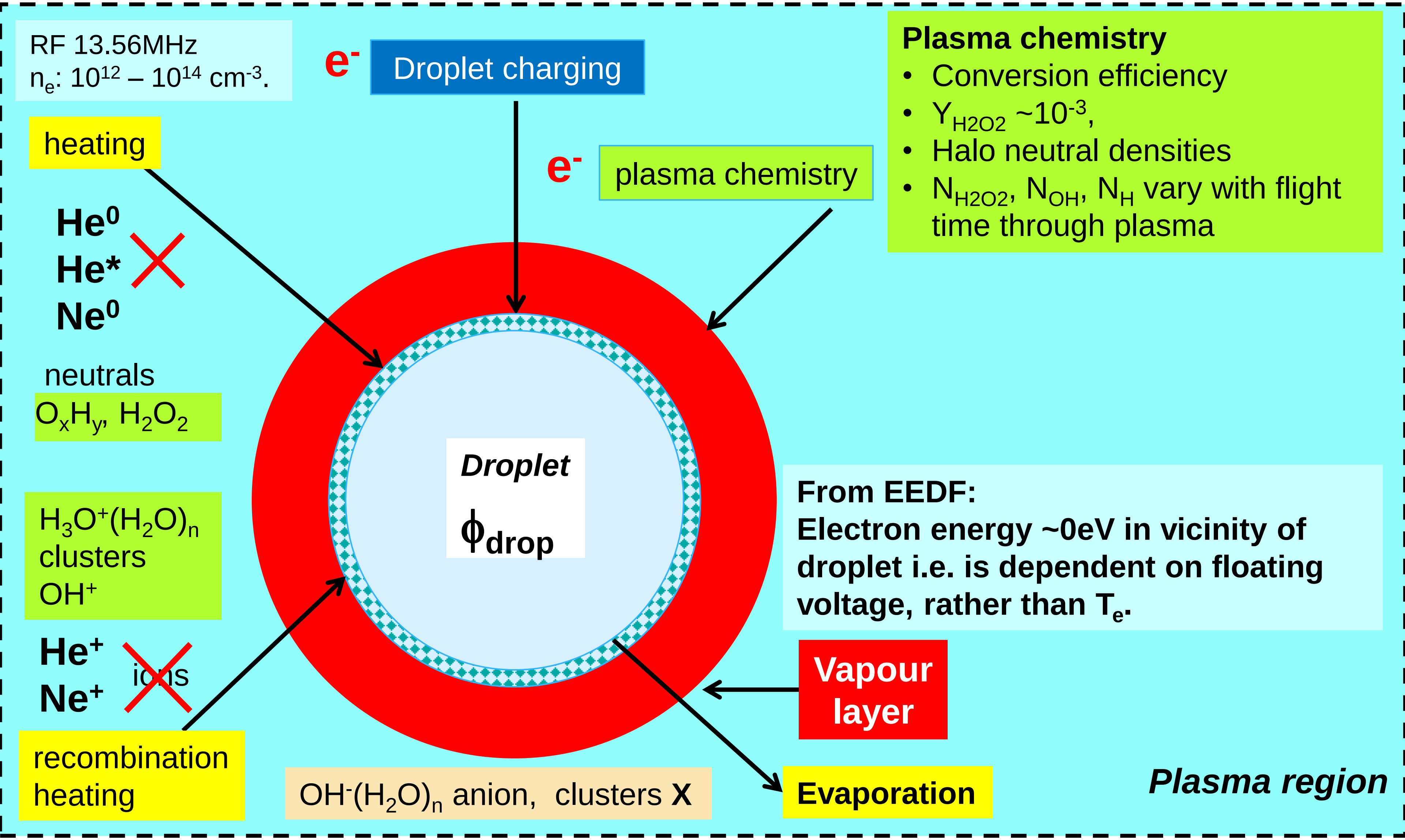

Droplet simulation: H_2O_2, OH

pd.maguire@ulster.ac.uk

Diameter
15um, 20um

Electron flux:
$10^{20} – 10^{23}$ m^{-2} s^{-1}.

Ions:
no chemical impact

H_2O_2:
Decreases with increasing electron flux

OH:
Optimum flux at 10^{22} m^{-2} s^{-1}.

15um: 1mM max conc. Decays by 10^{-4} over 1500nm

20um: 1μM max conc. Decays by 10^{-4} over 2500nm

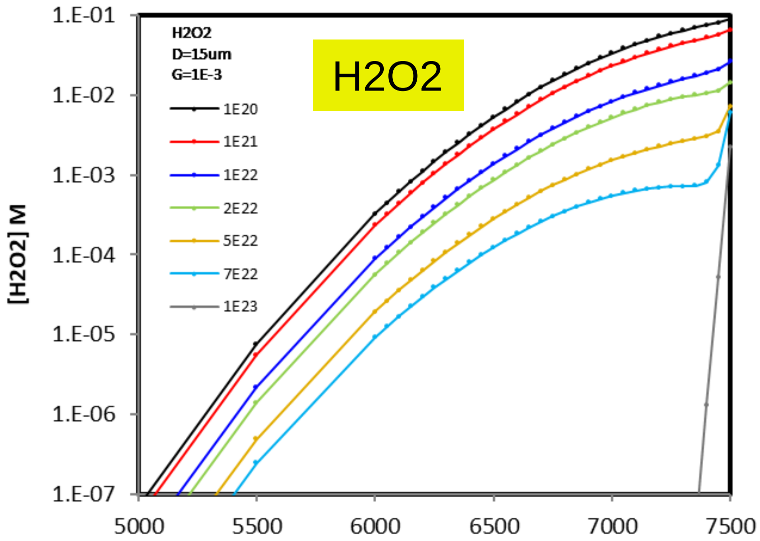

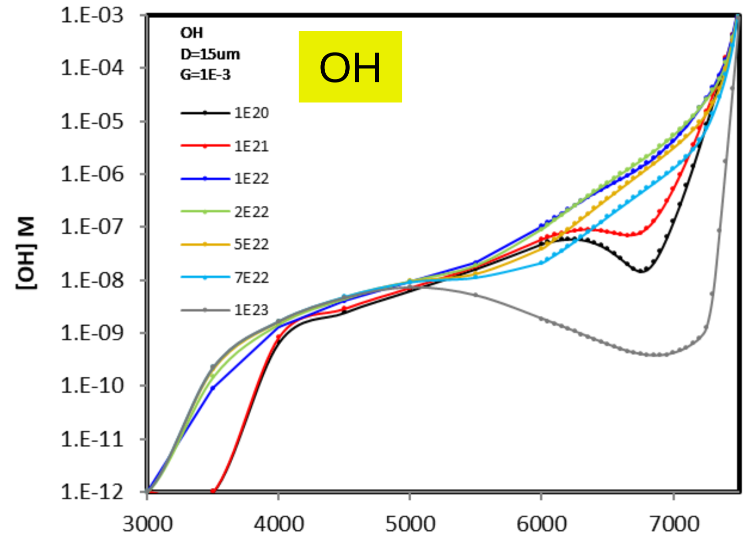

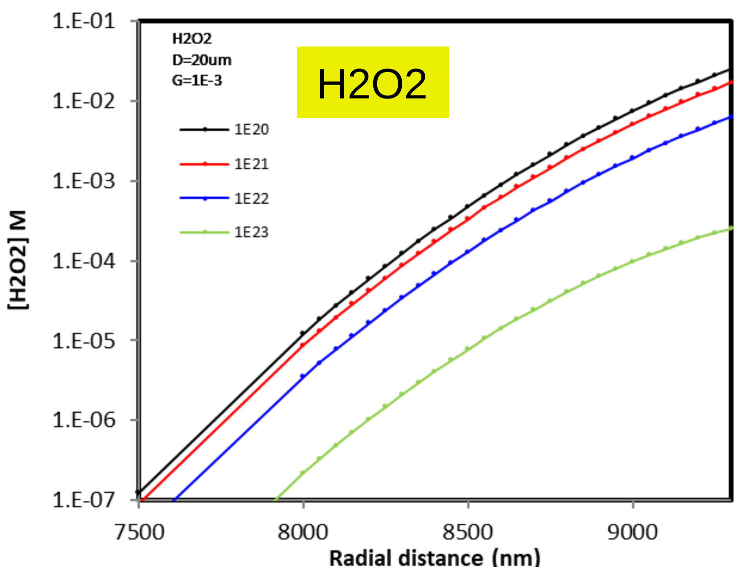

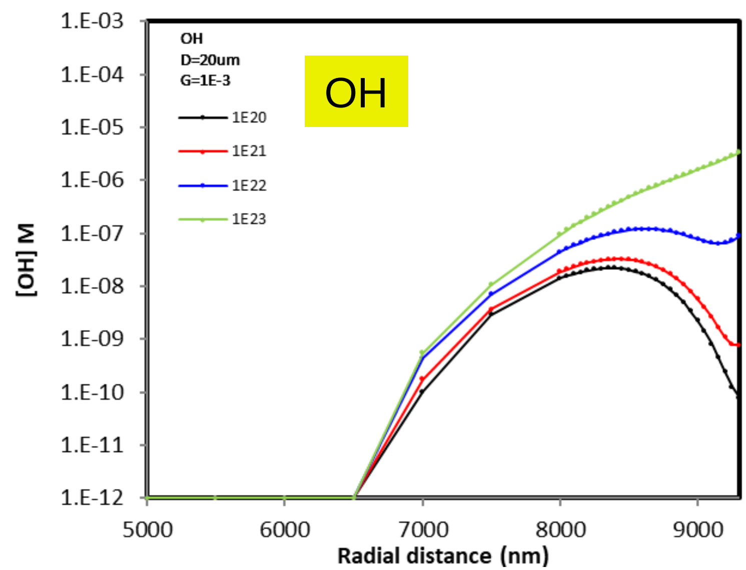

Droplet temperature dependent Henry's constant for OH and H2O2

Droplet simulation: H_2O_2, OH

pd.maguire@ulster.ac.uk

Diameter
15um, 20um

Electron flux:
$10^{20} – 10^{23}$ m^{-2} s^{-1}.

Ions:
no chemical impact

H_2O_2:
Decreases with increasing electron flux

OH:
Optimum flux at 10^{22} m^{-2} s^{-1}.

15um: 1mM max conc. Decays by 10^{-4} over 1500nm

20um: 1μM max conc. Decays by 10^{-4} over 2500nm

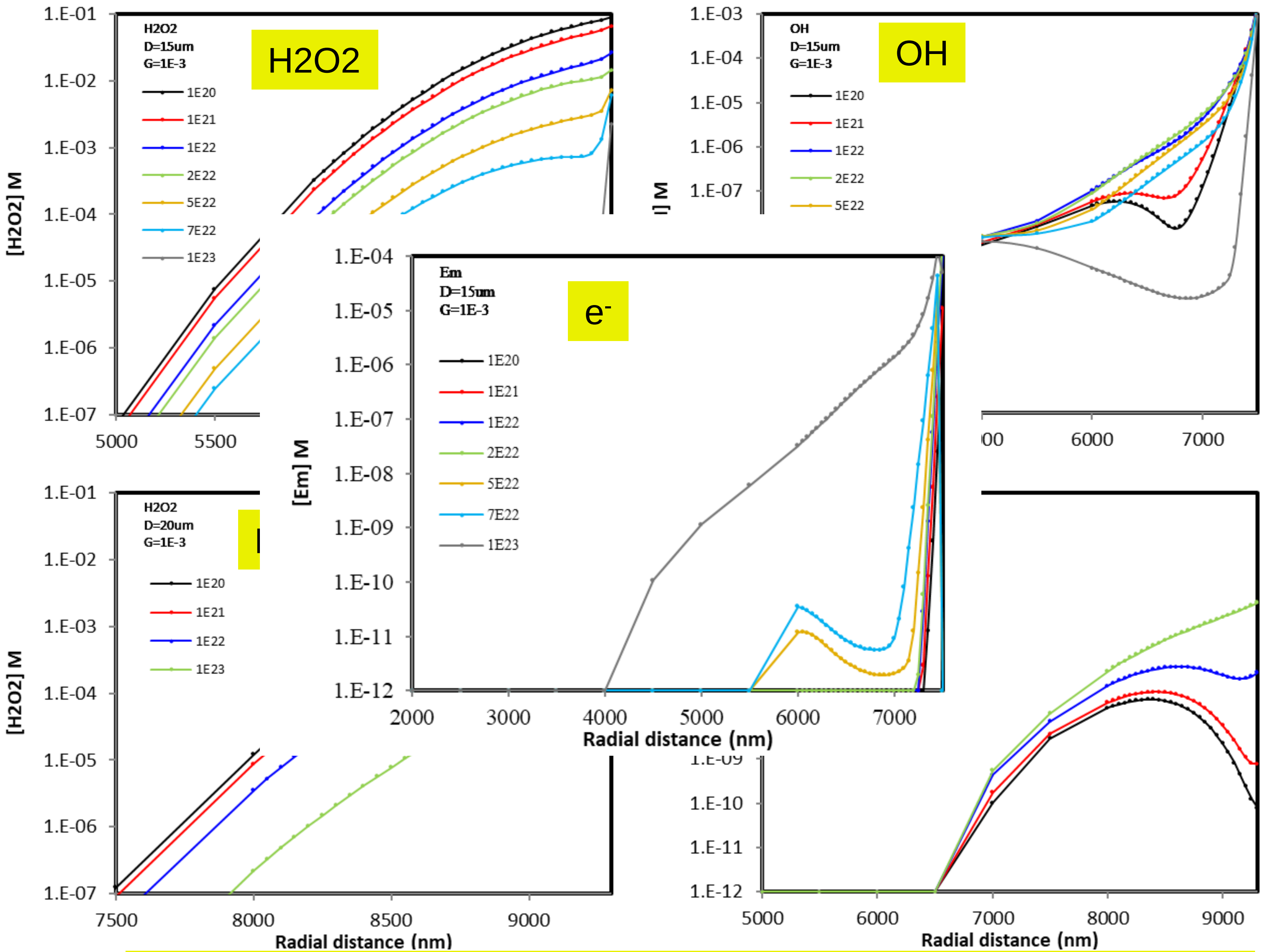

Droplet temperature dependent Henry's constant for OH and H2O2

Electron flux to droplet

Scale lengths

pd.maguire@ulster.ac.uk

- Reactor
  - 10^{-3}
- Droplet
  - 10^{-5}
- Sheath?
- Debye?
- Mean free path
  - 10^{-7}
- Solvated electron layer
  - 10^{-8} to 10^{-9}

pd.maguire@ulster.ac.uk

Standard orbital motion limited (OML) theory

Collisionless

Droplet potential obtained by equating ion and electron currents to and from the droplet i.e.

$$\left(\frac{T_e}{m_e}\right)^{1/2}\left[1-\exp\left(-\frac{e|\varphi_s|}{K_B T_e}\right)\right]=\left(\frac{T_i}{m_i}\right)^{1/2}\left(\frac{e|\varphi_s|}{K_B T_i}\right).$$

total flux Γ is given by

$$4\pi r_o^2 Z_i e n_{oi}\left(\frac{K_B T_i}{2\pi m_i}\right)^{1/2}\frac{e|\varphi_s|}{K_B T_i}$$

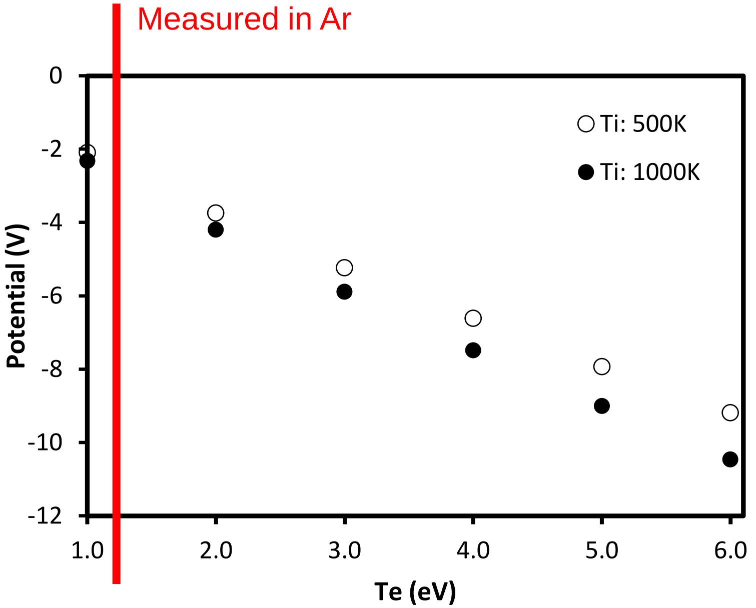

Droplet potential versus electron temperature, for two values of Ti = 500K, and 1000K calculated using Orbital Motion Limited (OML) theory.

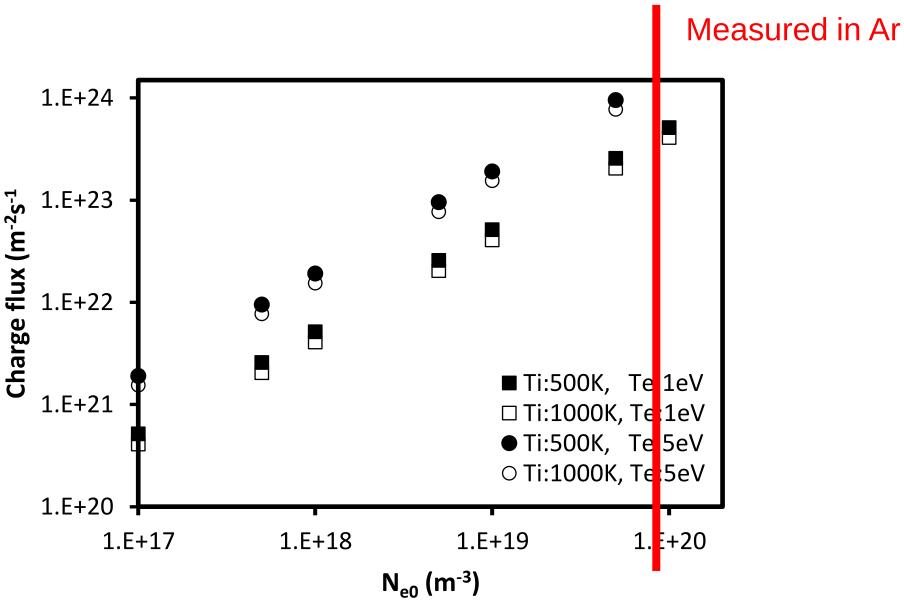

Ion/electron OML flux to 15 μm droplet versus plasma density (n_{e0}) for T_i = 500K, and 1000K and upper/lower values of T_e of 1 eV and 5 eV

Ulster University

Electron flux model

pd.maguire@ulster.ac.uk

Standard orbital motion limited (OML) theory
Droplet potential obtained by equating ion and electron currents to and from the droplet i.e.

$$\left(\frac{T_e}{m_e}\right)^{1/2}\left[1-\exp\left(-\frac{e|\varphi_s|}{K_BT_e}\right)\right]=\left(\frac{T_i}{m_i}\right)^{1/2}\left(\frac{e|\varphi_s|}{K_BT_i}\right).$$

total flux Γ is given by

$$4\pi r_o^2 Z_i e n_{oi}\left(\frac{K_BT_i}{2\pi m_i}\right)^{1/2}\frac{e|\varphi_s|}{K_BT_i}$$

High Pressure (Collisional)
In high pressure plasmas, ion and electron collisions with neutrals modify the charge flux to the surface.

Weak collisionality: ion mean free path λ_i, < Debye length λ_{Di},
Strong collisionality: electrons also suffer collisions i.e. $\lambda_e << \lambda_{De}$.

Simple expression for charge flux to a probe is not available.

1. COMSOL fluid model. 1D radial

2. 1D radial analytical / numerical model for both $\lambda_{i,e}$ and $\lambda_{Di,e}$ << D, the droplet diameter, based on mobility/diffusion assumptions

$$\begin{aligned}
\nabla\left(-\frac{\partial n_i}{\partial r}-\frac{1}{\tau}n_i\frac{\partial\phi}{\partial r}\right) &= 0\\
\nabla\left(-\frac{\partial n_e}{\partial r}+n_e\frac{\partial\phi}{\partial r}\right) &= 0\\
\nabla\left(\frac{\partial\phi}{\partial r}\right)-\frac{1}{\lambda_{De}^2}(n_e-n_i) &= 0
\end{aligned}$$

$$\nabla(x) = 1/r^2\partial/\partial r(r^2x)$$

$$\Gamma_i^p = \frac{N_\infty D_i}{R_p}\frac{\partial n_i}{\partial r}(r_p)$$

$$\Gamma_e^p = (N_\infty D_e/R_p)\partial n_e/\partial r(r_p)$$

Plasma charging, collisional model

pd.maguire@ulster.ac.uk

- Plasma – droplet collisional model

  $\lambda_e << \lambda_{De}$. λ_{De}. $<< r_{NP}$.

- Highly collisional
  - ➲Hydrodynamic solution
  - ➲No analytical approximations
  - ➲Simulations
  - ➲Asymptotic analytical approximations
  - ➲**Not experimentally verified**

$$\nabla\left(-\frac{\partial n_i}{\partial r} - \frac{1}{\tau} n_i \frac{\partial \phi}{\partial r}\right) = 0$$

$$\nabla\left(-\frac{\partial n_e}{\partial r} + n_e \frac{\partial \phi}{\partial r}\right) = 0$$

$$\nabla\left(\frac{\partial \phi}{\partial r}\right) - \frac{1}{\lambda_{De}^2}(n_e - n_i) = 0$$

$$\nabla(x) = 1/r^2 \partial/\partial r(r^2 x)$$

$$\Gamma_i^p = \frac{N_\infty D_i}{R_p}\frac{\partial n_i}{\partial r}(r_p)$$

$$\Gamma_e^p = (N_\infty D_e/R_p)\partial n_e/\partial r(r_p)$$

Patacchini, Leonardo, and Ian H. Hutchinson. "Continuum plasma solution surrounding non-emitting spherical bodies." Physics of Plasmas 16.6 (2009): 062101-16

Model Output

- Q_{drop} v R_{drop}
  - N_e:$1\text{x}10^{12} – 1\text{x}10^{14}$ cm^3.
  - Average R: Q_d = ~10^5e
  - Max. R: Q_d = ~10^6e
  - ***Electron flux***
  - $10^{20} – 5 \text{ x } 10^{23}$ m^{-2} s^{-1}
  - Nanoparticles (100nm) ~200 e
  - See simulation Nabiel H Abuyazid *et al* 2020 *Plasma Sources Sci. Technol.* **29** 075011

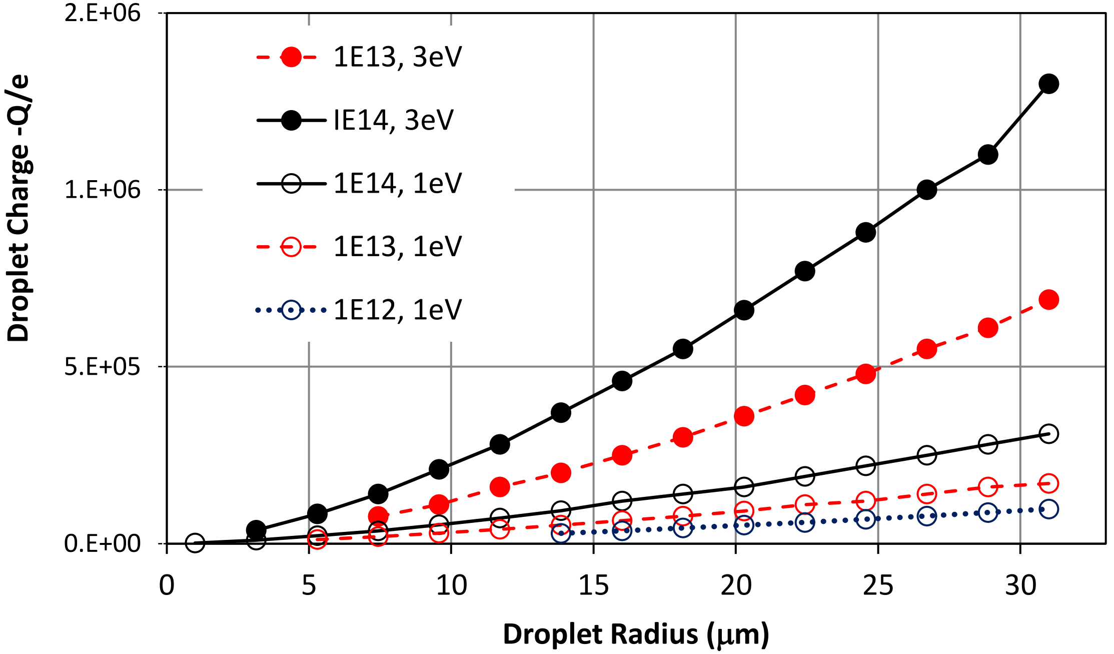

Plasma-induced droplet charge measurement

pd.maguire@ulster.ac.uk

Calibration

Droplet & Needle

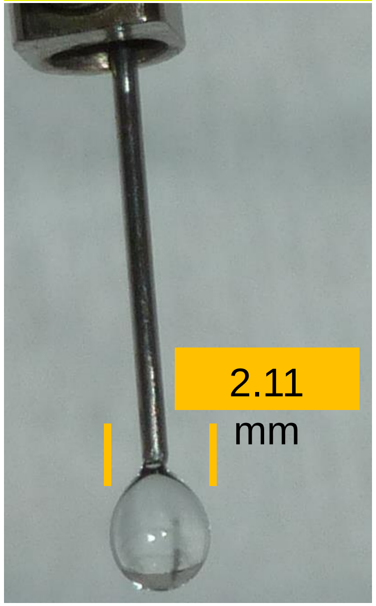

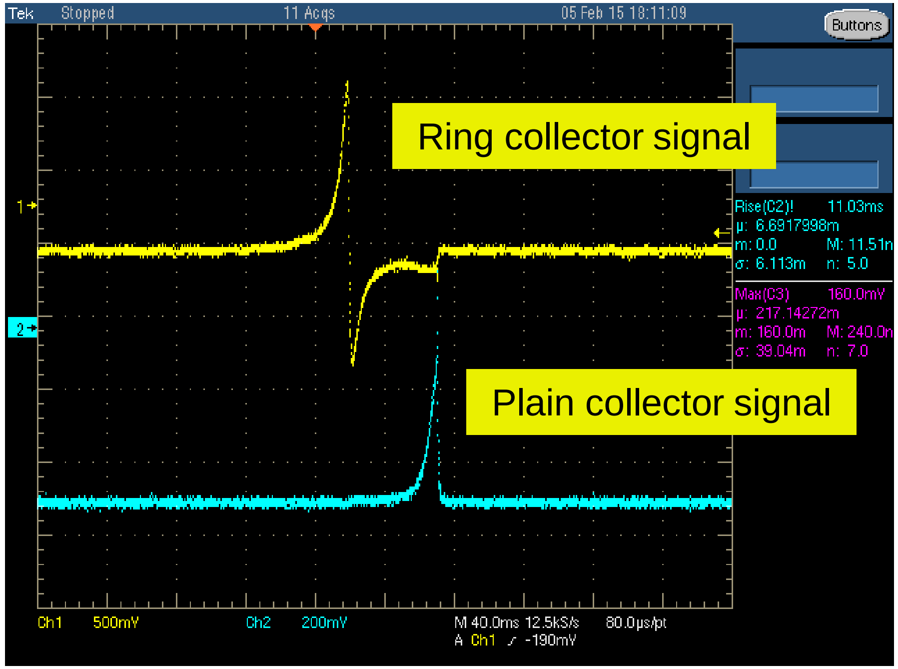

Comsol model: ring collector

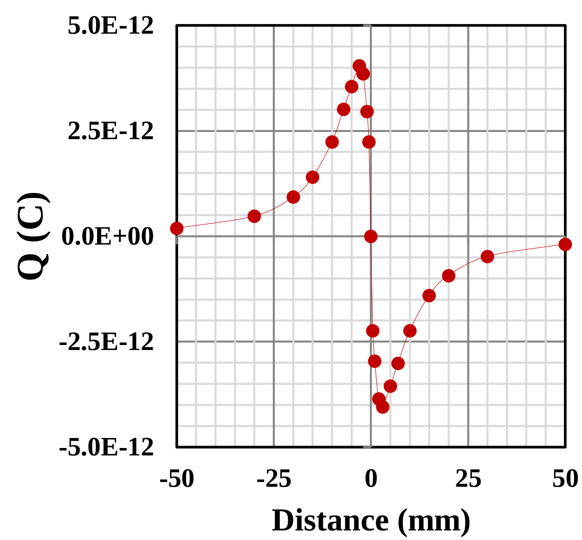

AMPLIFIER GAIN CALIBRATION: *A250F* x -1000 ± 50, *A250* x -300 ± 20

45° Plate Collector Measurements

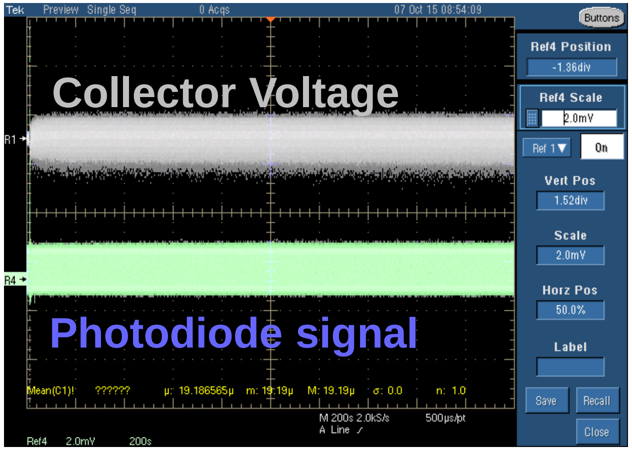

No droplets: 3.5 slm He, 1 slm Ne, 100 W power, collector 4.5 mm from quartz tube

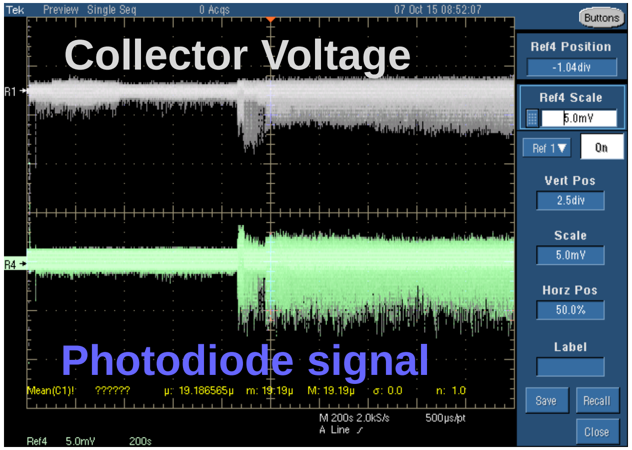

With droplets: H_2O 0.6 mL/h, 3.5 slm He, 1 slm Ne, 100 W power, collector 4.5 mm from quartz tube

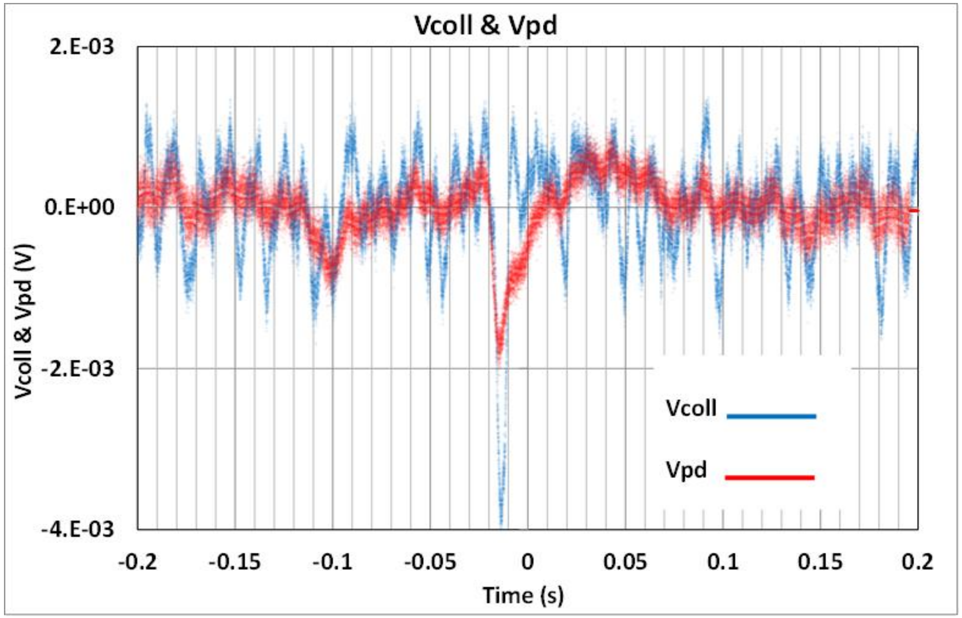

V_{coll} & V_{pd} waveforms cleaned by filtering 50 Hz & 13.56 MHz.

- Features in each waveform match.
- Likely indicator of change in plasma parameters
- and / or chemistry as droplet passes.

pd.maguire@ulster.ac.uk

Plate collector signal – high noise

Variation in pulse rate with gas flow

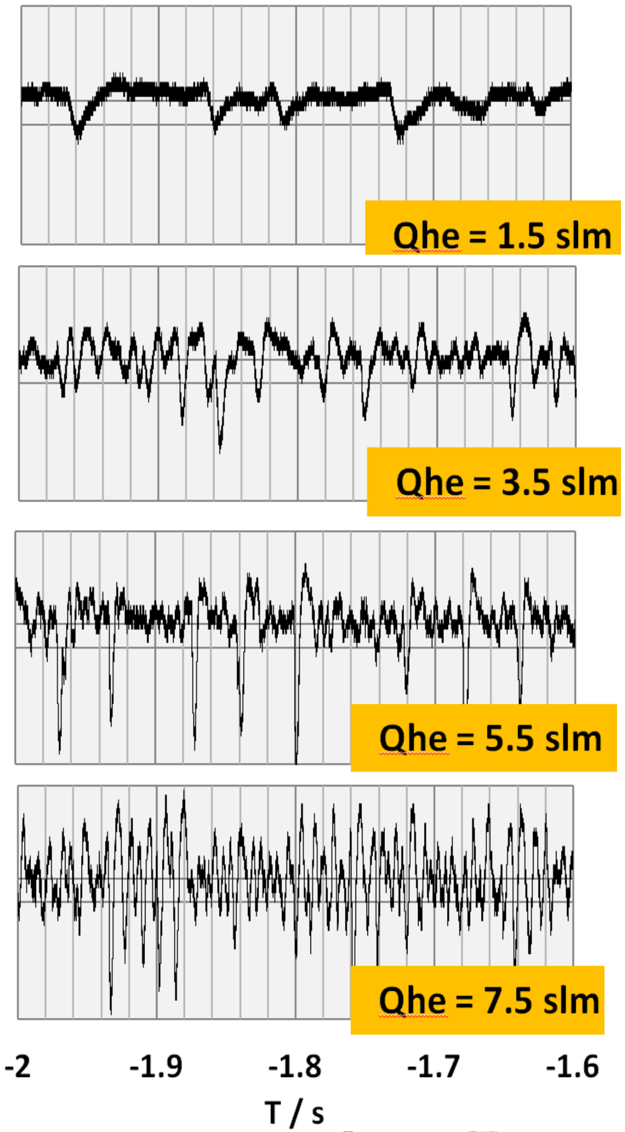

gas velocity x2

peak width ÷2

peak height increases

Pulse area (charge) = constant

Un-amplified data

DC voltage shift of - 0.53 mV

- commensurate with

[~ 10^5 droplets/second] * [with **>10^5** electrons each**]**

~ 10 - 20 micron diameter

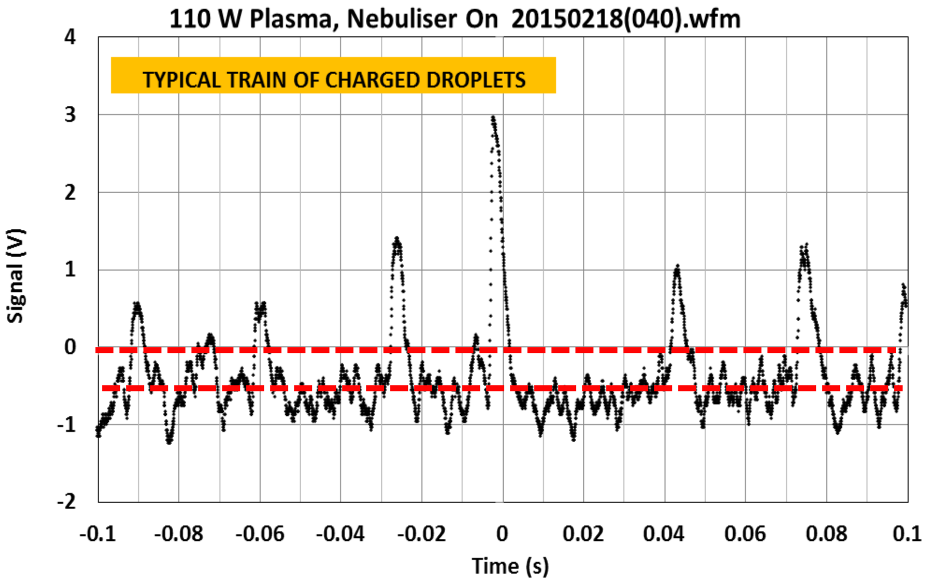

Ulster University
NIBEC Nanotechnology & Integrated Bioengineering Centre
plasma & nanofabrication
pd.maguire@ulster.ac.uk

Droplet average charge

Average charge determined from DC shift in waveform

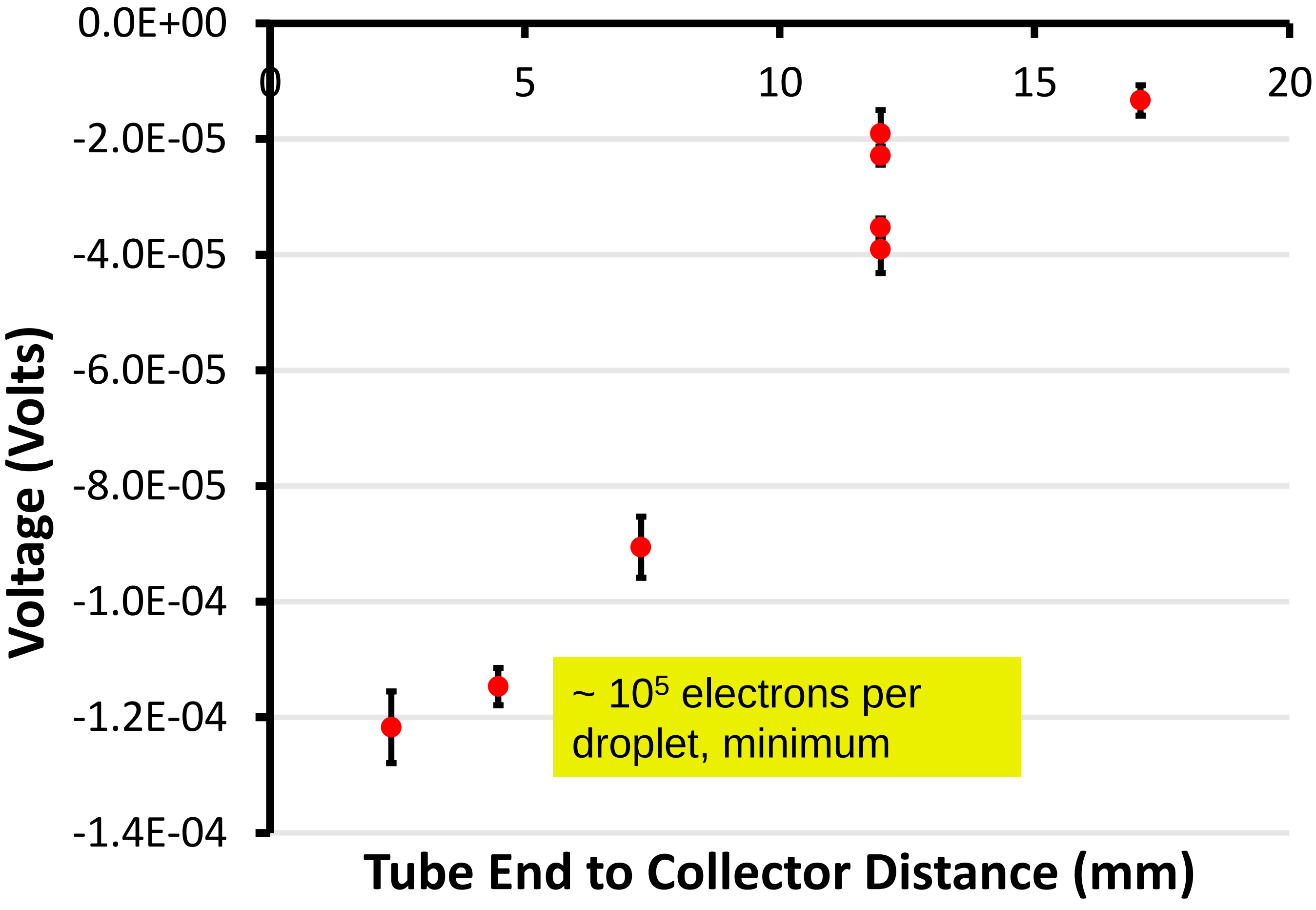

$V_{Plasma} - V_{NoPlasma}$:

Droplet individual charge

- Individual charge
  - ➲Very fast measurement to separate droplets
  - ➲Thin rings
  - ➲High accuracy to measure small fast moving charge
- Ring collectors
  - ➲Variable distance from plasma
  - ➲Variable inter-ring distance
  - ➲Is droplet charge neutralised in flight?
- High gain amplifiers
  - ➲Requires calibration
  - ➲Response time of detector and amplifiers

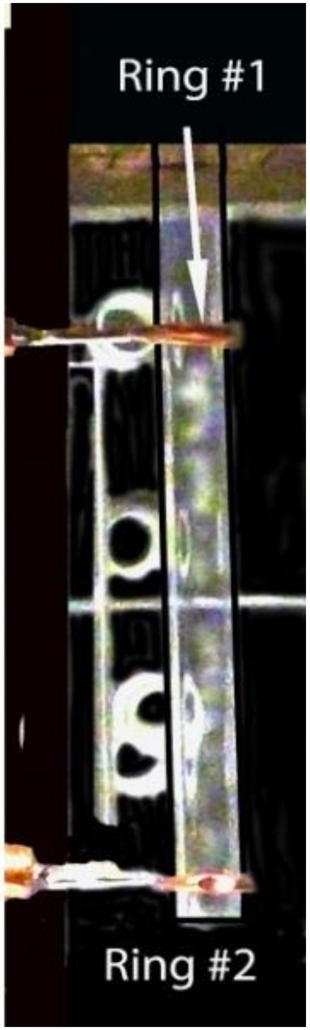

Charge decay with distance

Noise reduction & filtering of 13.56MHz, harmonics, 50Hz

- Signal
- Derivative

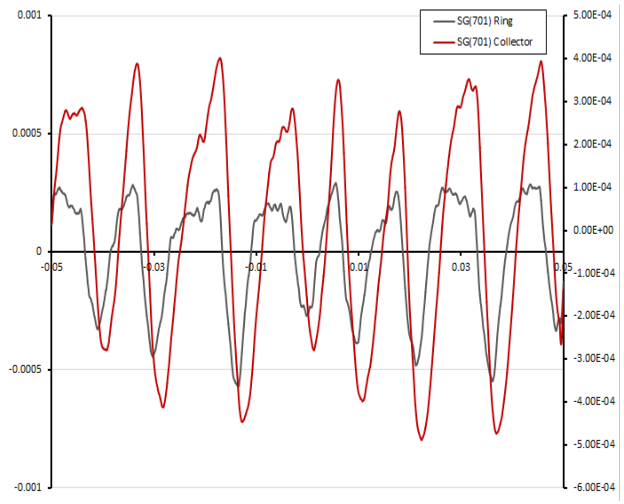

Derivative match ring #1 and ring #2 droplets – droplet speed

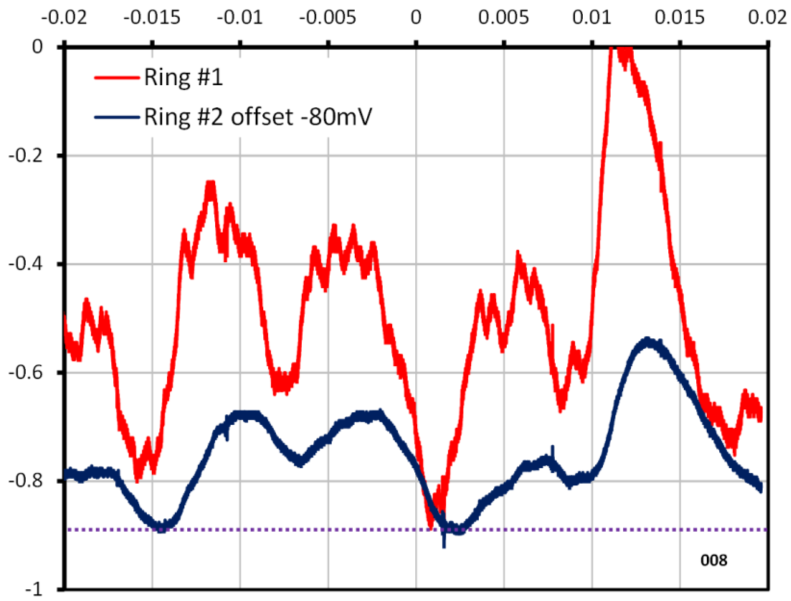

V_{rms} roll-off with distance from plasma for different gas velocities (10 ms^{-1} to 32 ms^{-1})

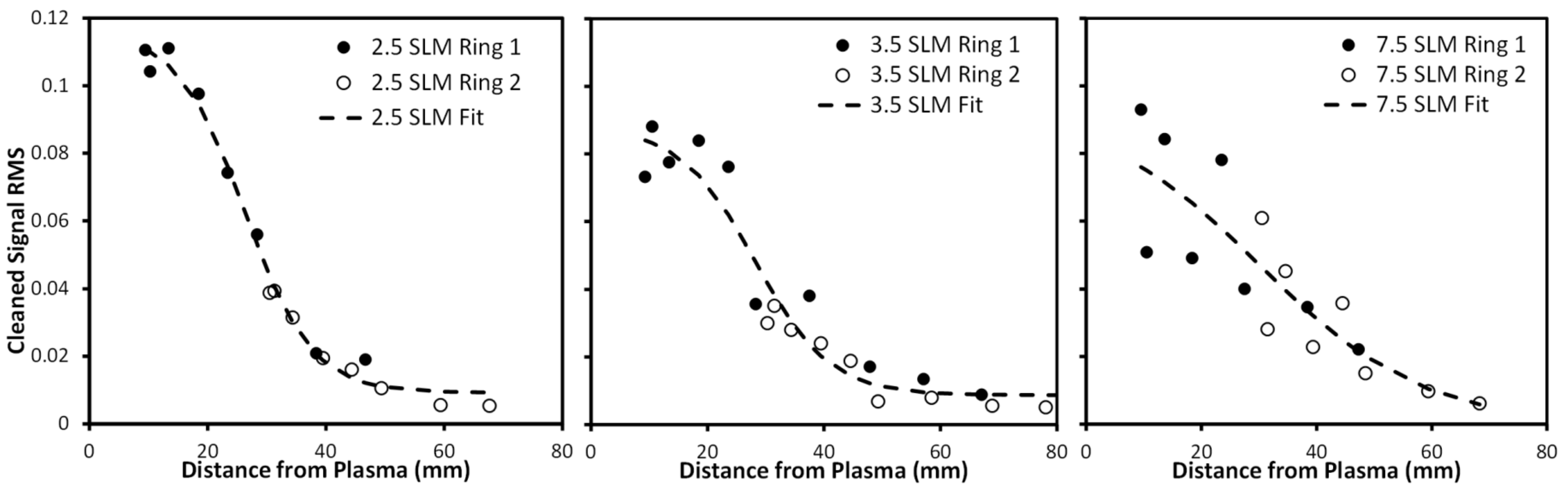

pd.maguire@ulster.ac.uk

Droplet velocity distribution

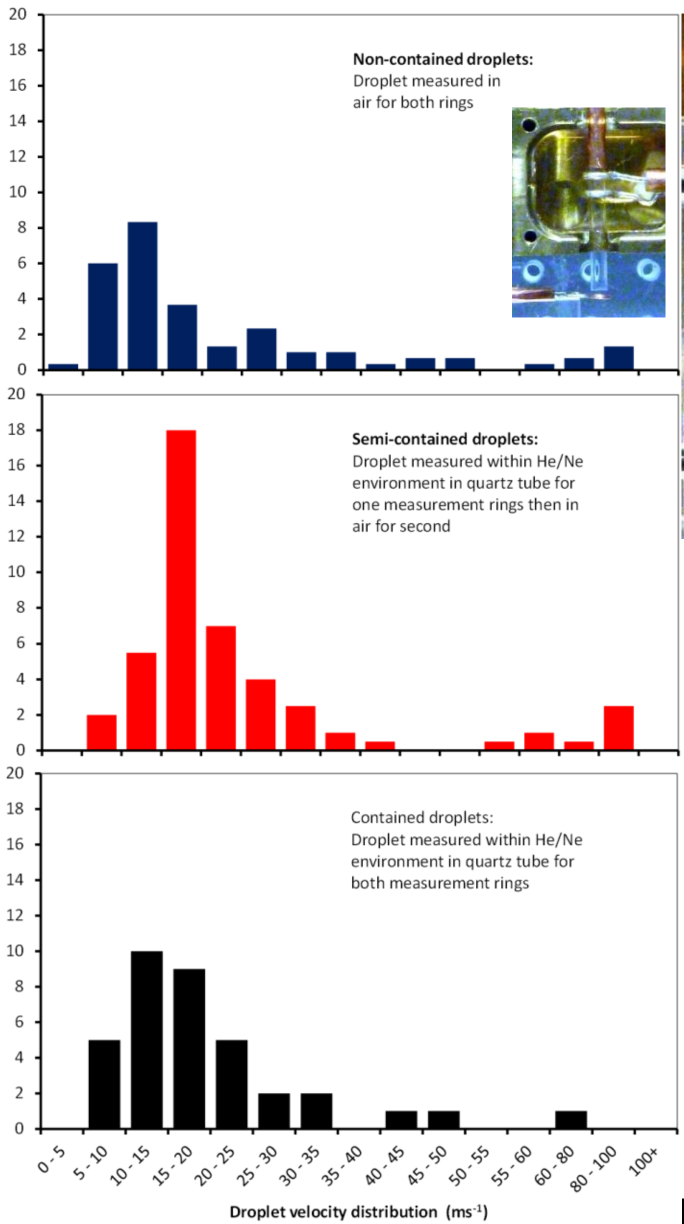

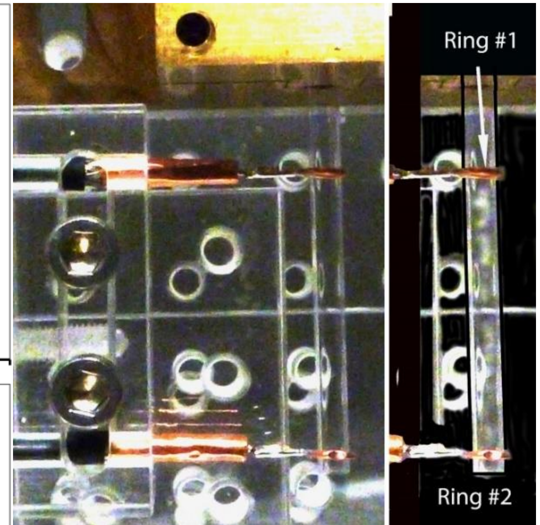

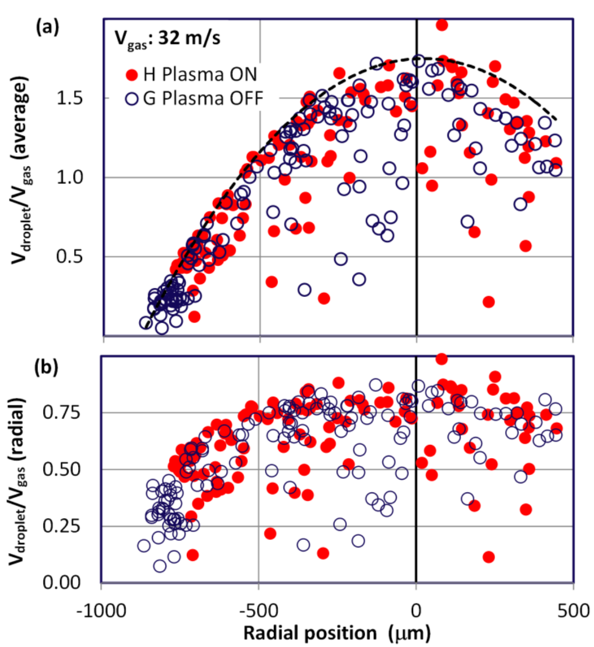

- Electrical
  - ➲Far left graphs
  - ➲Quartz tube position adjusted
  - ➲Speed estimated from pulse delay between rings
  - ➲Close to gas speed for droplets contained within quartz tube
  - ➲Droplets slower when outside tube
- Optical
  - ➲Left
  - ➲From high speed imaging
  - ➲Measurement possible outside quartz tube only
  - ➲Droplets typically ~75% of gas speed

Single-size droplet charge

Piezoelectric droplet generator coupled to plasma through custom stable directional coaxial laminar flow interface.

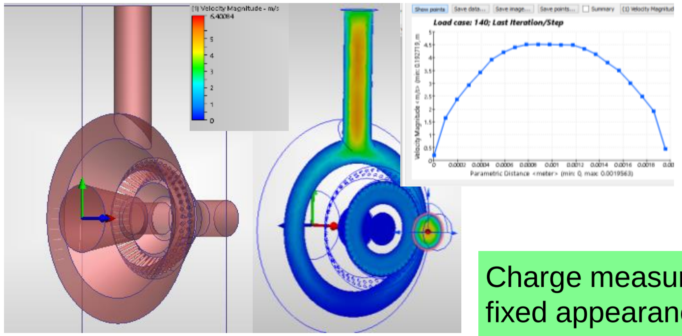

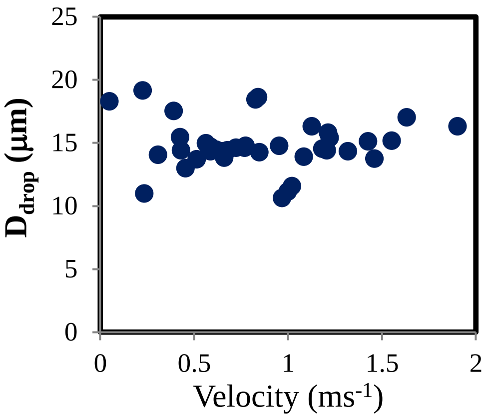

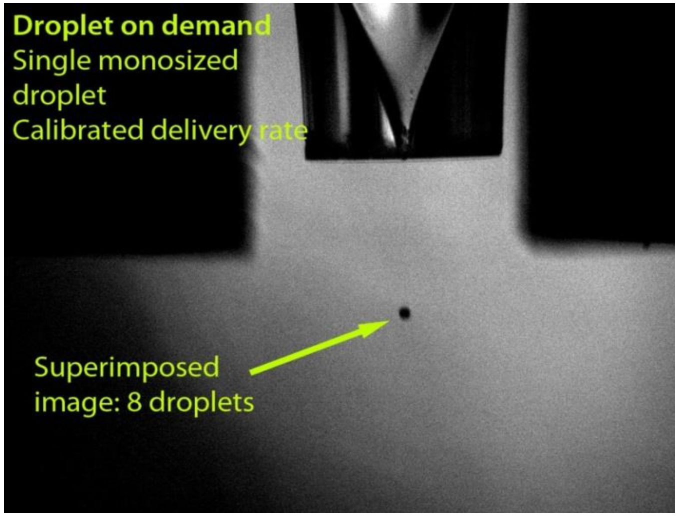

Charge measurement on isolated droplets with a fixed appearance rate. Signal averaging possible.

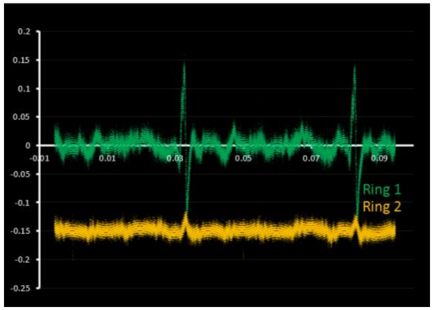

Charge estimate: >10^5e.

(i) Isolated sphere

(ii) Mutual capacitance of point charge and ring

(iii) Parasitic and measurement circuit capacitance

(iv) Distance off-centre

Ulster University
NIBEC Nanotechnology & Integrated Bioengineering Centre
plasma & nanofabrication
pd.maguire@ulster.ac.uk

Droplet in plasma charge: comparison with corona

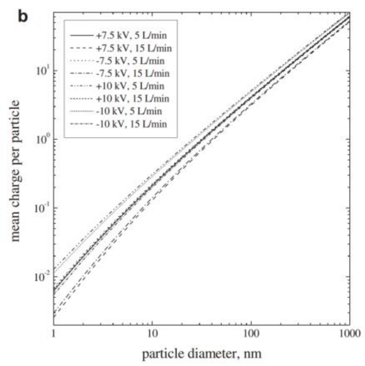

Fig. 8. Variation of mean charge per particle with particle diameter at different aerosol flow rate and applied voltage (a) 0 V and (b) 310 V.

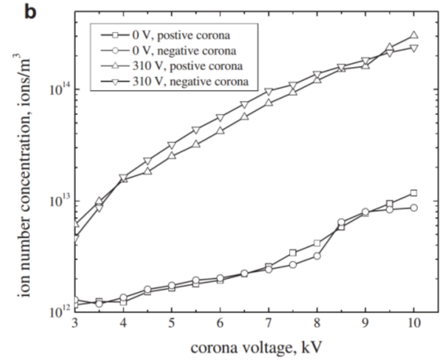

Fig. 5. Variations in ion number concentrations with corona voltage in the charger (a) discharge zone and (b) charging zone.

Corona discharge in a cylindrical triode charger for unipolar diffusion aerosol charging, P. Intra, J. Electrostat. **70** (2012) 136

Comparison with unipolar corona charging

Simulation: 10um particles,
Q_d = **7000** (8 kV), 3000 (5kV)

Measured: 1um particles,
Q_d = **68** (5kV)

Design and evaluation of a unipolar aerosol charger to generate highly charged micron-sized aerosol particles

J Park et al., J. Electrostat. ***69*** *(2011) 126*

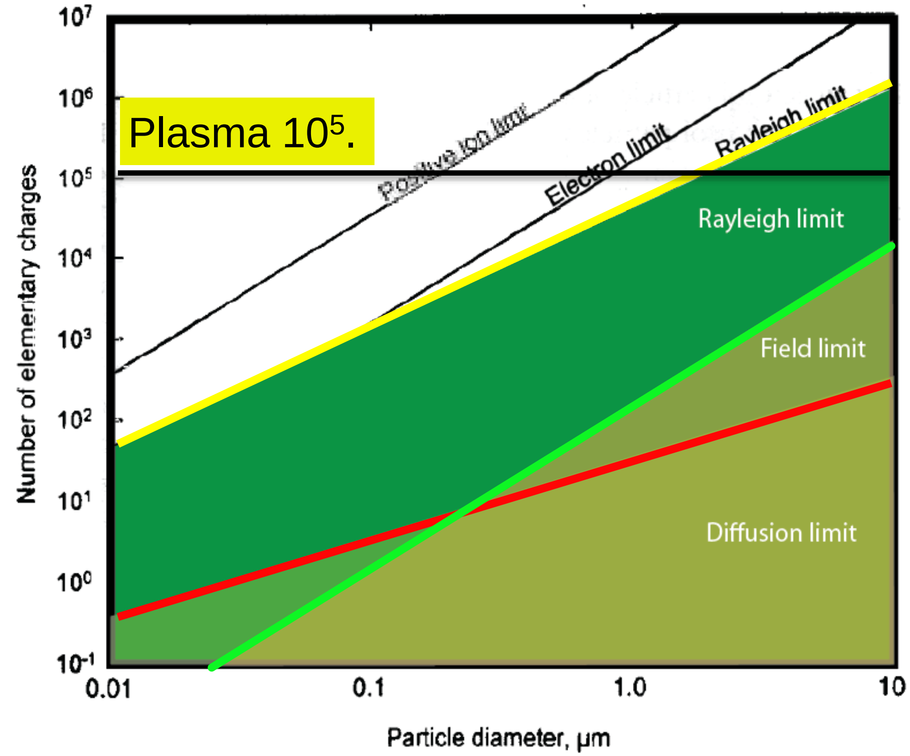

High electron density non-equilibrium atmospheric pressure plasma
(T_e >> T_{gas})

Plasma versus Radiolysis or e-Beam

- X $10^3 - 10^7$ faster
  - ➲**Similar dose rate as gamma radiation**
- Plasma-droplet
  - ➲Dose rate assuming **x%** plasma energy delivered to drop according to ratio $VOL_{drop} / VOL_{plasma}$
  - ➲5×10^{-2} kGy s^{-1}.
- Solvated Electron Reduction Hypothesis
  - ➲Reactions: 2nd order
  - ➲Droplet negatively charged
  - ➲**Electrons arrive with very low energy**
  - ➲**Electrostatically confined**
  - ➲**shallow surface layer**
  - ➲Very high local concentration

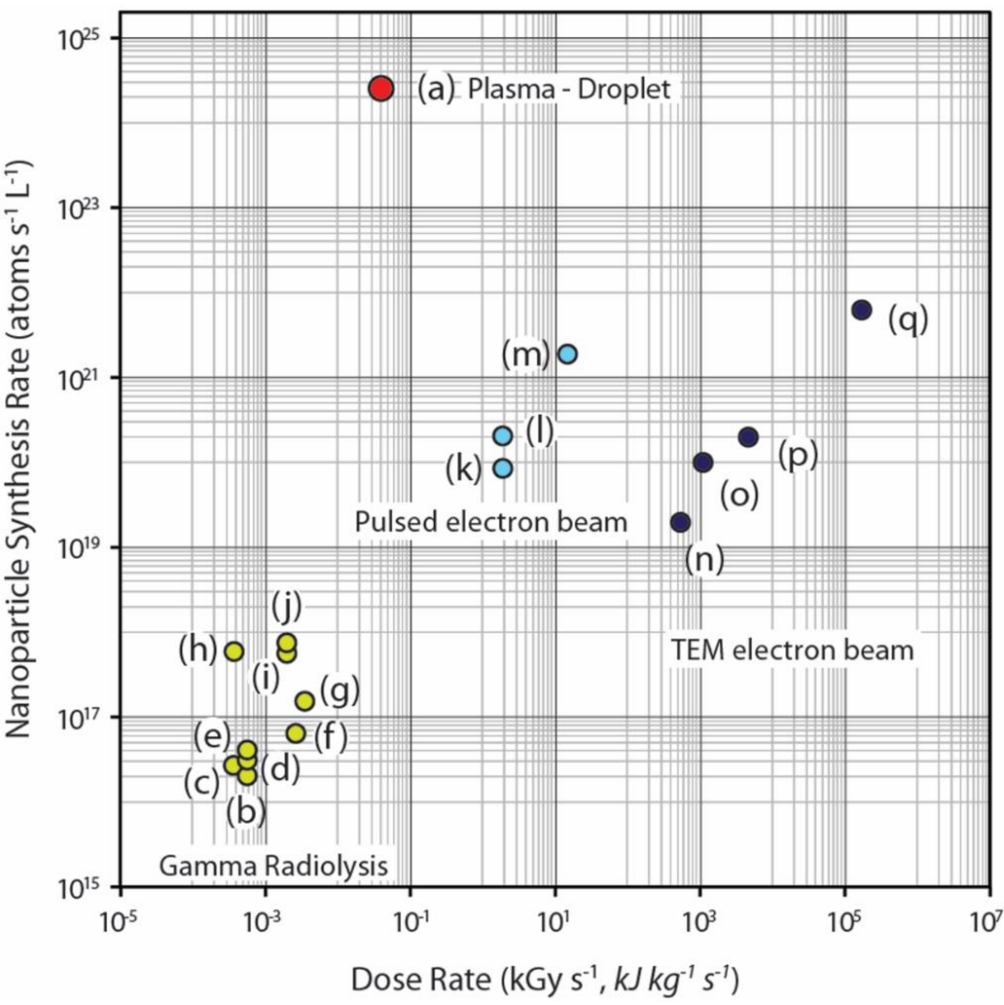

$HAuCl_4$. The reduction of **Au^{III}** proceeds via reactions as:

II	$Au^{III}Cl_4^- + e_{aq}^- \rightarrow Au^{II}Cl_4^{2-}$	(R1)
III / I	$2\ Au^{II}Cl_4^{2-} \rightarrow Au^{III}Cl_4^- + Au^{I}Cl_2^- + 2Cl^-$	(R2a)
0	$\mathbf{Au^{I}Cl_2^- + e_{aq}^- \rightarrow Au^{0}Cl_2^{2-}}$	**(R3)**
I / II	$Au^{III} + Au^{0} \rightarrow Au^{I}$ and Au^{II}	(R4)

Maguire et al., 2017, 10.1021/acs.nanolett.6b03440

pd.maguire@ulster.ac.uk

Ion impact … impact

pd.maguire@ulster.ac.uk

RF 13.56MHz
n_e: $10^{12} – 10^{14}$ cm^{-3}.

heating

e^- Droplet charging

e^-

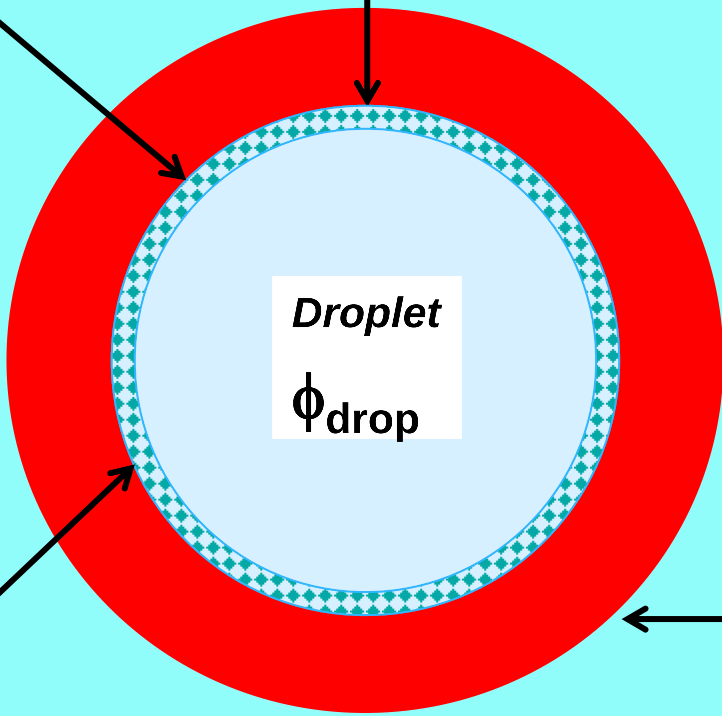

recombination
Heating?

He⁺ **Ne⁺** ions

Henry's constant ~0
Ion arrival energy ~0 eV because of collisions
KE ~0
PE ~24 eV (?)

Electron energy from EEDF:
Electron energy ~0eV in vicinity of droplet i.e. is dependent on floating voltage, rather than T_e.

Vapour layer

Evaporation

He^0
He^*
Ne^0

neutrals

Plasma region

Ions, metastables

Auger processes

pd.maguire@ulster.ac.uk

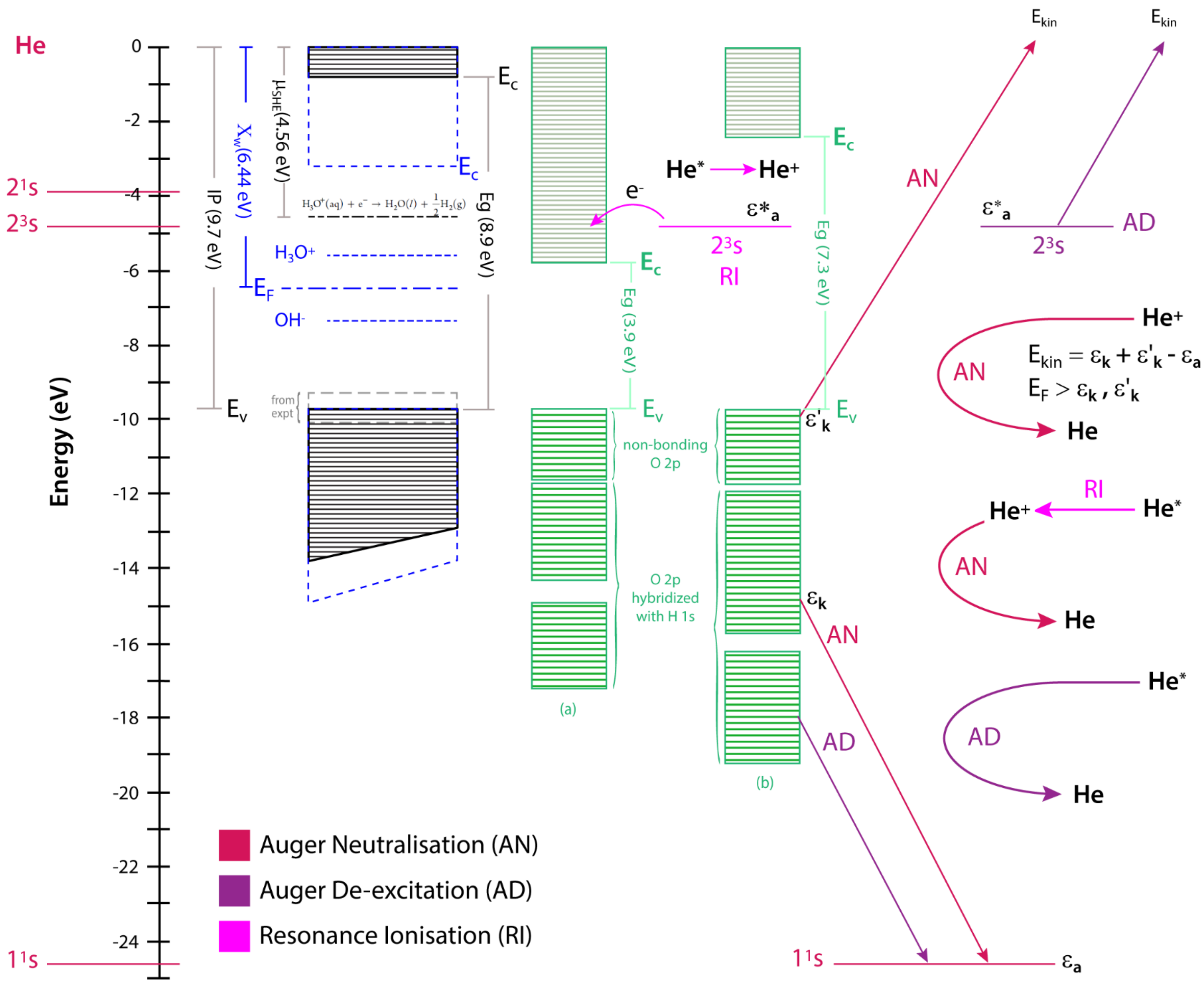

Auger Neutralisation

Without water ionisation, electrons required for AN would lead to the reduction in the number of surface negative charge, (solvated electrons and anions).

- From the requirement of zero net charge flux, the ion flux is diminished compared to electron flux by a factor of $(1 + \gamma)^{-1}$, where γ is the fraction of AN electrons emitted **into** the gas phase.
- Assuming emission occurs at random directions, the geometric yield for a droplet, γ_g, is ~50%.
- Remaining $1 - \gamma_g$ electrons penetrate 0.5 – 3 nm into the liquid. Ionisation, dissociation, further secondary emission and backscattering are possible, the latter two increasing the overall γ.
- In the energy range ≤ 25 eV, elastic scattering of electrons has largest cross-section.
- Data for backscattering coefficients in water or at sub-100 eV energies is absent.

Simulation

- $1 - \gamma$ electrons that enter the droplet participate in similar reactions as solvated electrons.

In each time step,

- surface solvated electron count is increased by $2(1 + \gamma)^{-1}\,\Gamma_n$
- negative charge count is decreased by $(1 + \gamma)^{-1}\,\Gamma_n$, where Γ_n is the nominal input flux.

Simulation

- 1 – γ electrons that enter the droplet participate in similar reactions as solvated electrons.

In each time step,

- surface solvated electron count is increased by $2(1 + \gamma)^{-1} \Gamma_n$
- negative charge count is decreased by $(1 + \gamma)^{-1} \Gamma_n$, where Γ_n is the nominal input flux.

H2O2

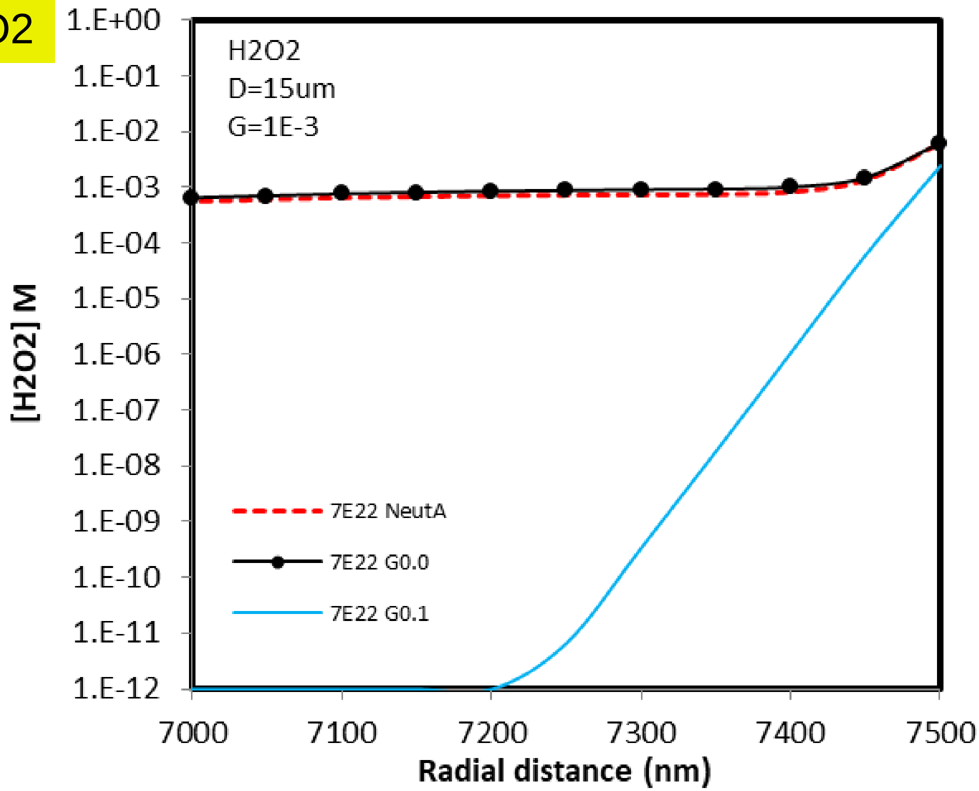

Simulation

- $1 - \gamma$ electrons participate in similar reactions as solvated electrons.
- surface solvated electron count is increased by $2(1 + \gamma)^{-1} \Gamma_n$
- negative charge count is decreased by $(1 + \gamma)^{-1} \Gamma_n$, where Γ_n is the nominal input flux.

OH decreases with γ increase

H Minimum effect at 5E22

OH

H

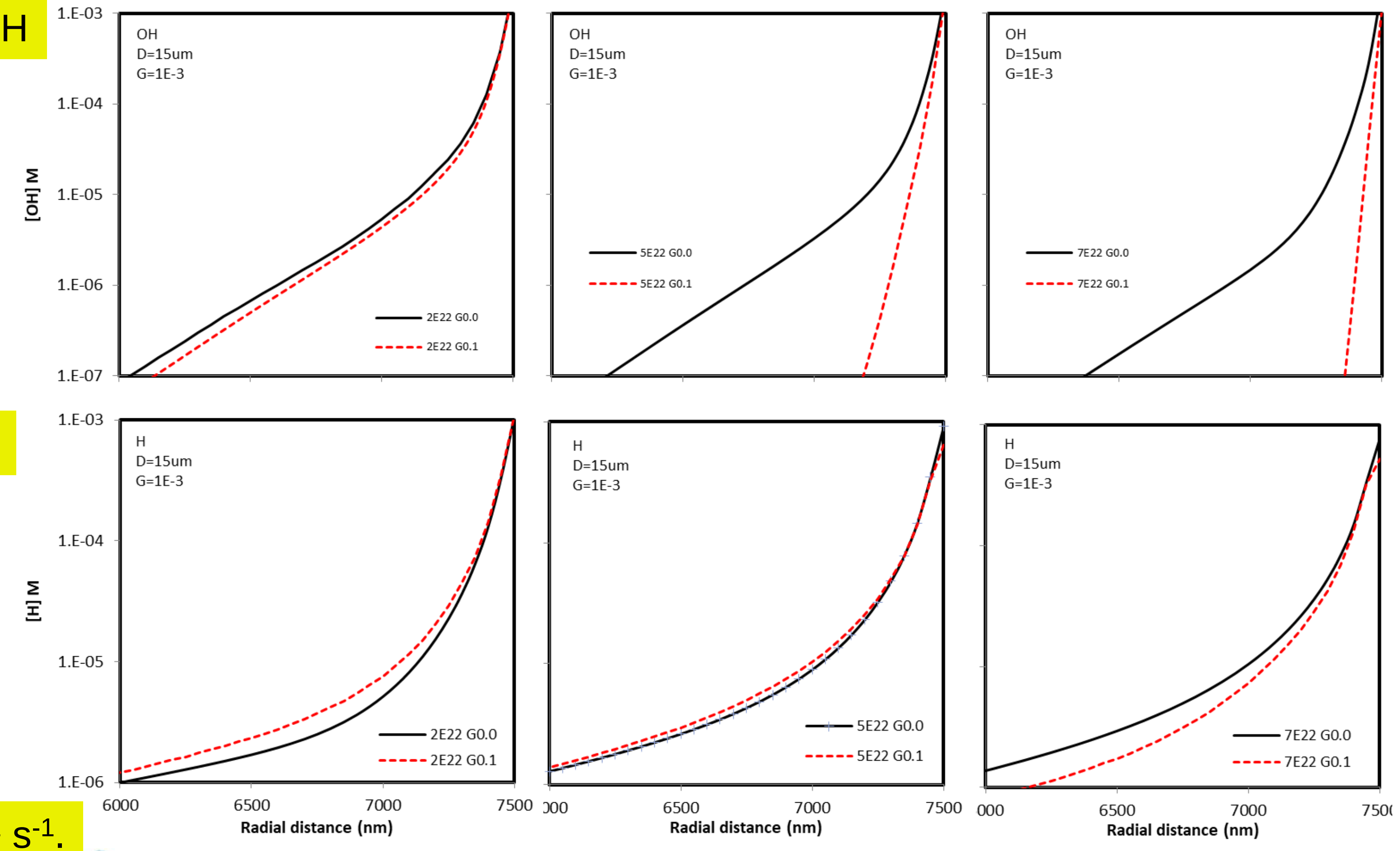

Γ_n= 2 - 7 x10^{22} m^{-2} s^{-1}.

New Diagnostics

1. XPS – UPS / REELS / ISS
2. Tunable mid-IR sources

Mid-IR

pd.maguire@ulster.ac.uk

- MIR absorption
  - Supercontimum broadband laser
  - 0.8 – 4um
  - Tunable filter
  - Other tunable lasers 4um – 12um
- Droplet diagnostics
  - In flight?
  - Stroboscopic?
  - Vapour halo?
  - Water clusters?
- Bulk liquid surface
  - 10 – 50 ns resolution?
  - 10 – 100nm penetration?
- Gas phase
  - H2O2, H2O average
  - FTIR mode

- Delivered
- 15th March 2020
- Still in boxes!

EPSRC Strategic Equipment

EP/R008841/1

"A multi-function XPS-UPS system with load-locked advanced sample preparation"

Davide Mariotti

Plasma Science &

Nanoscale Engineering Group

www.plasmamate.org

d.mariotti@ulster.ac.uk

Paul Maguire

Plasma Nanofabrication Group

pd.maguire@ulster.ac.uk

pd.maguire@ulster.ac.uk

XPS Escalab XI^{+}

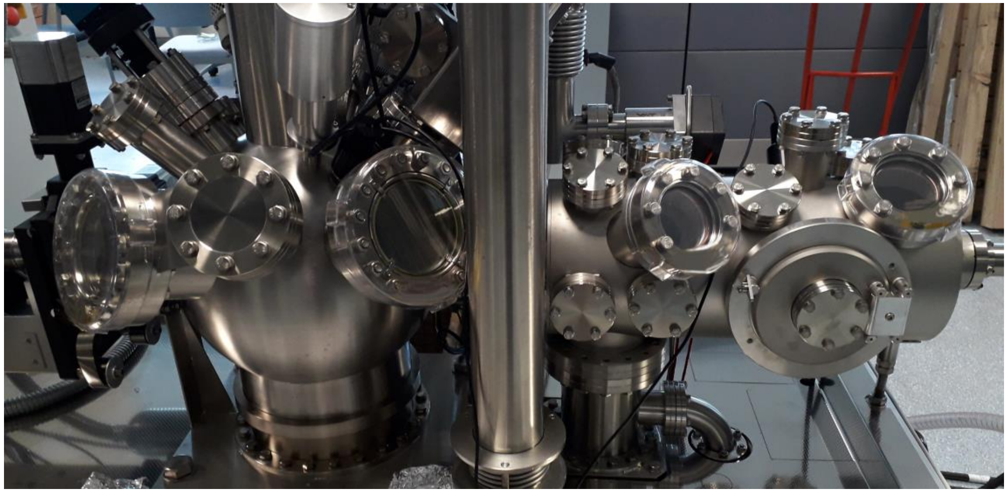

Sample holder available

From left to right:
- The normal substrate holder where thin samples lower than 2mm can be loaded
- The sample holder where thick sample can be loaded
- The heat sample holder can be heat until 1000°C
- The cooled sample holder, can be cooled to -50°C

Principle

Source Al kα (1486.7eV)

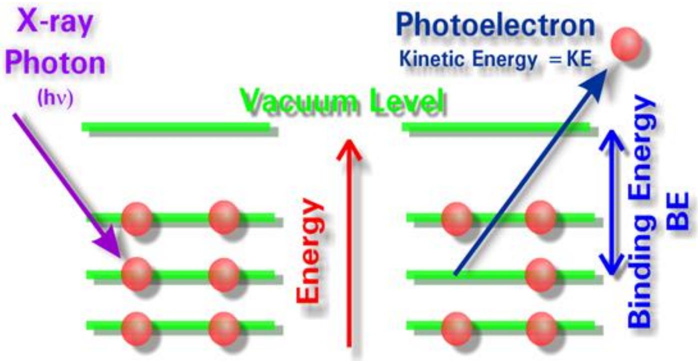

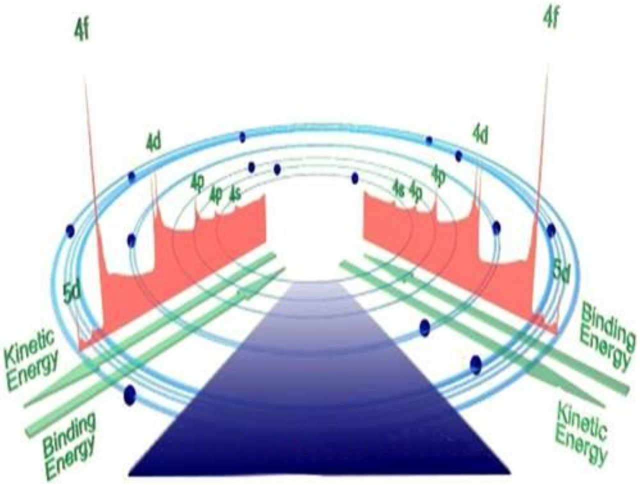

ESCALAB XI$^+$ Possibilities

pd.maguire@ulster.ac.uk

Controlled atmosphere

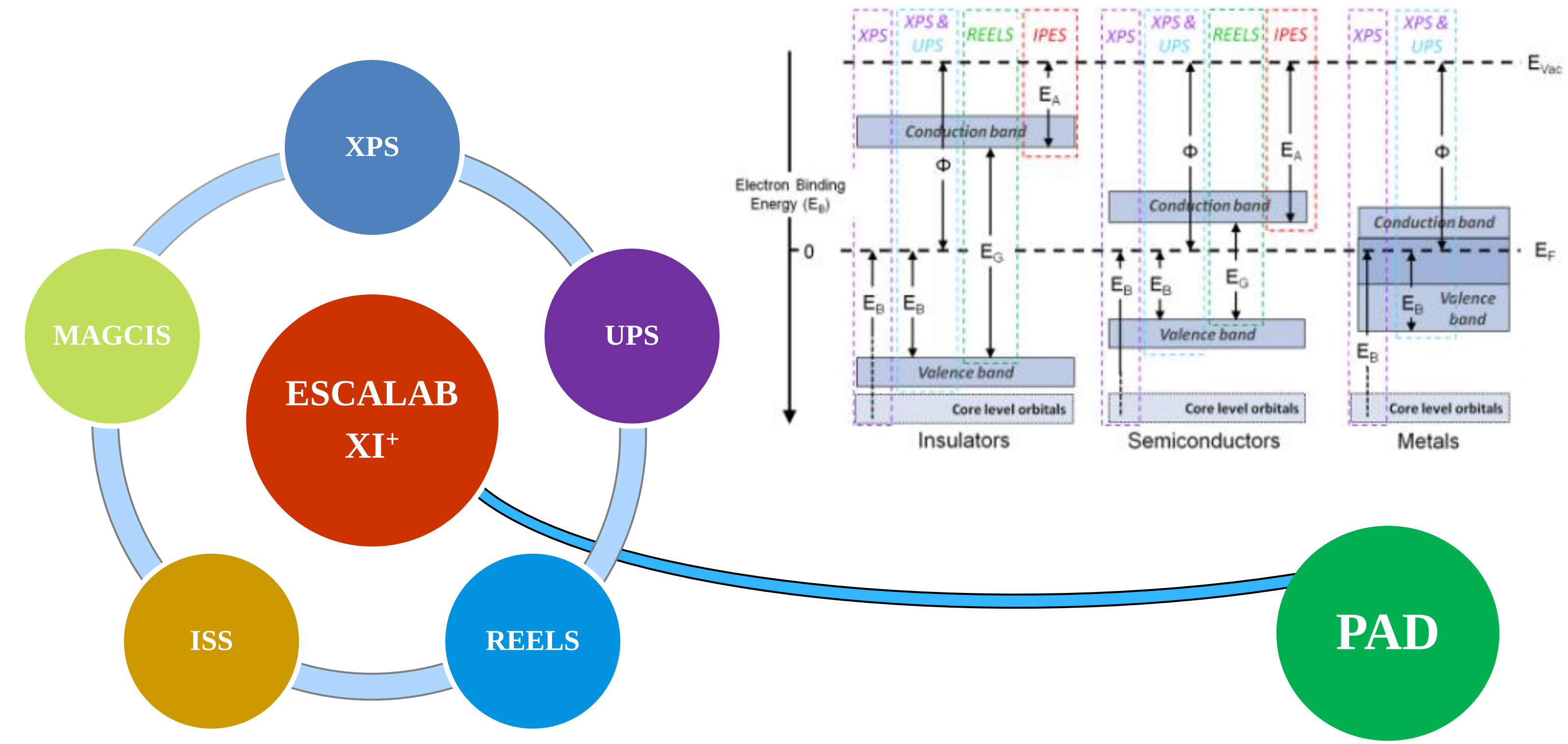

XPS : X-Ray Photoelectron Spectroscopy

MAGCIS: Mono Atomic/Gas Cluster Ions Source

ISS : Ions Scattering Spectroscopy

REELS : Reflection Electron Energy Losses Spectroscopy

UPS : UV Photoelectron spectroscopy

PAD : Plasma station

pd.maguire@ulster.ac.uk

X-Ray Photoelectron Spectroscopy (XPS)

- 10 nm surface analysis
- Non destructive
- Quantitative

Chemical bonding quantification:
from narrow region

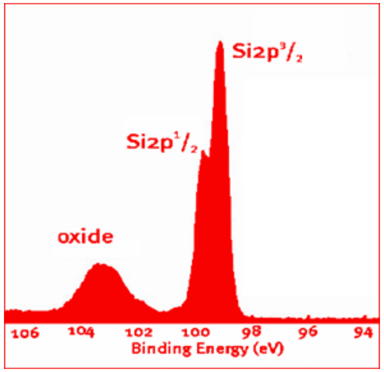

Elemental identification/quantification:
from survey spectra

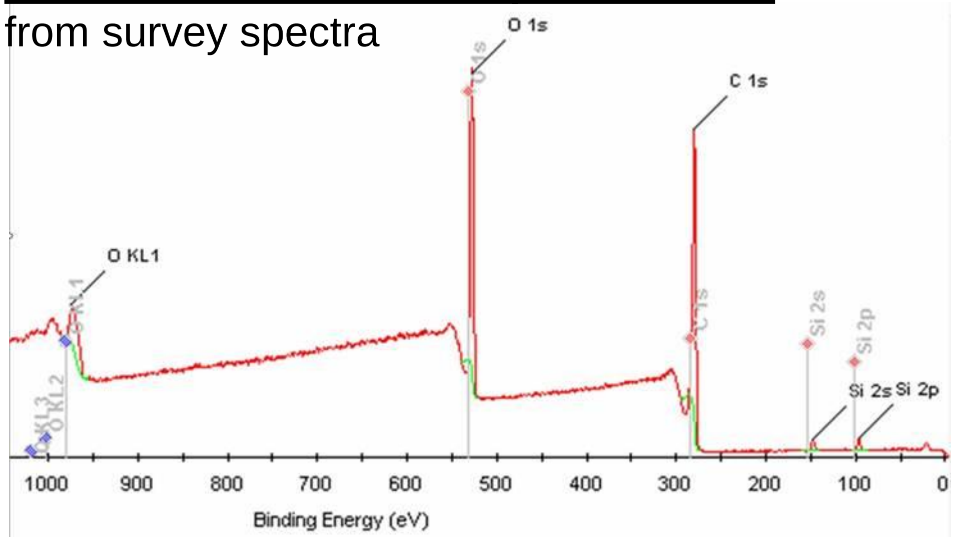

Available analysis

- Small area <20μm
- Point/Multipoint/Linescan
- Imaging
- Angle resolved
- Depth profile

Imaging:

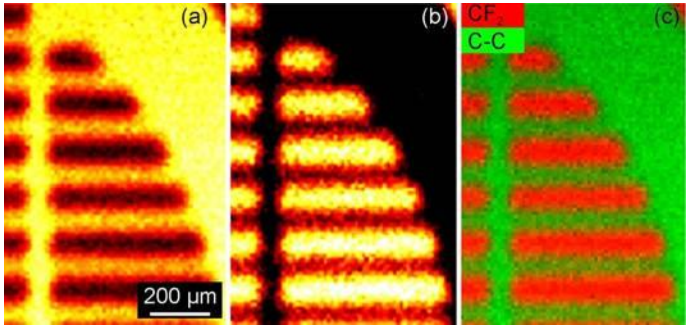

284.7 eV Hydrocarbon | 291 eV Fluorocarbon | Overlay

- Spatial localisation of the element

Angular resolved:

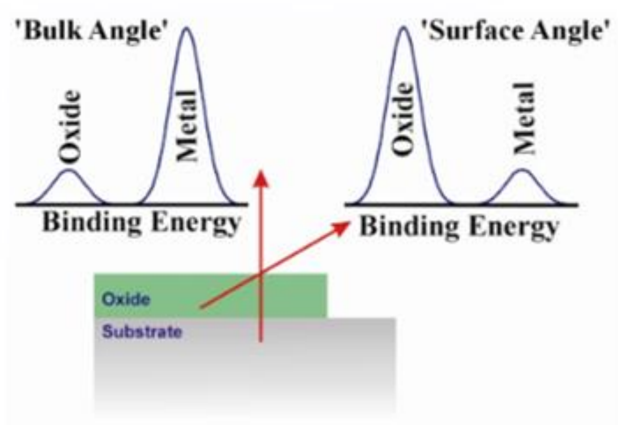

- Determination of the oxide layer thickness

Depth profile:

- Information of the thickness sample
- The sample need to be etched with Ar gun
- Locally destructive analysis

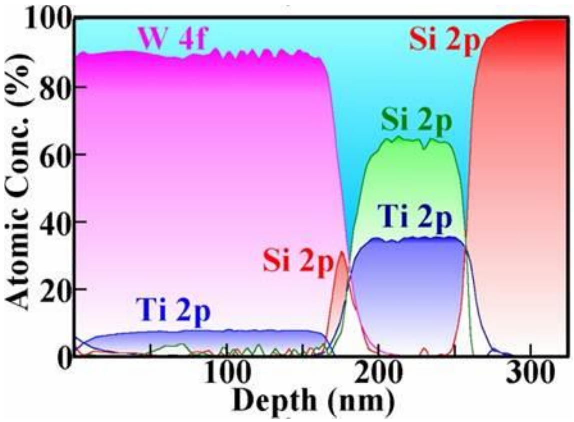

Cleaning/Etching process

* Monoatomic ions (Ar^+) : Used to etch/clean hard material

  - High energy per atom (200eV-4keV)
  - High etch rate
  - Can damage the surface
  - Can change the chemistry

* Cluster ions (Ar^+_n): Use for etch/clean soft material

  - Low energy per atom (cluster size 300-2000)
  - Very low etch rate
  - Soft material
  - Non damaging to the surface chemistry

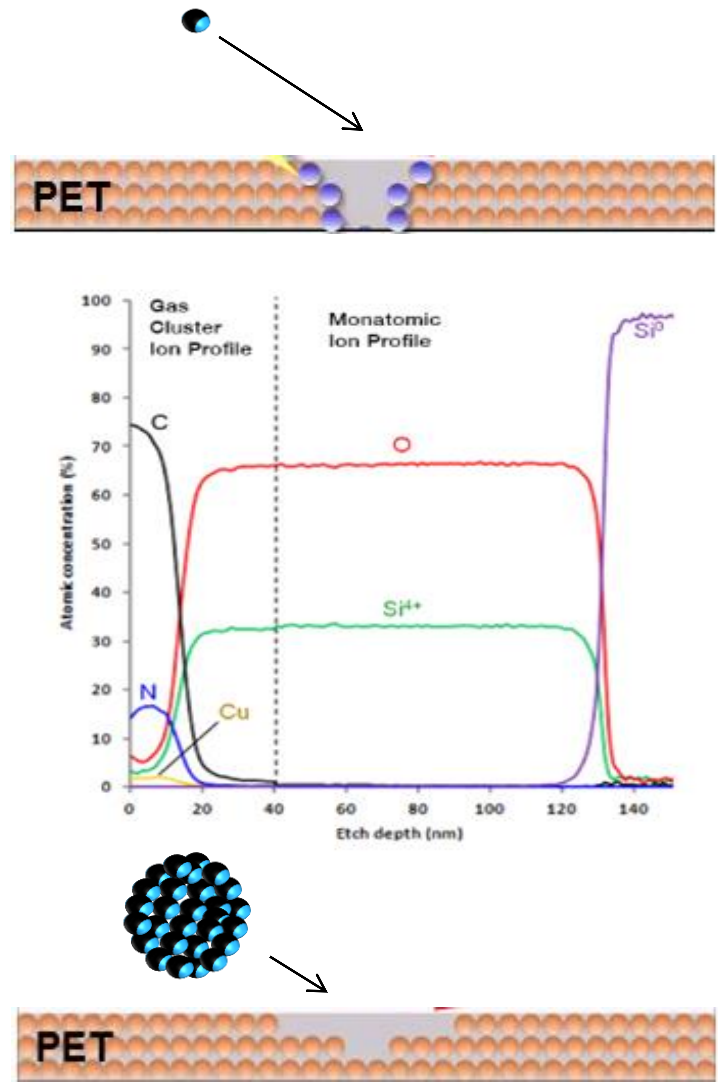

pd.maguire@ulster.ac.uk

Ion Scattering Spectroscopy (ISS) :

Involves firing a beam of He^+ ions at a surface, and measuring the kinetic energies of the ions that are scattered back.

- Non destructive
- Top surface analysis
- One peak for each element

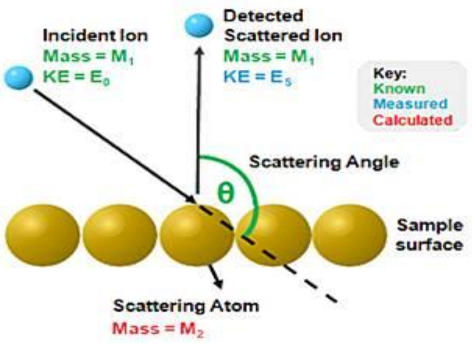

$$\frac{E_s}{E_o} = \left[\frac{\cos\theta \pm \left[\left(\frac{M_2}{M_1} \right)^2 - \sin^2\theta \right]^{\frac{1}{2}}}{1 + \left(\frac{M_2}{M_1} \right)} \right]^2$$

Unknown Recorded Spectra

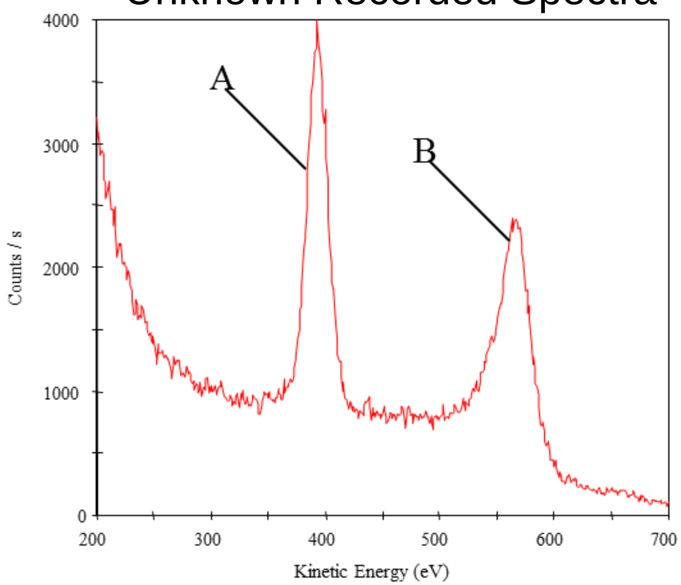

The primary beam energy (E_o) is usually determined by measuring the scattered peak energy (E_s) from a sample of known composition (such as gold E_0=910 eV)

Peak A : E_s = 393 eV $\Rightarrow$ M_2 = 16
Peak B : E_s = 568 eV $\Rightarrow$ M_2 = 28

Peaks A and B correspond to O and Si respectively.

REELS spectra:

A. The shape of the scattered background – this can help understand the scattering processes near the surface of the solid.

B. The onset of the scattered background – possible measurement of the electronic band gap of a sample.

C. Plasmon, shake-up or other loss peaks – visible without interference from XPS peaks

D. Peaks due to hydrogen – allowing semi-quantitative analysis

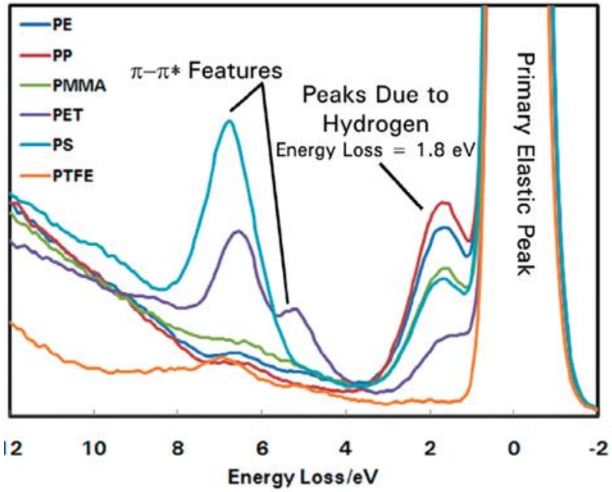

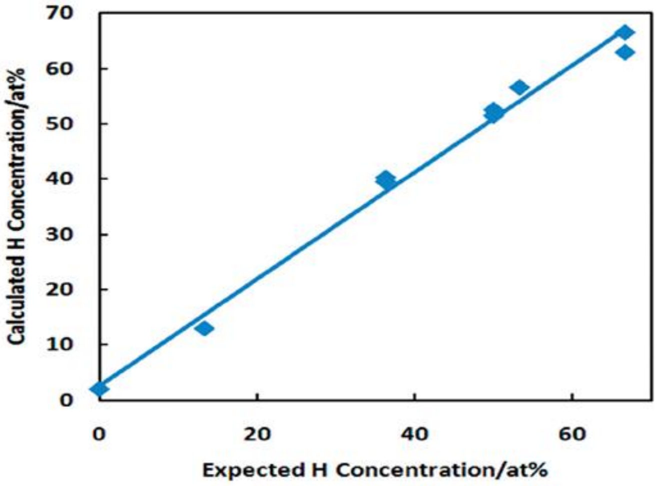

- Surface sensitive 2-3 nm
- Give chemistry and structure of top surface
- Can be used on soft sample

pd.maguire@ulster.ac.uk

Ultraviolet Photoelectron Spectroscopy (UPS)

- Works on the same principles as XPS with lower photon energy, generally below 50 eV (He (II)) and commonly 21.2 eV (He(I))
- Valence band analysis
- Work function analysis
- Fermi Level

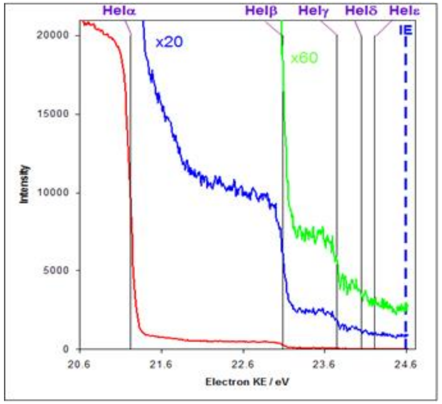

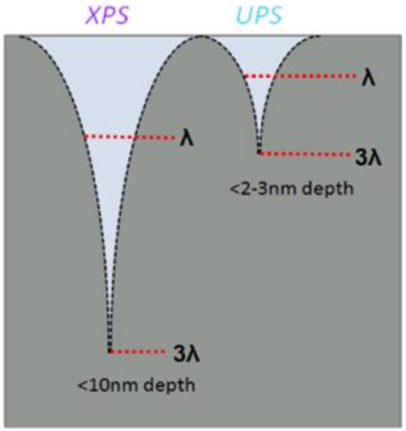

Emission line	Photon Energy / eV	Relative intensity (%)
He (I) α	21.22	97.7
He (I) β	23.09	1.9
He (I) γ	23.74	0.4
He (I) δ	24.04	0.2
He (I) ε	24.21	0

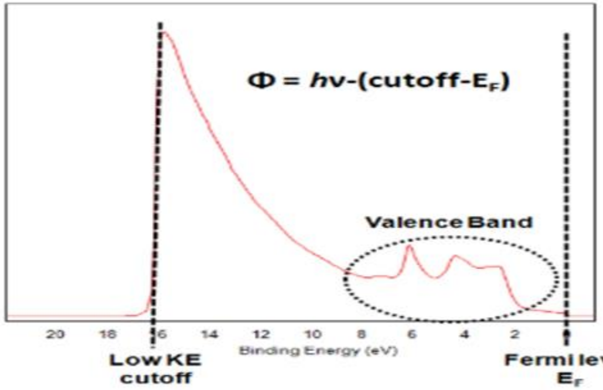

Standard, substrate with no liquid:
- Nanomaterial deposition
- Plasma surface treatment

Plasma - liquid with stopped or continuous flow
- Plasma - liquid treatment
- Nanomaterial synthesis in liquid
- Nanomaterial deposition into liquid
- Plasma – liquid – biological

Plasma - static liquid
- Plasma - liquid treatment
- Nanomaterial synthesis in liquid
- Nanomaterial deposition into liquid
- Plasma – liquid – biological

Plasma - treated microdroplets
- Plasma - droplet treatment
- Droplet deposition, instant freezing
- Nanomaterial deposition into liquid
- Plasma – liquid – biological

- ❖ **Plasma**
- ❖ Different plasma gases available
- ❖ Low to Radio frequency plasma
- ❖ Easy to transfer to XPS
- ❖ XYZ stage for large surface treatment

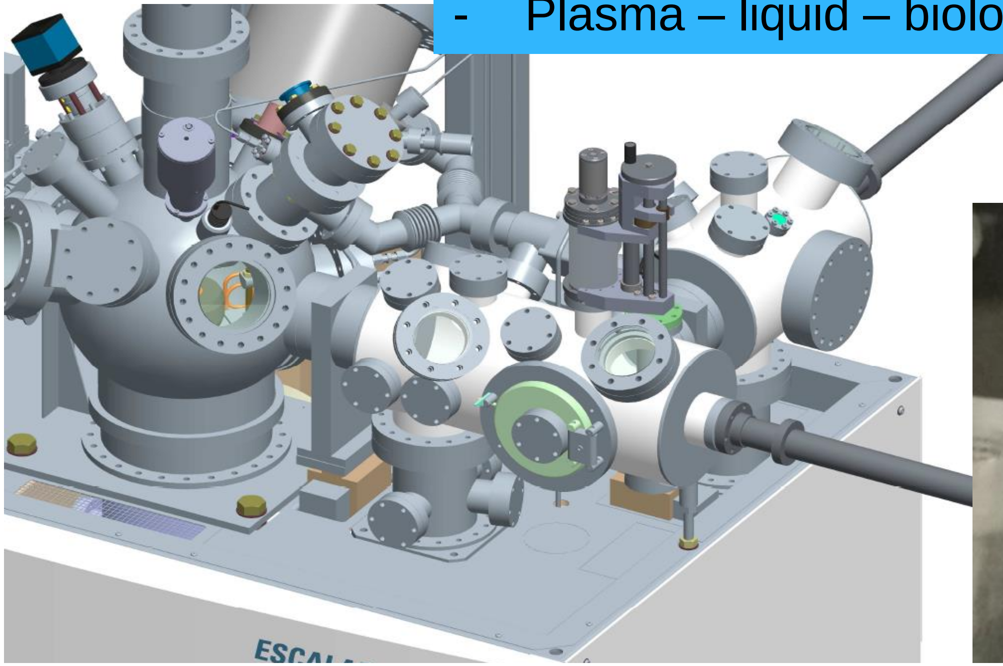

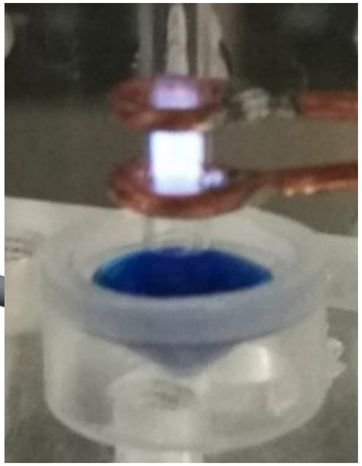

Funding Sources

EPSRC
Pioneering research and skills

THE ROYAL SOCIETY

National Science Foundation
WHERE DISCOVERIES BEGIN

The Leverhulme Trust

Department for Employment and Learning
www.delni.gov.uk

sfi Science Foundation Ireland

European Union
European Regional Development Fund
Investing in your future

JAPAN SOCIETY FOR THE PROMOTION OF SCIENCE · FOUNDED 1932 ·

Invest Northern Ireland

MARIE CURIE ACTIONS

NATO OTAN

University of St Andrews

RUB
RUHR-UNIVERSITÄT BOCHUM

NUI Galway
OÉ Gaillimh

Queen's University Belfast

University of Glasgow
Declan Diver
Hugh Potts
Euan Bennet

University of Glasgow

UNIVERSITY OF CAMBRIDGE

SCRIPPS INSTITUTION OF OCEANOGRAPHY UC San Diego

NATO
SfP 984555

National Institute of Advanced Industrial Science and Technology (AIST)
独立行政法人　産業技術総合研究所

Ulster University
NIBEC Nanotechnology & Integrated Bioengineering Centre
plasma & nanofabrication
pd.maguire@ulster.ac.uk